ASHRAE Guideline 36 Open-Source Supervisory Control Technology Development and Demonstration

Final Report

ET22SWE0039

Image: https://www.michaudcooley.com/news/chiller-plants/

Prepared by:

Tharanga Jayarathne, Rupam Singla – TRC
Carlos Duarte, Aoyu Zou, Paul Raftery - UC Berkeley, CBE
Reece Kiriu, Hwakong Cheng - Taylor Engineers

October 31, 2025

Acknowledgements

The authors of this report would like to thank Domenico Caramagno, Danny Pestal, Maria Hassid, and Chris Ellis for their support at the demonstration sites.

Disclaimer

Executive Summary

ASHRAE Guideline 36 (G36) establishes industry best practice standardized sequence of operations for heating, ventilation, and air conditioning systems, including airside systems, chilled water plants, and hot water plants. Previous research studies have implemented airside system sequence of operations to show up to 35 percent energy savings over existing control strategies. This project demonstrated a scalable approach to implementing G36 sequence of operations for chilled water and hot water plants in existing buildings. The research team deployed selected G36 sequences of operations in one chilled water plant and two hot water plants across two buildings, using a layered architecture that combined a supervisory control platform, Control Description Language programming, and Brick ontology tagging.

The team used the supervisory control layer to coordinate G36 logic with existing building automation systems without requiring major infrastructure changes. Using Control Description Language, the team implemented control logic to promote transparency, modularity, and alignment with G36 specifications, and applied Brick ontology to tag heating, ventilation, and air conditioning system data points. This created a machine-readable semantic model that supported scalable integration and diagnostics, allowing for an implementation pathway that enabled standardized control deployment across diverse systems while minimizing engineering effort. Prior to the implementation, the team performed a thorough evaluation of the existing heating, ventilation, and air conditioning system including the control setpoints and sequences to identify and rectify issues that might impact G36 implementation.

To evaluate performance, the research team conducted measurement and verification using measured energy data and regression modeling with typical meteorological weather data to calculate weather-normalized annual energy consumption. G36 implementation resulted in weather-normalized annual energy savings of 7 percent and 11 percent in the two hot water plants, corresponding to $ 0.095 per square foot per year and $0.17 per square foot per year cost savings. The implementation also led to 15 percent energy savings in the chilled water plant, corresponding to $0.12 per square foot cost savings—excluding June through August—when compared to existing controls strategy.

These results confirm both the energy efficiency benefits and the technical viability of using a modular and scalable approach for adopting G36. The findings also highlight the importance of reviewing existing systems and performing thorough retro-commissioning to ensure system operation as expected, especially in critical environments, before deploying advanced control strategies. For context, the team estimated that the in-depth retro-commissioning measures in the chilled water plant saved 16 percent energy in this building and were a critical first step to ensuring that the more advanced supervisory controls could operate over the maximum possible range of temperatures and yield correspondingly higher performance.

Abbreviations and Acronyms

Acronym	Meaning
AHU	Air handling unit
ASHRAE	American Society of Heating, Refrigerating, and Air-Conditioning Engineers
BACnet	Building Automation and Control Network
BAS	Building automation system
CAC	Computer air conditioning
CCF/min	Hundred cubic feet per minute
CDL	Control Description Language
CHW	Chilled water
CVRMSE	Coefficient of variation of the root mean square error
DHW	Domestic hot water
DOAS	Dedicated outside air system
FMU	Functional mockup unit
FPT	Functional performance testing
GPM	Gallons per minute
HVAC	Heating, ventilation, and air conditioning
HW	Hot water

Acronym	Meaning
IPMVP	International Performance Measurement and Verification Protocol
IOU	Investor-owned utility
kWh	Kilowatt-hour
kBtu	Thousand British thermal units
LBNL	Lawrence Berkeley National Laboratory
NDBE	Normalized deviation of the bias error
NMEC	Normalized Metered Energy Consumption
M&V	Measurement and verification
RAHU	Recirculating air handling units
sMAP	Simple Measurement and Actuation Profile
SOO	Sequence of operations
TOWT	Time-of-Week and Temperature
T&R	Trim and respond
VAV	Variable air volume

Table of Contents

Figures

Tables

Introduction

The American Society of Heating, Refrigerating, and Air-Conditioning Engineers (ASHRAE) Guideline 36—hereafter ASHRAE G36 or G36 (ASHRAE, 2021)—was first published in 2018 and establishes industry best-practice standardized sequence of operations (SOOs) for heating, ventilation, and air conditioning (HVAC) systems. These include airside control sequences introduced with the original G36 in 2018, and chilled water and hot water control sequences introduced in the 2021 update. Standardization of control sequences allows HVAC system manufacturers to centrally program the control logic and then distribute it to installers for field implementation, including possible field adjustment and customization. This approach, in theory, should reduce cost and the risk of errors inherent in current practice. Designers can specify G36 rather than writing their own SOOs and installers can draw from a library of G36 control logic options rather than programming their own logic.

The California Energy Commission recently adopted the 2025 updates to California's Building Energy Efficiency Standards (CA Title 24), establishing a prescriptive requirement for using ASHRAE G36 sequences (Singla, et al., 2022) for airside systems in all non-residential building types, including new constructions, additions, and alterations except for healthcare buildings. This is expected to save 44.5 gigawatt-hours in electricity, 0.71 million therms in natural gas, and more than 50 million gallons of water in the first year alone.

Previous field demonstration research studies in California have implemented airside SOOs of G36 and estimated energy savings. One 2022 study (Taylor Engineering, TRC, Integral Group, 2022) implemented ASHRAE G36 airside SOOs for variable air volume (VAV) systems in seven non-residential buildings and estimated electricity savings of 11 percent to 35 percent (Raftery, Cheng, & Wendler, 2024). The research team did not find similar studies that demonstrate the SOOs for hydronic systems, such as the chilled water plant and hot water plant. This project implemented the hydronic system G36 SOOs and evaluated the energy savings compared to an established baseline. The research team expects the outcomes of this project will support future energy code adoption of G36 chilled water and hot water system SOOs.

In this project, the team successfully implemented G36 SOOs in one chilled water system and two hot water systems in two buildings using a layered architecture that combined a supervisory control platform, Control Description Language (CDL) programming, and Brick ontology tagging. The team evaluated the energy savings of G36 against the existing control strategy and the implementation process of G36 in existing buildings, including challenges to implement these control system updates.

This implementation methodology of using a supervisory control layer to perform the advanced controls calculations, using standardized CDL and Brick ontology for mapping between the control logic and BAS points, streamlines the deployment in a manufacturer-agnostic manner and avoids the need to program G36 in each unique system. It also provides options if the existing system cannot accommodate control algorithm intensity or controllability of equipment. The energy savings analysis showed 86,672 kilowatt-hours (kWh)—0.61 kilowatt-hours per square foot, or 14.6 percent—weather

normalized savings from September through May in the chilled water plant, due to reduced overcooling and improved system efficiencies at revised temperature setpoints.

The two hot water plants showed 1,431,580 thousand British thermal units (kBtu) per year (10.15 kBtu per square foot per year, or 11.5 percent) and 126,953 kBtu units per year (3.28 kBtu per square foot per year, or 7.5 percent) annual weather normalized savings, mainly from reduced thermal losses when operating at lower supply water temperatures. The team also evaluated the value of using semantic interoperability to enable standardized controls deployments that increase adoption of industry standard and high performing control sequences across the building stock.

Background

Project Overview

The goal of this project is to demonstrate implementation of ASHRAE G36 SOOs related to hydronics systems using open-source supervisory control technology. The hydronic system SOOs implemented in this project include chilled water plant control and hot water plant control serving a multizone VAV system and a radiant heating system. Open-source supervisory control technology used a higher-level control layer to calculate and set control parameters for the local control layer of the building automation system (BAS). Using an open-sourced technology to implement G36 through a supervisory control layer demonstrates the scalability of G36 adoption in both new construction and in retrofits in a BAS-agnostic manner.

The team selected two buildings at which to demonstrate the implementation that have supervisory control hardware and software platforms in place. These platforms utilize CDL for documenting and implementing control logic (Wetter, et al., 2022); CDL is built on the equation-based modeling language, Modelica, and is used to express control sequences for BAS in a structured, verifiable, and vendor-independent format to ensure that the design intent of the control sequences is met. Many G36 SOOs and other high-performance HVAC control sequences are currently available in a repository of engineering models for building energy systems called Modelica Buildings library (Wetter, Zuo, Nouidiu, & Pang, 2014), so the research team did not have to duplicate effort in the programming of G36 SOOs used in these field demonstrations. The Brick ontology (Brick Consortium, 2015) is an open-source effort to standardize descriptions of physical and logical assets in buildings, as well as the relationships between them. It allows for the creation of digital, machine-readable representations of buildings where information can be retrieved in a standardized format to input into control logic including CDL function blocks. Together, CDL and Brick ontology enable the testing and implementation of ASHRAE G36 standardized sequences of operations, as shown in Figure 49 later in this report.

In this project, the team established baseline HVAC system control methods, implemented the G36 sequences, and performed measurement and verification (M&V) to calculate energy savings for the two buildings. As part of establishing baseline control methods, the team analyzed BAS trend data, verified the performance of the existing controls, and made updates discussed in the G36 Sequences Implementation and Plant Optimization section so that the baselines were representative of a well-functioning system. This included increasing the space temperatures of clean rooms from 68°F to 72°F, lowering AHU preheat coil leaving air temperature setpoints from 55°F to 50°F, and

increasing AHU dewpoint setpoints from 45°F to 55°F. These updates led to substantial savings on their own as discussed in the Energy Consumption Analysis – Site 1 Chilled Water Plant section and allowed to achieve far higher energy savings when combined with G36 SOOs implementation. Under the new control sequence implementation, the team developed Brick data models for the buildings to develop and test portable controls applications of the G36 SOOs. To perform M&V, the team verified the existing metering and installed new metering where necessary. The Methods and Approach and Findings sections below discuss the activities the team conducted.

Existing Control Strategies for HVAC Chilled Water and Hot Water Plants

Conventional control methods for chilled water plants and hot water plants involve regulating temperatures and flowrates using feedback from thermostats, pressure sensors and flow meters but can vary between fixed values to resets. *ASHRAE Handbook: HVAC Systems and Equipment* (ASHRAE, 2020) discusses control strategies used in chilled water and hot water plants that include temperature and flow rate reset based on cooling and heating demand. Some of these strategies, such as chiller and boiler staging, are part of the standardized sequences presented in ASHRAE G36.

These control strategies represent a range of possible approaches to managing chilled water and hot water plants in existing buildings. Some of these control strategies are often combined, for example, variable primary flow with chiller staging for optimization. However, many buildings use sub-optimal controls, like fixed supply water temperature setpoints.

Chilled water plants:

1. **Fixed Supply Chilled Water Flow Rate:** Maintaining a constant flow rate through the system, regardless of the cooling load.
2. **Variable Primary Flow:** Adjusting the flow rate of chilled water based on the cooling load using variable speed pumps.
3. **Primary-Secondary Pumping:** Using separate primary and secondary loops to maintain constant flow through chillers while adjusting flow in the secondary loop to meet the cooling load.
4. **Constant Flow with Variable Temperature:** Keeping the flow rate constant but varying the temperature of the chilled water supply based on the cooling load.
5. **Variable Flow with Variable Temperature:** Adjusting both the flow rate and temperature of the chilled water based on real-time cooling demand.
6. **Differential Pressure Control:** Using differential pressure sensors to maintain a set pressure difference across the system, ensuring adequate flow while optimizing pump energy use.
7. **Demand-Based Control:** Monitoring cooling demand in different zones and adjusting flow and temperature accordingly.
8. **Chiller Staging:** Sequencing multiple chillers to turn on or off based on the cooling load.

Hot water plants:

1. **Fixed Supply Hot Water Flow Rate:** Maintaining a constant flow rate through the system, regardless of the heating load.
2. **Variable Primary Flow:** Adjusting the flow rate of hot water based on the heating load using variable speed pumps.

3. **Primary-Secondary Pumping:** Using separate primary and secondary loops to maintain constant flow through boilers while adjusting flow in the secondary loop to meet the heating load.
4. **Constant Flow with Variable Temperature:** Keeping the flow rate constant but varying the temperature of the hot water supply based on the heating load.
5. **Variable Flow with Variable Temperature:** Adjusting both the flow rate and temperature of the hot water based on real-time heating demand.
6. **Differential Pressure Control:** Using differential pressure sensors to maintain a set pressure difference across the system, ensuring adequate flow while optimizing pump energy use.
7. **Demand-Based Control:** Monitoring heating demand in different zones and adjusting flow and temperature accordingly.
8. **Boiler Staging:** Sequencing multiple boilers to turn on or off based on the heating load.
9. **Outdoor Reset Control:** Adjusting the hot water supply temperature based on the outdoor temperature to match heating demand.
10. **Night Setback Control:** Reducing the hot water supply temperature during unoccupied periods to save energy.

ASHRAE G36 provides standardized sequences of control and uses combinations of control strategies, including some from the above list to minimize energy use while meeting heating and cooling demand.

ASHRAE Guideline 36 Control Methods

ASHRAE G36, titled "High-Performance Sequences of Operation for HVAC Systems," establishes current industry best-practice SOOs for HVAC systems, including chilled water plant and hot water plant control, which is the focus of this study. The aim of G36 is to maximize the energy efficiency and overall performance of HVAC systems, provide control stability, and allow for real-time fault detection and diagnostics. The sequences provided in this guideline complement other ASHRAE standards and help maintain occupant comfort and acceptable indoor air quality.

Chilled Water Plant Control Sequences

Chilled water plant control sequences in ASHRAE G36 include standardized control sequences for the entire plant, such as chiller control, waterside economizer control, pump control, and pressure control. The primary G36 energy measure this demonstration considered for the chilled water plant was the chilled water supply temperature setpoint reset. This strategy uses trim and respond (T&R) reset logic based on demand from associated chilled water valves to reset both the supply temperature setpoint as well as the differential pressure setpoint. For this project, the team decided to focus on the supply temperature reset, since this can have the biggest impact on energy efficiency. When there is less demand for cooling, G36 logic will gradually increase (trim) the chilled water supply temperature up to a maximum limit and when there is cooling demand as calculated from the number of cooling requests, the plant will reduce (respond) the chilled water supply temperature down to a low limit.

Hot Water Plant Control Sequences

Hot water plant control sequences in G36 include control sequences for the entire plant including boiler staging and control, hot water supply temperature reset, and hot water pump control. The primary energy saving measure from G36 considered for the hot water plant as part of this

demonstration is the hot water supply water temperature reset. G36 resets the temperature using T&R logic based on the demand from building hot water valves. Where there is less demand for hot water, the plant will reduce the hot water temperature (trim) down to a minimum limit and when there is heating demand as calculated by the number of heating requests, the plant increases the hot water temperature (respond) up to a maximum limit.

Open-Source Semantic Tools for Scalable Deployment

Supervisory control technologies are important to unlocking scalable, vendor-agnostic, and high-performance control strategies across diverse building types. Achieving this vision requires standardized G36 SOO, corresponding CDL control logic and two critical elements: standardized communication protocols that enable consistent access to real-time building data, and semantic data models that give data descriptions and context that are machine-readable. Together, these elements allow advanced supervisory controls, such as those based on G36, to interpret building conditions, execute control logic, and adapt to diverse HVAC configurations. In this project, the research team leveraged Building Automation and Control Networks (BACnet) for data communication and Brick ontology to organize and structure building metadata, enabling a digital representation of the physical system. These standardized frameworks supported the implementation of supervisory control strategies using vendor-independent programming tools, such as CDL, to deploy pre-tested G36 sequences in real buildings. The following sections describe how these components are integrated and used to overcome implementation barriers and improve the scalability and reliability of advanced control solutions.

Standardized Control Sequences and Programming Logic

G36 includes high performance sequences of operation for a range of airside HVAC systems, as well as chilled and hot water plants, to facilitate the implementation of high-performance HVAC controls. The control strategy uses T&R logic described in Section 5.1.14 of G36 (ASHRAE, 2021). G36 solves the problem of having each design engineer develop and specify their custom control sequences. The design engineer reduces time and effort when specifying these existing sequences, which have been developed by HVAC control experts and proven to have high performance. G36 sequences are presented as English-language specifications of controls and not the actual programming code syntax that will eventually be uploaded to the building's BAS; control programmers still need to convert this text into computer language specific to the building's HVAC and BAS and adapt it to the BAS point naming conventions. Furthermore, control programmers may have their own interpretation of the sequences, leading to various programmed G36 variants with varying field performance.

The design engineer might save costs in specifying standardized G36 but might then shift costs and effort to the control vendor, who must program and implement the more complex G36 sequences. The higher complexity of ASHRAE G36 exposes the system to more errors during the programming and implementation stages. This is where manufacturers' efforts to pre-program G36, and projects such as the OpenBuildingControl (Lawrence Berkeley National Laboratory, 2024), come at a great advantage.

The OpenBuildingControl project aims to digitize the design, specification, deployment, and verification of building control sequences such as G36 (Wetter, et al., 2022). The researchers in the project developed the CDL by building on the equation-based modeling language, Modelica, and used this to express control sequences for BAS in a vendor-independent (Wetter, Grahovac, & Hu,

Control Description Language, 2019). CDL is formally defined in the proposed standard, *ASHRAE 231P – A Control Description Language for Building Environmental Control Sequences* and has already been used to program G36 airside and hydronic sequences. Furthermore, these CDL representations are currently available in the Modelica Buildings library, a repository of engineering models for building energy systems and their control sequences (Wetter, Zuo, Nouidiu, & Pang, 2014)—building designers can take the standard CDL implementation of G36 to simulate the performance of the sequences in their specific buildings. The end goal is to use the same control sequence specifications and programming syntax through various stages of the building lifecycle, e.g., design, simulation, testing, deployment, and commissioning.

The research team took advantage of the Modelica library by using the preprogrammed and tested G36 sequences to deploy hydronic control interventions at the two demonstration sites. The team can use the CDL representation of G36 sequences by exporting them as a functional mockup unit (FMU), conforming to the functional mockup interface standard (Blochwitz, et al., 2012). Developers created FMU to allow model exchange and co-simulation models from different simulation environments. The FMU is a packaged file that contains details about the model parameters, variables, equations, and other relevant information to run the control sequences in our field demonstrations.

In order to develop control sequences for the two sites, the project team gathered and reviewed drawings and information from the existing building automation systems to identify the equipment and control configurations, determine compatibility with G36, and identify which strategies are likely to provide energy savings opportunities.

Standardized Communication Protocol and Semantic Data Model

BACnet is a communication protocol that defines a set of rules that allows the building automation system (BAS) network to exchange information in a standardized format (ASHRAE, 2020). BACnet represented a significant breakthrough in the BAS industry because it frees building stakeholders from relying on a single manufacturer or control vendor with proprietary communication protocols to procure equipment and controls for building services. BACnet is an abstraction of the inputs, outputs, and properties of BAS objects, but advanced control sequences, such as those found in G36 described above, need more information to perform well. This information can be the type and location of a sensor, the size of the HVAC zone, or the interconnections of the equipment in mechanical systems (Bergmann, et al., 2020). Building drawings, BAS software, or BACnet property fields may contain this type of information, but they are usually found in text and graphical descriptions that may not be easily queried or processed by computers. Furthermore, naming and other description conventions are not standardized, making point-mapping exercises unique to the building (Butler & Veelenturf, 2010). The team used the Brick ontology to solve these shortfalls.

Just as BACnet standardized the communication protocol for data transmitted over BAS, semantic metadata ontologies and schemas such as Brick standardize the meaning of that data to ensure consistent access and analysis. As shown in Figure 1, Brick is an ontology that uses a class hierarchy with three root nodes—Equipment, Point, and Location—to create a standardized data model for a building that identifies and characterizes the “things” inside the building and the relationship between them (Bharathan, et al., 2016). Brick refers to these “things” as entities, and to their relationships—such as feeds, hasPoint, and hasPart—as edges, which it describes using Brick

classes. For example, a physical device that provides some service to part or all the building can be described with the root class Equipment or its more specific subclasses, such as Centrifugal Chiller or Boiler. Point generally refers to entities that provide a source of data or control input. For example, Sensor, a subclass of Point, refers to the digital source of measurements, not the actual physical devices or transducers. Brick uses Location and its subclasses to describe physical and logical spaces grouped by common characteristics, e.g., an HVAC zone. Assigning nameplate information, floor area size, and electrical circuit leg phase as properties to the relevant Brick classes is possible. A set of two entities is connected by one edge, forming a triple in the Brick data model. The collection of interconnected triples forms the graph data structure known as the Brick data model.

The team built a Brick data model for each of the demonstration buildings. Figure 1 illustrates how the Brick classes and relationships come together to describe the hot water plant for Site 2, one of the demonstration sites described in detail later in this report. The developers of the Brick ontology built it on modern Semantic Web technologies typically used in the exchange of information over the internet e.g., Resource Description Framework and Web Ontology Language. It can be integrated and linked with other Semantic Web ontologies to develop a more complete representation of the built environment and data it produces (Delgoshaei, Heidarinejad, & Austin, 2022). This means that a Brick data model is a digital, machine-readable representation of the building and its contents that can be queried and is interoperable with a wide array of open-source and commercial software.

As part of the first steps for these field demonstrations, the team connected a small PC without a fan to the buildings' BAS network infrastructure, which allowed us to read and write to BACnet objects. The team used the open-source project BACpypes to provide the BACnet application and network layer, which established our PC's communication to the BAS (Bender, 2018). With this communication in place, the team performed a BACnet network scan and BAS point list retrieval using open-source network discovery utilities, such as Nmap (Nmap, 2022). The BACnet point list gave the research team the starting point to follow a five-step process that would build a Brick data model for each of the demonstration buildings.

The five-step process is as follows:

1. Collect siloed metadata for the building.
2. Organize it into more manageable formats.
3. Transform metadata into a Brick model.
4. Apply inference and reasoning to the initial Brick model to discover implied information.
5. Validate the Brick model to ensure the data modeler uses Brick classes and relationships correctly.

The research team also embedded BACnet object information within the Brick model and information for an external database access, collecting historical data from the buildings' BAS. Duarte Roa et al. describe the five-step Brick model development process in more detail (Duarte Roa, et al., 2022).

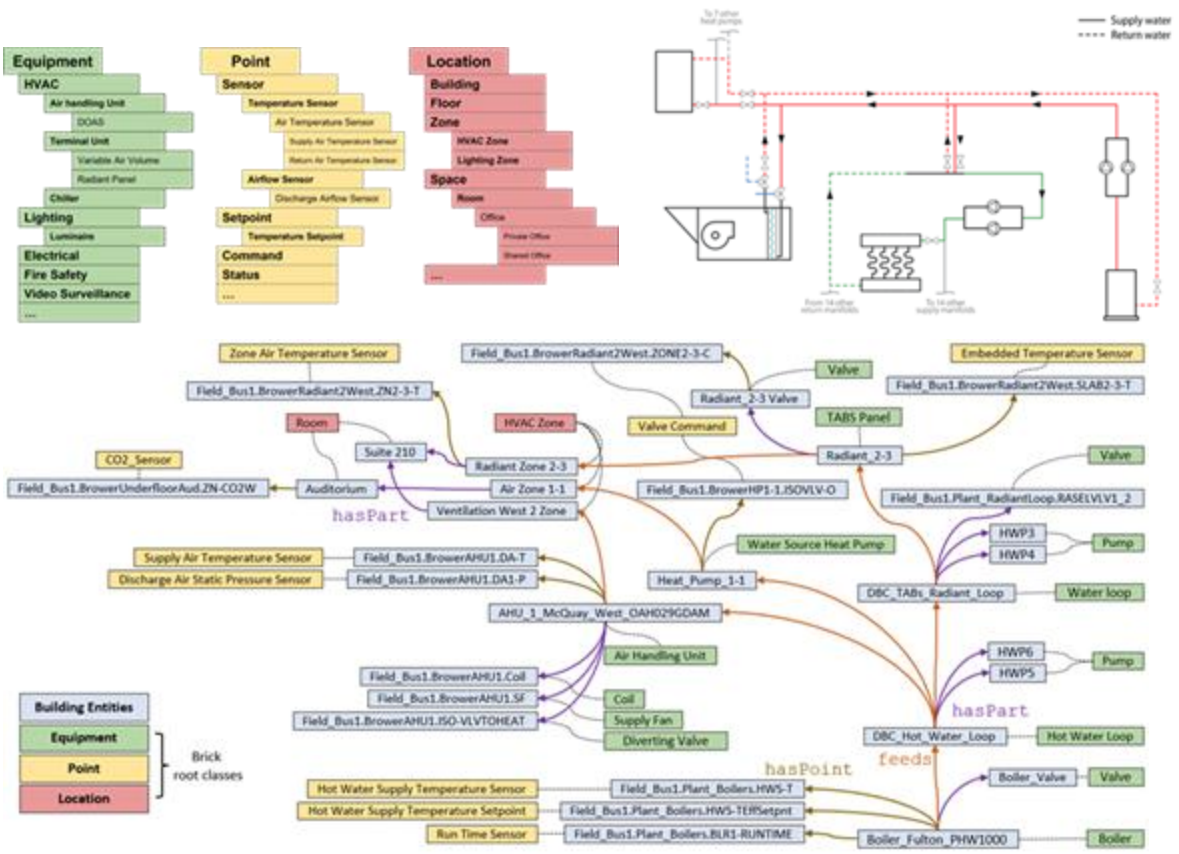

Figure 1: Diagram of Brick ontology and schematic of Site 2's hot water plant.

Top left: Excerpt of the Brick ontology class hierarchy with three root nodes (Equipment, Point, and Location). Top right: Schematic of Site 2's hot water plant. Bottom: Brick data model example for the hot water plant shown in top right figure.

Objectives

The objectives of this project are to:

1. Implement ASHRAE G36 hydronics SOOs at two test sites and evaluate energy savings.
2. Document the lessons learned from implementing G36 hydronic SOOs in existing buildings.
3. Demonstrate the proof of concept of using supervisory controls and semantic interoperability with tools such as the Brick ontology that standardizes building and HVAC system descriptions, and CDL that standardizes the control logic programming language to provide advanced HVAC controls logic.

The team successfully completed the project work and achieved all three objectives.

Methods and Approach

Field Study Buildings and Site Climate

Site 1

Site 1, located in Berkeley, CA, is a seven-floor, 141,000-square-foot (13,000-square-meter) building belonging to a major California University that primarily contains open-plan and private offices. There is also a multi-level cleanroom facility for silicon-based nanofabrication, classrooms, laboratory and workshop areas, a 149-seat auditorium, and a cyber cafe within the building. University faculty, students, and staff occupy most of the office space on floors four through seven.

Site 1 has a building-wide HVAC system with two parallel 600-ton, 2.1 megawatt chillers, which provide chilled water to the air handling units (AHU) and process loads. One chiller (CH1) is an absorption chiller that runs on excess steam from campus's cogeneration plant during summer conditions. The other chiller (CH2) is a centrifugal chiller that mostly operates during winter conditions, when the steam resource is less abundant. The chillers do not run in parallel except during the transition from the operation of one chiller to the other. The chilled water plant also contains modular chillers (CH3) to provide cooling to server rooms, in case the main chillers go down.

The chilled water plant serves 38 cooling coils in four large AHUs, two small AHUs, several computer air conditioning systems (CAC), and a fan coil unit. The chilled water plant also serves a heat exchanger that supplies cooled water for process loads in the cleanroom facility. Two of the large AHUs (AH2A and AH2B) with air-side economizers distribute air to variable air volume (VAV) terminal units in floor areas of the building not associated with the cleanroom facility, e.g., office spaces, classrooms, and the auditorium. The other two large AHUs (AH1A and AH1B) serve as a dedicated outside air system (DOAS) that distributes 100 percent outside air to nine reheat coils, which reheat the AHUs' discharge air to 68°F (20°C). The reheat coils in turn discharge air into plenums in which recirculating air handling units (RAHUs) recirculate and cool air to 70°F (21.1°C) for the cleanroom chambers. The fans in the large AHUs have variable-frequency drives. Meanwhile, the two smaller AHUs supply conditioned air to electrical rooms, while the CACs provide cooling for server rooms.

The hot water plant uses a heat exchanger connected to the campus's steam resource to supply hot water to the building. The system distributes hot water to 130 heating coils in the four large AHUs, cleanrooms' reheating coils, and the office space VAV terminal units with reheat coils. Most of the VAV terminal units with reheat coils have a discharge air temperature sensor.

Below, Figure 2 shows a schematic of the chilled water plant and Figure 3 shows one for the hot water plant.

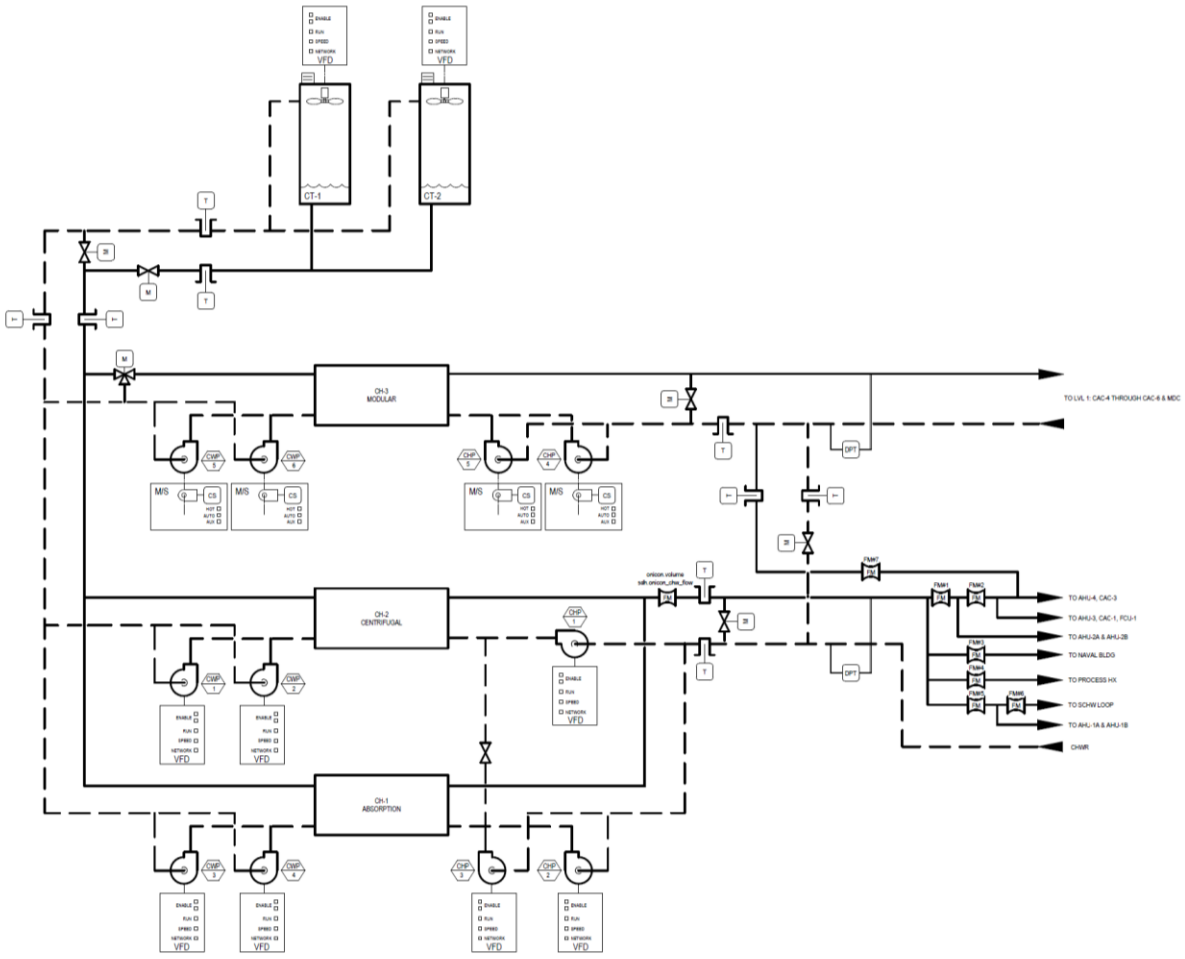

Figure 2: Schematic of chilled water plant in Site 1.

Note: The solid line indicates the supply-side pipes while the dashed lines represent the return pipes.

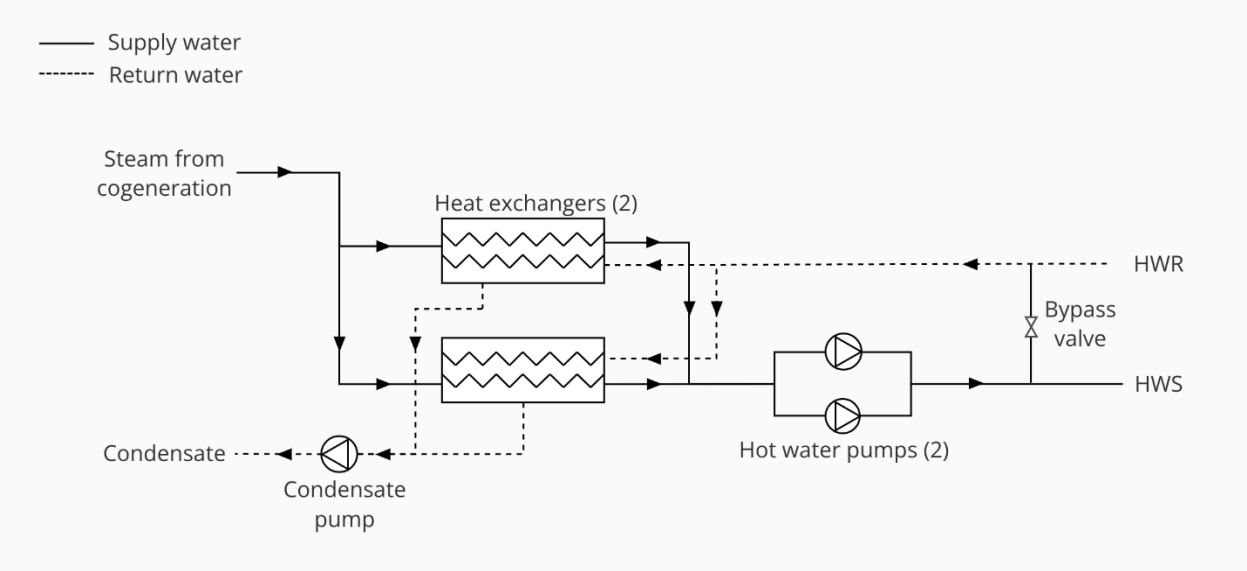

Figure 3: Schematic of the hot water plant in Site 1.

Note: The solid line indicates the supply-side pipes while the dashed lines represent the return pipes.

Site 2

Site 2 is a LEED Platinum, four-story, mixed-use building in downtown Berkeley, California. Site 2 consists of private and open-plan offices, conference rooms, an auditorium, a restaurant, and a gallery with 38,600 square feet (3,590 square meters) of conditioned area and 3,300 square feet (307 square meters) of unconditioned area. The restaurant, auditorium, and gallery are on the first floor, and office spaces are mainly on floors two through four. The restaurant's natural gas and electricity are metered separately from the Site 2's office space and are not part of the M&V analysis. The building's main tenants are nonprofit environmental organizations, with a current total building occupancy of about 150 people.

The HVAC system for Site 2 includes two gas condensing boilers for hot water, a cooling tower with a heat exchanger for cooled water, and two AHUs with underfloor air distribution system makeup the DOAS system and combined with natural ventilation through operable windows provide ventilation to Site 2. Each AHU contains a single coil with three-way valves that switch to either provide heating or cooling. Eight water-to-air heat pumps connected to the hot water loop condition the gallery, conference rooms on the first and second floors, and the auditorium. A two-pipe thermally activated building radiant system supplies heating and cooling to floors two through four.

Figure 4 shows a schematic of the hot and cool water plant. Hot water production is available 24 hours a day and each of the boilers has an input capacity of 26 Btu per hour per square foot (82 watts per square meter). The boilers have a lead-lag operation and efficiency range between 85 percent and 95 percent, depending on the operating mode and return water temperature when operating at or above the minimum turndown capability of the boilers.

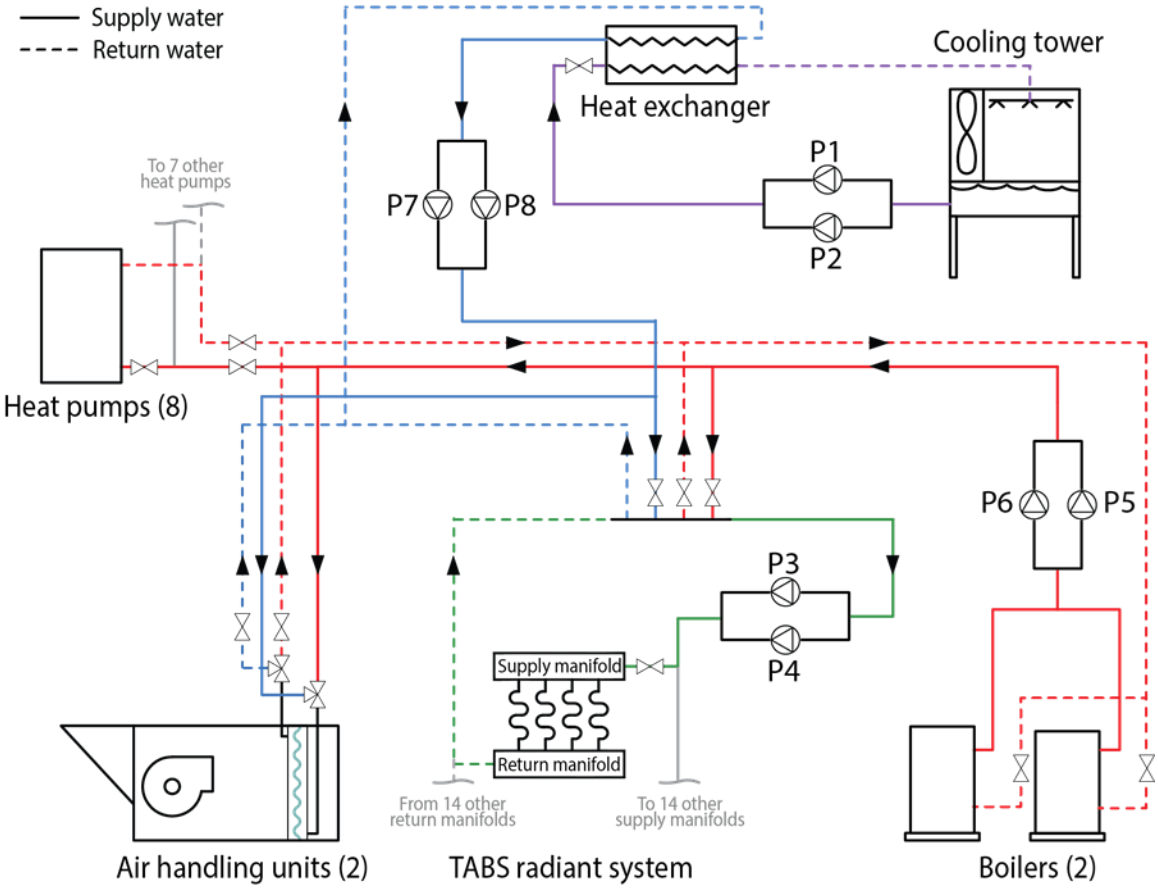

Figure 4: Schematic of the water loops at the plant level in Site 2.

Note: Colored lines represent different water loops, with hot water in red, cool water in blue, condenser in purple, and radiant system in green.

Site Climate

Berkeley, California is in California Climate Zone 3 and ASHRAE Climate Zone 3C, characterized by moderate temperatures year-round with dry summers and wet winters. Average high temperatures throughout the year range from 58°F to 75°F (14.7°C to 23.9°C), and the average low temperatures range from 42°F to 54°F (5.6°C to 12.2°C). The 99 percent winter design day has an outside dry-bulb air temperature of 34°F (1.1°C) and 1 percent summer design day of 85°F (29.4°C), with relative humidity of 65 percent.

ASHRAE G36 Implementation

ASHRAE G36 Sequence Development and Implementation

Once the research team developed the Brick data models, our G36 control intervention can be centered on it. At a high level, the team used the buildings' Brick model to query and retrieve HVAC system design information and pertinent BACnet object information to obtain the HVAC's current operating status, e.g., the valve positions in coils to infer requests for colder or hotter supply water

temperatures. The system forwards the queried information for further processing, including sending it to the CDL G36 T&R control block to calculate a new setpoint for the water plant supply water temperature. The new supply water setpoint is then deployed by writing it back to the plant equipment.

Once again, the team used Brick to retrieve the required BACnet object information so the equipment can use it. Figure 5 shows a schematic of the G36 controls implementation enabled with the Brick ontology in the demonstration buildings. In theory, the only block that needs to be replaced when porting over this controls implementation is the Brick data model for the new building. The rest of the application will remain the same.

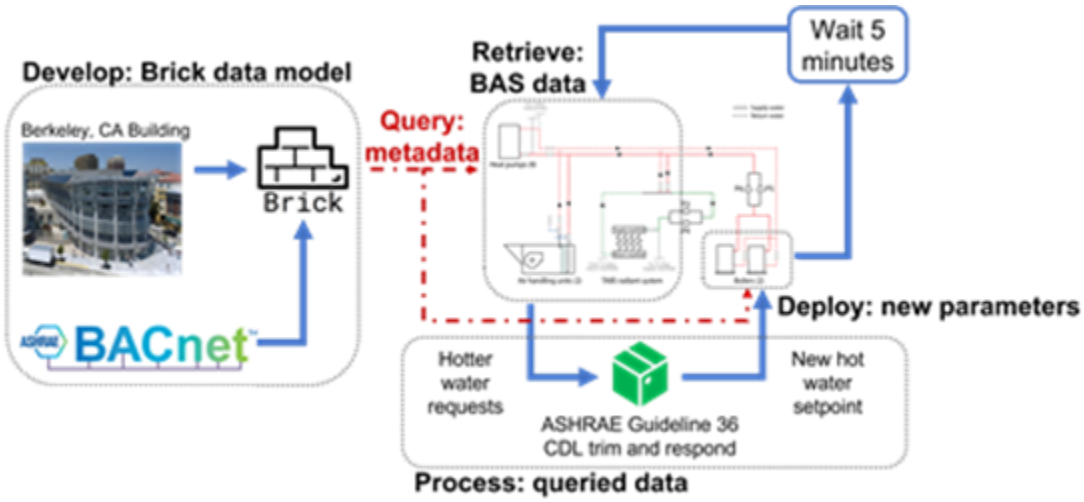

Figure 5: ASHRAE G36 schematic using Brick ontology to reset plant supply water temperature.

In our implementation, the research team developed an interactive controls application where the user can find equipment that can run the G36 sequences and specify control parameters. The basic interactive component of the control application is to demonstrate a workflow of how a user might input information so that the sequences operate within the building's needs and constraints. In the first step of this interactive control application, generalized programmatic queries search the building's Brick model for the equipment that provides the energy source for hot or chilled water. In some cases, such as in the Site 1 demonstration site, there is a secondary water loop with independent temperature control that supplies chilled water to the RAHUs. Thus, the research team added the capability to search for water loops and deploy the G36 T&R reset strategy if the water loop has temperature control.

The team used the results of this search to initiate a configuration file for the building, as shown in Figure 6. Users can now indicate which chillers or water loops they want to deploy G36 sequences. In this example implementation, users would do this by switching the "isToBeControlled" parameter to true. In the Site 1 demonstration, the team switched this parameter for CH2 and the secondary chilled water loop. Once this is done, the controls application continues by asking the temperature range the user would like to reset the supply water temperature for each equipment selected. The specific temperature range will depend on the plant or water loop that G36 reset strategy is

implemented on and reported below. At this stage, the application also queries the equipment's BACnet information to read and write its supply water temperature setpoint and stores it in memory. The controls application proceeds by identifying all end users for each equipment selected using the building's Brick data model and initializing default parameters, such as the request multiplier and the thresholds in terms of the valve positions, to consider a request for colder water and when to release the request.

It also collects BACnet information from each end user to later poll the end user's water valve position and stores the information in memory. The user has the option to customize the end user parameters if desired. After this process, the system generates a configuration file that the controls application can use directly. If the application receives the configuration at initialization, it skips the search for equipment and end users, using the information in the configuration file to set up the G36 sequence operation parameters.

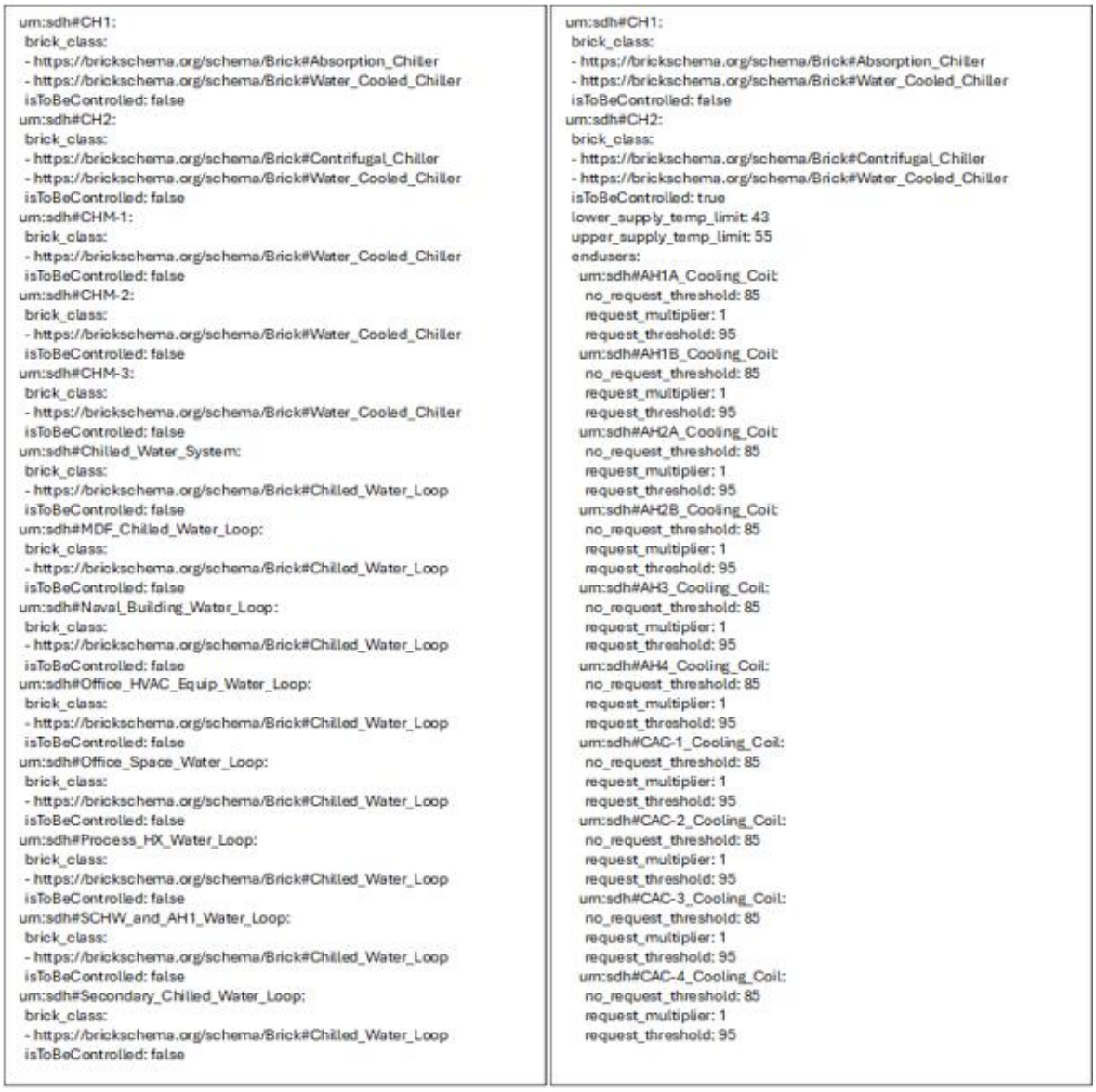

```
um:sdh#CH1:
 brick_class:
 - https://brickschema.org/schema/Brick#Absorption_Chiller
 - https://brickschema.org/schema/Brick#Water_Cooled_Chiller
 isToBeControlled: false
um:sdh#CH2:
 brick_class:
 - https://brickschema.org/schema/Brick#Centrifugal_Chiller
 - https://brickschema.org/schema/Brick#Water_Cooled_Chiller
 isToBeControlled: false
um:sdh#CHM-1:
 brick_class:
 - https://brickschema.org/schema/Brick#Water_Cooled_Chiller
 isToBeControlled: false
um:sdh#CHM-2:
 brick_class:
 - https://brickschema.org/schema/Brick#Water_Cooled_Chiller
 isToBeControlled: false
um:sdh#CHM-3:
 brick_class:
 - https://brickschema.org/schema/Brick#Water_Cooled_Chiller
 isToBeControlled: false
um:sdh#Chilled_Water_System:
 brick_class:
 - https://brickschema.org/schema/Brick#Chilled_Water_Loop
 isToBeControlled: false
um:sdh#MDF_Chilled_Water_Loop:
 brick_class:
 - https://brickschema.org/schema/Brick#Chilled_Water_Loop
 isToBeControlled: false
um:sdh#Naval_Building_Water_Loop:
 brick_class:
 - https://brickschema.org/schema/Brick#Chilled_Water_Loop
 isToBeControlled: false
um:sdh#Office_HVAC_Equip_Water_Loop:
 brick_class:
 - https://brickschema.org/schema/Brick#Chilled_Water_Loop
 isToBeControlled: false
um:sdh#Office_Space_Water_Loop:
 brick_class:
 - https://brickschema.org/schema/Brick#Chilled_Water_Loop
 isToBeControlled: false
um:sdh#Process_HX_Water_Loop:
 brick_class:
 - https://brickschema.org/schema/Brick#Chilled_Water_Loop
 isToBeControlled: false
um:sdh#SCHW_and_AH1_Water_Loop:
 brick_class:
 - https://brickschema.org/schema/Brick#Chilled_Water_Loop
 isToBeControlled: false
um:sdh#Secondary_Chilled_Water_Loop:
 brick_class:
 - https://brickschema.org/schema/Brick#Chilled_Water_Loop
 isToBeControlled: false
```

```
um:sdh#CH1:
 brick_class:
 - https://brickschema.org/schema/Brick#Absorption_Chiller
 - https://brickschema.org/schema/Brick#Water_Cooled_Chiller
 isToBeControlled: false
um:sdh#CH2:
 brick_class:
 - https://brickschema.org/schema/Brick#Centrifugal_Chiller
 - https://brickschema.org/schema/Brick#Water_Cooled_Chiller
 isToBeControlled: true
 lower_supply_temp_limit: 43
 upper_supply_temp_limit: 55
 endusers:
  um:sdh#AH1A_Cooling_Coil:
   no_request_threshold: 85
   request_multiplier: 1
   request_threshold: 95
  um:sdh#AH1B_Cooling_Coil:
   no_request_threshold: 85
   request_multiplier: 1
   request_threshold: 95
  um:sdh#AH2A_Cooling_Coil:
   no_request_threshold: 85
   request_multiplier: 1
   request_threshold: 95
  um:sdh#AH2B_Cooling_Coil:
   no_request_threshold: 85
   request_multiplier: 1
   request_threshold: 95
  um:sdh#AH3_Cooling_Coil:
   no_request_threshold: 85
   request_multiplier: 1
   request_threshold: 95
  um:sdh#AH4_Cooling_Coil:
   no_request_threshold: 85
   request_multiplier: 1
   request_threshold: 95
  um:sdh#CAC-1_Cooling_Coil:
   no_request_threshold: 85
   request_multiplier: 1
   request_threshold: 95
  um:sdh#CAC-2_Cooling_Coil:
   no_request_threshold: 85
   request_multiplier: 1
   request_threshold: 95
  um:sdh#CAC-3_Cooling_Coil:
   no_request_threshold: 85
   request_multiplier: 1
   request_threshold: 95
  um:sdh#CAC-4_Cooling_Coil:
   no_request_threshold: 85
   request_multiplier: 1
   request_threshold: 95
```

Figure 6: Query results and configuration file.

Note: The left column shows the results of a query performed on Site 1's Brick data model to search for available chillers and water loops. This initial search serves as the basis for a configuration file for the deployment of Guideline 36 sequences enabled with Brick. The right column is an **illustration of the configuration file at the end of the search for equipment and its end users with operational parameters defined.**

Once the configuration steps are complete, the controls application proceeds with performing the G36 T&R sequences at five-minute intervals. At each iteration, the application goes through each equipment's list of end users and polls their valve position, comparing the current valve position with the defined thresholds to determine the total requests for the equipment. In these demonstrations, the control system generates a request when the valve is open over 95 percent and the request is

released when the valve position is less than 85 percent. The total number of requests for each equipment is then sent to the T&R block pre-programmed with CDL and encapsulated in a FMU as described above. The T&R block then outputs a new supply water temperature setpoint that is written back to the equipment using the BACnet information queried previously in the configuration step.

SITE 1

The chilled water plant at Site 1 has undergone multiple retrofits since the initial construction, so available existing drawings and schematics were incomplete or incorrect. The project team developed a new system schematic based on detailed review of existing documentation and extensive field verification to confidently understand control requirements, as well as metering requirements for measurement and verification.

The team implemented chilled water plant reset as the primary energy measure from G36 for the chilled water plant. The plant reset uses T&R reset logic based on demand from associated chilled water valves to reset the supply temperature setpoint.

Table 1 below shows the variables used for the T&R logic and includes the parameter values implemented for different equipment and water loops in Site 1. Though the chilled water plant alternates between operating the absorption and the centrifugal chillers, this effort will only apply the control strategies when the centrifugal chiller is in operation. The team implemented chilled water supply temperature setpoint reset from 43°F to 52°F to lower chiller energy and chilled water loads by reducing pipe losses. The team did not make any other changes to the chilled water plant controls. The baseline control strategy is a fixed chilled water supply temperature setpoint of 43°F and a fixed differential pressure setpoint of 26 pounds per square inch.

During the initial review of the system operation, the team observed that some of the connected chilled water valves were continuously fully open, which they investigated and then resolved by updating the system controls. Left unresolved, the fully open valves would prevent the chilled water supply temperature setpoint from being able to reset.

Using T&R reset logic based on demand from associated hot water valves, the team reset the hot water supply temperature setpoint between 120°F to 190°F—the primary energy measure from G36 implemented for the hot water plant;

Table 1 below shows the T&R variables. As a steam-to-hot water exchanger serves the hot water system, the primary energy savings from this measure is limited to reduced pipe losses, which vary as a function of water temperature. The baseline control strategy is a fixed hot water supply temperature setpoint of 190°F.

Table 1: Trim and respond variables and parameter values for each equipment and water loop.

Variable	Definition	Centrifugal Chiller (CH1)	Secondary Chilled Water Loop	Hot Water Loop
Device	Associated device (e.g., fan, pump)	Chiller	Water loop	Water loop
SP0	Initial setpoint	43 °F	43 °F	190 °F
SPmin	Minimum setpoint	43 °F	43 °F	120 °F
SPmax	Maximum setpoint	52 °F	52 °F	190 °F
Td	Delay timer	5 minutes	5 minutes	5 minutes
T	Time step	5 minutes	5 minutes	5 minutes
I	Number of ignored requests	1	1	2
R	Number of requests from zones/systems	Actual requests	Actual requests	Actual requests
SPtrim	Trim amount	+ 0.75 °F	+0.75 °F	- 2 °F
SPres	Respond amount (must be opposite in sign to SPtrim)	- 1 °F	- 1 °F	+ 3 °F
SPres-max	Maximum response per time interval (must be same sign as SPres)	- 2.5 °F	- 2.5 °F	+7 °F

Note: The number of ignored requests (I) should be set to zero for critical zones or air handlers.

SITE 2

The hot water system at Site 2 serves a range of loads including the radiant floors, perimeter radiators, preheat coil in the dedicated outdoor air system, and supplemental heat for the water source heat pump loop. Because the two condensing boilers are staged by the internal boiler controls, rather than by the building automation system, the primary energy measure from Guideline

36 the team implemented was resetting the hot water supply temperature setpoint from 90°F to 130°F. To do this, we used T&R reset logic based on demand from associated hot water valves. The remaining T&R variables of T_d, T, I, R, $SP_{trim,}$ SP_{res}, and $SP_{res\text{-}max}$ are the same values for the hot water plant at Site 1 shown in

Table 1. The team expected this measure to improve the efficiency of the condensing boilers by reducing loop temperatures, thereby enhancing condensing performance, as well as to reduce hot water loads by reducing pipe losses. The baseline control strategy is a fixed hot water supply temperature setpoint of 130°F.

Commissioning

The HVAC system commissioning for the demonstration sites included functional testing and trend reviews.

FUNCTIONAL PERFORMANCE TESTING

The team conducted functional performance testing (FPT) to systematically test the BAS and verify that it programs the G36 SOOs correctly. This involves manually overriding the system conditions to drive the control system through the full range of expected operating conditions and evaluating the observed responses against expected responses. FPT allows HVAC system testing under artificial conditions—for example, heating system testing can occur during summer when it may not otherwise be operating.

The project team developed functional performance test scripts to evaluate chilled water and hot water temperature reset by G36 SOOs. The test scripts are Microsoft-Excel-based, with macros allowing the team to perform the test as specified, record the relevant data from the BAS to verify performance, and save any screenshots of BAS related to the reaction of performance testing for the review of test results. Detailed step-by-step instructions and training videos developed by Taylor Engineers are available in the test scripts to demonstrate how to use them.

These FPTs evaluate:

1. How the system generates number of requests for both chilled water and hot water plants when the hot water (HW) and chilled water (CHW) valve positions change.
2. Trim and respond control behavior with number of requests for both the main loop (CHW and HW) and secondary loop (CHW).
3. CHW plant reset percentage and differential pressure reset.

Members of the research team who implement G36 SOOs performed the FPTs using the scripts and shared them with the rest of the research team, who evaluated independently if the results indicated successful implementation of G36. The FPTs revealed a few minor issues that were relayed to the Lawrence Berkeley National Laboratory (LBNL) OpenBuildingControls research team to resolve for future releases of the CDL Modelica Buildings library. The minor issues included the inability to vary the timestep at which the CDL T&R block returned a new setpoint, the existence of a time delay before trimming the setpoint after reaching the maximum setpoint, and inconsistent sign conventions between the G36 text document and the CDL T&R programming.

TREND DATA REVIEW

The team performed a detailed trend data review to evaluate G36 SOOs correct implementation. The goal of this analysis is to ensure chilled water and hot water temperatures behave as expected with varying cooling and heating requests under G36 control strategy. For Site 1, both chilled water and hot water G36 SOOs operated at the same time when using rapid M&V method; therefore, the data for both systems were collected at the same time.

Data Collection

The team conducted FPT to systematically test the BAS and verify that the G36 SOOs were programmed correctly. For both demonstration sites, the research team compiled a list of required data points—as shown in Table 2 below—and evaluated HVAC plant mechanical drawings, BAS datapoints list, onsite inspections, and recent trend data to establish sensor availability, data connection availability on the BAS, trend data availability, and quality of data.

Data Points

Table 2: Data points used for G36 SOO controls and energy savings analysis.

Site/System	Data Point	Source	Unit	Sampling Interval	Use
Site 1 – CHW plant	CHW pump 1, 3, CW pump 1,2 power	BAS	kW	5 minutes	Energy savings
	Chiller 2 power	BAS	kW	5 minutes	Energy savings
	Cooling tower 1, 2 power	BAS	kW	5 minutes	Energy savings
	CHW sup/ret temperature	BAS	F	5 minutes	Energy savings
	CHW flowrate FM 1, 3, 4, 5	BAS	GPM	5 minutes	Energy savings
	Supply chilled water temperature setpoint	BAS	F	5 minutes	G36
	CHW end-user water valve positions	BAS	%	5 minutes	G36
Site 1 – HW plant	Sup/Ret HW temperature	BAS	F	5 minutes	Energy savings
	HW flowrate	TRC-installed Dynasonic meter	GPM	1 minute	Energy savings

Site/System	Data Point	Source	Unit	Sampling Interval	Use
	HW pump 1, 2 power	BAS	kW	5 minutes	Energy savings
	Supply hot water temperature setpoint	BAS	F	5 minutes	G36
	HW end-user water valve position	BAS	%	5 minutes	G36
Site 2 – HW plant	Building natural gas use	TRC-installed VataVerks meter and utility meter data	Rotations/ CCF	5 minutes (Vata), 1 day (utility)	Energy savings
	HW pump 5, 6 operation time	BAS		5 minutes	Energy savings
	Supply hot water temperature setpoint	BAS	F	5 minutes	G36
	HW end-user water valve position	BAS	%	5 minutes	G36

BAS Meter Validation

SITE 1

The team implemented ASHRAE G36 SOOs in both the chilled water plant and hot water plant at Site 1. Table 3 below summarizes the data points that the team field validated. The team also used additional measurements, such as using the Fluke power quality logger, Flexim flow meter, and a thermistor for power, flow rate, and temperature. We compared these values with BAS readings to identify potential metering issues and during the field validation, tested a range of flow and pump power conditions by changing the pump speeds through VFDs.

Table 3: Field-validated data points at Site 1.

System	Data Point	Validation Method	Results
Site 1 – CHW plant	CHW, CW pump power	Fluke power quality logger	No issues
	Cooling tower fan power	Fluke power quality logger	No issues
	CHW sup/ret temperature	External thermistor	No issue
	CHW flowrate	Flexim ultrasonic meter	Didn't match with main BAS flow meter reading. Further testing found sum of four downstream meters to be accurate.
Site 1 – HW plant	HW pump power	Fluke power quality logger	No issues

Hot water flow rate is not measured at Site 1; therefore, the research team installed an external clamp on flow meter that measures the flow rate and saves data into a cloud drive for remote access, which is described in the Findings section of this report. The team also considered using a steam-side heating energy calculation. While steam flow rate was available, temperatures were not; due to this, as well as the known accuracy issues in typical steam meters, we decided to use the hot-water-side calculation using flow rate and temperatures. For the G36 implementation, the research team evaluated heating and reheat coil valve operation and tuned the reheat coil valves to improve temperature stability, which is also discussed in Findings.

SITE 1 CHILLED WATER FLOW RATE VERIFICATION

As part of meter verification, the research team identified the need to field verify total chilled water flow rate at Site 1. As seen in Figure 6, there are multiple flow meters, and the team wanted to ensure that the summing of the correct flow meters captured the total flow rate. For this validation, the research team temporarily installed a Flexim Fluxus F601 clamp on an ultrasonic flow meter before any branching on the CHW pipe near the chiller. The team used the chilled water return line because it had a length of straight pipe required for the flow meter's accuracy. While the flow meter was installed and recording data, the team changed the chilled water pump speeds from 100 percent down to 70 percent (typical operating range) and measured the flow rate through the clamp-on flow meter and plant flow meters. The chiller plant includes an Onicon flow meter that measures the total chilled water flow rate shown in Figure 6 below, which is a section of the chilled water schematic shown in Figure 2. However, the team observed differences up to 21 percent between this meter and the Flexim meter for different pump speeds and concluded that this meter does not measure the total flow rate correctly.

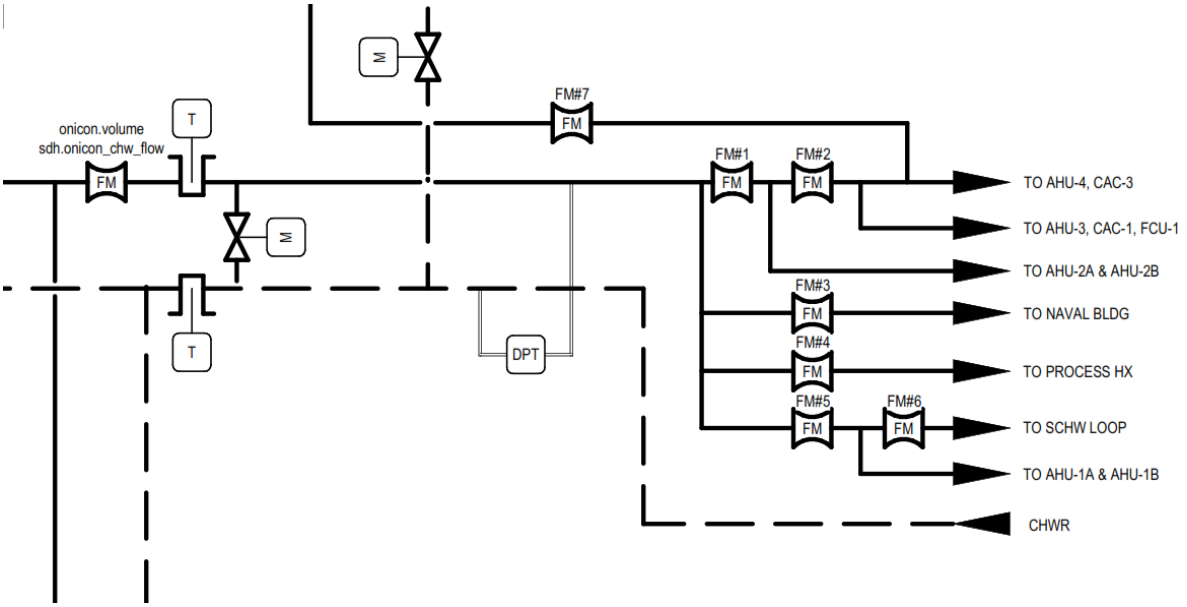

Figure 6: Schematic section of the flow meters in Site 1 chilled water plant.

Note: See Figure 2 for full schematic.

The research team identified that summing the downstream flow meters 1, 3, 4, and 5 provides the total chilled water flow rate, and that this agrees with the clamp on ultrasonic flow meter within 2 percent; Figure 7 shows the comparison of the measured flow rate from the two methods. The team used readings from flow meters 1, 3, 4 and 5 for calculating cooling energy (thermal).

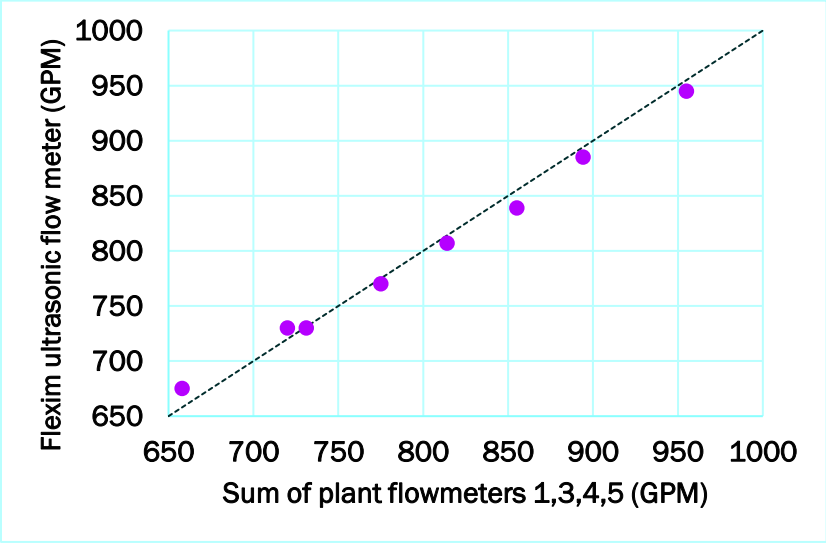

Figure 7: Comparison of total chilled water flow rate from clamp-on Flexim ultrasonic flow meter and the sum

of plant flow meters 1, 3, 4, and 5.

SITE 2

The team implemented G36 SOOs in the hot water plant at Site 2. They evaluated the hot water supply and return temperatures, flow rate, hot water pump speed and status, and outside air temperature for M&V purposes. The data values were reasonable, with some common historical data gaps due to BAS trending being offline or sensor issues that have since been fixed. In addition, the building had historically turned off the boiler used to generate hot water for space heating during the summer months. The team decided no specific meter validation was required due to the quality of historical trend data, as well as recent studies conducted in the same building. However, we identified two issues:

1. There is a lack of hot water pump power data. Hot water pump power was not monitored at Site 2, but the pumps were small, with a capacity of 0.5 horsepower, and historical data suggested they mostly operated at the full load. Therefore, the team decided to use the pump speed percentage and speed-power relationship to calculate total power and energy use for M&V. We used the following equation to calculate the pump power (kW).

$$Pump\ Power\ (kW) = 0.7456\left(\frac{kW}{HP}\right) \times 0.5HP\ \times (\%Speed)^3$$

2. The natural gas usage was not available through the BAS due to a connectivity issue. After investigating the connectivity, the team decided to install an external natural gas meter, which is further discussed in the New Meter Installation and Validation section below.

New Meter Installation and Validation

SITE 1 HOT WATER FLOW RATE MEASUREMENT AND NEW FLOW METER INSTALLATION

The Site 1 hot water plant does not measure the hot water flow rate, which made calculating heating energy use in the building challenging. The team decided to install a clamp-on ultrasonic flow meter for the duration of the project to measure the hot water flow rate.

The team acquired a Dynasonic TFX-5000 ultrasonic clamp-on flow meter and conducted lab tests to verify flow measurement accuracy for flow rates between 45 to 70 gallons per minute (GPM), which is typical range. In addition, the meter was factory calibrated for flow speeds of up to 20 feet per second, which translates to up to 3,000 GPM in an 8-inch diameter pipe. The research team installed this flow meter on the return line pipe of the hot water loop, captured the data, and transferred it via cellular modem to a cloud storage that is accessible remotely.

SITE 2 NATURAL GAS METERING AND EXTERNAL METER INSTALLATION

Natural gas meter data at Site 2 was not available through the BAS, so the team decided to install an external meter to capture the natural gas usage. The building has a Dresser gas flow meter, and the team installed a VataVerks VV-302-02-R wireless rotary gas meter monitor at the existing meter, coupled with a HOBO data logger to collect the pulse data captured by the VataVerks meter. We periodically retrieved the data from the HOBO data logger via wired connection to a computer.

Measurement and Verification

Energy Consumption Data Collection and Calculation

SITE 1 – CHILLED WATER PLANT

Energy consumption calculation at the chilled water plant at Site 1 required two types of energy uses: cooling energy through a water-side calculation and power use of the chiller, chilled water pumps, condenser water pumps, and cooling tower fans. Table 4 summarizes the data type requirement, energy consumption field, and M&V approach. The team separately evaluated energy use for water cooling energy and plant equipment (chiller, pumps, fans) energy listed in the table by using the standard International Performance Measurement and Verification Protocol (IPMVP) procedure. The chilled water cooling energy included process loads for the laboratory equipment, as well as space cooling. The team assumed that these process loads stayed constant over the total M&V period.

Table 4: Summary of data used and M&V approach for chilled water plant at Site 1.

Energy End Use	M&V Method	Data Points Used
Chilled water cooling energy	IPMVP Op B: Retrofit isolation	Chilled water supply/return temperature $T_{CHW,sup}$, $T_{CHW,ret}$ (F), chilled water flow rate FM 1,3,4,5 $Q_{FM1,2,4,5}$ (GPM), outside air temperature T_{OA} (F)
Chiller, chilled/condenser water pump, and cooling tower fan energy	IPMVP Op B: Retrofit isolation	Chiller $P_{CHILLER}$, CHW pump 1,3 $P_{CHW1,3}$, CW pump 1,2 $P_{CW1,2}$, CT 1,2 fan power $P_{CT1,2}$ (kW), site outside air temperature T_{OA} (F)

Chilled water cooling energy consumption (power) was calculated using the water-side data of calculated total flow rate ($\hat{Q}_{CHW,Tot}$), while temperature differences were calculated using the equation below, where $\hat{P}_{cooling}$ is the calculated cooling power, ρ is the water density, and $T_{CHW,sup}$ and $T_{CHW,ret}$ are the water supply and return temperatures. Power was integrated over time to calculate the total energy consumption for a given timeframe.

$$\hat{Q}_{CHW,Tot} = Q_{FM1} + Q_{FM2} + Q_{FM4} + Q_{FM5}$$

$$\hat{P}_{cooling} = \hat{Q}_{CHW,Tot} \times \rho \times \left(T_{CHW,ret} - T_{CHW,sup}\right)$$

The team used cooling energy consumption and outside air temperature to develop regression models that accounted for weather changes and the day of the week for both the intervention and baseline. These regression models also estimated energy savings of G36 compared to the baseline.

Plant equipment power was the sum of power of the chiller, chilled water pumps, condenser water pumps, and cooling tower fans.

$$\hat{P}_{Equip.} = P_{CHILLER} + P_{CHWP1} + P_{CWP1,2} + P_{CT1,2}$$

Similar to the cooling energy models, the team used chiller, pumps, fan power and energy measured, and outside air temperature to develop regression models, considering the weather and the day of the week for both the intervention and baseline to estimate energy savings of G36.

SITE 1 – HOT WATER PLANT

The hot water plant at Site 1 uses campus steam, which is supplied to a heat exchanger to produce hot water. The team calculated the heating energy use in the building through hot water temperatures and flow rates, and Table 5 summarizes the data type requirement, energy consumption field, and the M&V approach. We separately evaluated energy use for water heating energy and pump energy listed in the table, as the pump energy is expected to increase due to higher hot water flow rate.

Table 5: Summary of data used and M&V approach for hot water plant at Site 1.

Energy End Use	M&V Method	Data Points Used
Hot water heating energy	IPMVP Op B: Retrofit isolation	Hot water supply/return temperatures $T_{HW,sup}$, $T_{HW,ret}$ (F), hot water flow rate Q_{HW} (GPM), outside air temperature T_{OA} (F)
Hot water pump energy	IPMVP Op B: Retrofit isolation	HW pump 1,2 energy $P_{HWP1,2}$ (kW), site outside air temperature T_{OA} (F)

The team calculated hot water heating energy consumption (power) using the water flow rate and the temperature difference using the equation below.

$$\hat{P}_{heating} = Q_{HW} \times \rho \times (T_{HW,sup} - T_{HW,ret})$$

We used energy consumption data to develop regression models to account for outside air temperature and the day of the week for both the intervention and baseline strategies.

Similarly, the team used hot water pump power $P_{HWP1,2}$ to calculate pump energy use and savings.

SITE 2

Energy consumption calculation in the hot water plant of Site 2 required two types of energy uses: In addition to energy-use-related data, the team collected outside air temperature data to develop M&V regression models. Table 6 summarizes the data type requirement, energy consumption field, and M&V approach. Heating energy consumption was calculated using natural gas usage ($Q_{Nat\ gas,Tot}$) in hundred cubic feet per minute (CCF/min), where the team assumed a standard energy density ($U_{Nat\ gas}$) of natural gas using the equation below. Total natural gas usage monitored at the building level was used by the two space-heating boilers, as well as by a separate boiler that generated domestic hot water (DHW).

Since the boilers used for domestic hot water were turned on continuously, the team used the days where the boiler for space heating was turned off, such as during summer and winter breaks, to determine the average natural gas usage for DHW ($\tilde{Q}_{Nat\ gas,DHW}$). We found that daily natural gas usage for DHW is consistent between days and small compared to the space heating boiler natural gas usage. The team decided not to adjust for the DHW-related natural gas usage but removed the days when the space heating boiler was turned off completely due to building closures or boiler breakdowns from the analysis.

$$\hat{P}_{Nat\ gas} = \hat{Q}_{Nat\ gas,Htg} \times U_{Nat\ gas}$$

To estimate the savings of G36 SOOs over the baseline conditions, the team used natural gas energy consumption data to develop regression models that normalized for weather conditions and the day of the week for both the intervention and the baseline.

Table 6: Summary of data used and M&V approach for hot water plant at Site 2.

Energy Consumption Type	M&V Method	Data Points
Building natural gas energy	IPMVP Op C: Whole facility	Building natural gas consumption (CCF/min), outside air temperature (F)
Hot water pump energy	IPMVP Op B: Retrofit isolation	Hot water pump speed (%), site outside air temperature (F)

The electricity savings used the formula below to determine the energy consumption of the pump, which the team considered reasonable approach, as the hot water pumps are only 0.5 horsepower and were rarely observed to operate at partial load.

$$P_{HW,pump} = \left(\frac{0.7456\ kW}{HP}\right)(Pump\ HP)(\%Speed)^3$$

For electricity consumption, the team will develop separate regression models that normalize the energy use for the site conditions—e.g., weather, time of the week, etc.—and use these models to estimate the energy savings when the proposed measures are implemented.

DATA COLLECTION AND QUALITY CHECK

The Simple Measurement and Actuation Profile (sMAP) tool recorded the trend data above meters at both sites. sMAP captured data from the BAS and stored it in a cloud that the team can access remotely, and from which they can periodically download data to a local drive for analysis and quality assurance. The team will check for the range of values, outliers, and repeated values for each data type to identify poor accuracy or erroneous sensors. Table 7 below summarizes the data cleaning solutions we will conduct for the anticipated data quality issues.

Table 7: Data quality issues and possible solutions.

Source	Data Quality Concern	Potential Solution
Data acquisition connectivity	Short – intermittent data gaps	Linear interpolation
Data acquisition connectivity	Large – intermittent data gaps	Regression/ omit timeframe
Sensor failure	Poor accuracy	Data source alternative sensor correction
Building behavioral change	Non-routine events/non-routine adjustments	Engineering adjustment/ omit timeframe

Rapid M&V Procedure

The measurement and verification (M&V) used in this project leverages a novel method that randomly switches between the existing control sequence—i.e. the baseline—and a new control sequence—i.e. the intervention—each day (Raftery, Zou, Parkinson, & Hancock, 2023). Therefore, this method is ideal, albeit limited, for determining the savings of a retrofit that can be switched on and off, e.g. most control retrofit. Conventional M&V requires a 12-month baseline measurement and another 12-month intervention measurement, and though it has a broader application, that means it takes 24 months to estimate energy savings. It is also inherently vulnerable to incurred errors due to changes in building operation that are unrelated to the measure being studied. The team chose not to adjust for the DHW-related natural gas usage but excluded the days when the space heating boiler was completely turned off due to building closures or boiler breakdowns from the analysis. This study demonstrates that by using the novel randomized method, a building analyst can estimate control retrofit savings more rapidly and reliably.

The novel M&V method is based on a randomized block experimental design where confounding variables such as day-of-week variables are accounted for—i.e., blocked. In other words, the novel M&V produces a control implementation schedule for a given blocking period that ensures not only sampled baseline days and intervention days are equal in total but also ensures that each day of the week is sampled equally between the two strategies. After the schedule is generated, the analyst can sequentially evaluate the collected measurements to inform whether a target effect of the intervention has been detected through statistical hypotheses test, such as a t test. This allows an early report of M&V results with any given desired uncertainty level.

As mentioned, the randomized schedule consists of the existing baseline control strategy discussed in the ASHRAE G36 Sequence Development section and the proposed G36 T&R control. The method randomly samples one strategy at 50 percent/50 percent probability at each sampling interval at 00:01 a.m. Although most of the buildings can sample at daily intervals (such as the rapid M&V implementation at Site 1, which switches at one-day intervals), this isn't true for all buildings. Those with thermal mass radiant systems like Site 2 need to sample at a three-day interval to account for the lingering results of the previous implemented strategy, which is commonly known as "carryover

effect." Therefore, the team sampled between the baseline and the intervention daily for Site 1, but sampled every three days for Site 2, with non-consecutive days dropped. In the context of building mechanical systems, due to the substantial thermal storage in Site 2, any operational strategy sampled would continue to influence the system's performance even after it switched. Therefore, selecting a longer sampling interval allowed the analyst to drop or exclude non-consecutive data points from the analysis. For example, a three-day sampling interval allowed the analyst to drop the first non-consecutive day—i.e., the "washout" day—and include the following day in the analysis, though this meant losing one-sixth of all samples.

The team generated a randomized switchback schedule for Site 1 starting on July 22, 2024, and another randomized schedule for Site 2 starting on November 1, 2024.

Energy Savings Analysis

The team conducted energy savings analysis using the trend data for energy use between the baseline control strategy and G36 intervention, for which we used standard IPMVP procedures. We also conducted an initial data quality check and a preliminary check on energy consumption calculations to identify issues and compare against the expected patterns. The team then extended this to the full M&V analysis, presented in the Findings section below.

REGRESSION MODEL DEVELOPMENT

The team developed regression models associated with the two strategies being evaluated: baseline conditions and interventions (ASHRAE G36) for the plants and subsystems in the two demonstration buildings.

Starting on the date of implementation, the strategies alternated as described in the rapid M&V procedure to allow the team to capture the performance of the system while operating under the different strategies. We separately used the resulting data to develop baseline and intervention regression, using the Time-of-Week and Temperature (TOWT) approach to model each strategy.

An example regression equation is shown below.

$$E_i = \alpha_i + \sum_{j=1}^{6} \beta_j T_{c,j}(t_i) + \sum_{k=1}^{n} \gamma_k S_k$$

Where:

E_i = Energy consumption at time interval i
t_i = i^{th} time interval
$T_{c,j}(t_i)$ = Component temperature computed based on algorithm
α_i = Coefficient for time of day and week estimated by regression
β_j = Coefficients for component temperatures estimated by regression
γ_k = Coefficients for independent variables
S_k = Independent variables (e.g., number of occupants, thermostat setpoints)

The research team followed modeling best practices and aimed to collect a dataset that included the maximum range of energy and independent variable values. We assessed the model accuracy for different energy use data separately and judged them using the following targets for the coefficient

of variation of the root-mean-square error (CVRMSE), based on ASHRAE Guideline 14 (ASHRAE, 2023) and normalized deviation of the bias error (NDBE):

- CVRMSE: Less than 30 percent when using hourly or sub-hourly data, and less than 20 percent when using daily data
- NDBE: Less than 0.005 percent

ONE-TAILED HYPOTHESIS TEST

The team used a one-tailed hypothesis test to compare the measurement distribution of the two sampled control strategies. The null hypothesis is stated as follows: the mean daily energy usage sampled from the intervention measurement set is greater than or equal to the mean daily energy usage sampled from the baseline measurements (H_0: $\mu_{interv} \geq \mu_{base}$).

The alternative hypothesis, which describes the target effect, is stated as: the mean daily power usage sampled from intervention measurement set is less than the mean daily power usage sampled from the baseline measurements (H_a: $\mu_{interv} < \mu_{base}$).

By comparing the test statistic specifically—the p-value—an analyst can evaluate whether there is sufficient evidence to reject the null hypothesis in favor of the alternative. In this context, a low p-value (typically < 0.05) indicates that the observed energy savings are statistically significant and unlikely to have occurred by random chance. A p-value below the chosen significance level supports rejecting H_0, thereby validating that the intervention (G36) results in lower average energy use compared to the baseline. Conversely, a high p-value suggests that the observed differences may not be statistically distinguishable, and the null hypothesis cannot be confidently rejected.

ESTIMATED NORMALIZED ANNUAL ENERGY CONSUMPTION

To estimate normalized annual energy consumption, the research team used the Time-of-Week and Temperature (TOWT) regression model in conjunction with typical meteorological year (TMY3) (NREL, 2020) weather data. Specifically, the model calculated predicted energy consumption for each 15-minute interval over a full calendar year using TMY3 outside air temperature as input. Because the TOWT models were developed using measured data that may not span the entire temperature range represented in the TMY3 dataset, certain periods required extrapolation beyond the model's original training range. As shown in Figure 1, some TMY3 temperature values fall outside the observed temperature range in the demonstration period. While this introduces some uncertainty, the TOWT model framework is designed to provide reasonable extrapolations based on the underlying time-of-week and temperature-response patterns captured during the training phase. This approach enables a standardized comparison of energy performance across different strategies under consistent weather conditions.

Findings

Overview

This section presents the findings from the G36 implementation and challenges, energy and cost savings analysis, and a brief discussion on the research team's thoughts on market scalability of G36 hydronic sequences in existing commercial buildings.

Energy and Cost Savings Analysis section includes a detailed summary of the energy consumption comparison, regression model results, and normalized annual energy consumption between strategies and the potential of G36 sequences, as well as related retrofit efforts to save energy and cost.

G36 Sequences Implementation and Plant Optimization

Table 8: Status and timeline for G36 implementation and M&V data collection.

	Implementation and Cx	M&V Data Collection
Site 1: HW	Completed 07/2024	7/22/2024 – 9/30/2025
Site 1: CHW	Completed 11/2024	11/1/2024 – 9/30/2025
Site 2: HW	Completed 11/2024	11/15/2024 – 9/30/2025

The research team encountered several challenges deploying G36 CHW plant sequences in Site 1, which serves both a critical nanofabrication facility and non-critical office spaces. The cleanrooms in the nanofabrication facility have strict environmental control requirements, 68°F space temperature and 55 percent ±5 percent relative humidity, which initially appeared incompatible with G36 supply water reset strategies aimed at improving energy efficiency.

After conducting psychrometric analysis and temperature testing, the team proposed the following initial modifications:

1. Raise cleanroom space setpoints from 68°F to 72°F.
    a. Keep reheating coils' discharge setpoint at 68°F.
    b. Raise recirculated air handling units' discharge setpoints from 68°F to 72°F.
2. Lower AH1A and AH1B preheat coil leaving air temperature setpoints from 55°F to 50°F.
3. Increase AH1A and AH1B dewpoint setpoints from 45°F to 55°F.

The team implemented these changes on March 22, 2024, with facility manager approval and a caveat to revert if necessary. The goal was to enable G36 control sequences while maintaining cleanroom conditions of 72°F ±2°F and 55 percent ±5 percent relative humidity. The initial control changes led to elevated cleanroom temperatures and performance issues with nanofabrication tools. Although lowering the AHU discharge setpoint to 70°F helped, the increased dewpoint setpoints caused unstable relative humidity, prompting a return to the original 45°F by June 2024. This limited the ability to reset the chilled water supply temperature and reduced potential energy savings from G36. To address the humidity instability, the team identified and corrected unstable

discharge air temperatures in the cleanrooms' recirculated AHUs by retuning their reheating coils' Proportional-integral-derivative (PID) controls using methods outlined in (Lin, et al., 2023).

It was a laborious and complex process to find a set of parameters that worked well at both the maximum (190°F) and minimum (120°F) temperatures in the hot water plant. With improved temperature control, the team proposed a more moderate dewpoint increase to 50°F to balance relative humidity stability with energy saving potential. Facility managers approved this revised plan, enabling a second attempt at G36 deployment. Table 9 shows the evolution of temperature and dewpoint setpoints from pre-demonstration to current baseline conditions. As discussed in the section Energy Savings from Plant Optimization, this resulted in 14.6 percent savings in the chilled water plant thermal energy consumption.

Table 9: Summary of temperature and dewpoint setpoints pre-demonstration vs. baseline condition.

Operational Change Date and Reason	Space thermostat (°F), Relative Humidity Setpoint (%)	RAHU SAT Setpoint (°F)	AH1A & AH1B Leaving Air setpoint (°F)	AH1A & AH1B Dewpoint Setpoint (°F)
Pre-demonstration, set by facility manager.	68°F, 55% +/- 5%	68	68	45
Team suggested to improve energy performance, March 2024. Resulted in nanofab tool performance issues unacceptable to facility manager.	72°F +/- 2°F, 55% +/- 5%	72	68	55
Facility manager changes to improve operation, May 2024.	72°F +/- 2°F, 55% +/- 5%	72	68	45
Team suggested to meet operational requirements and improve energy performance, September 2024.	72°F +/- 2°F, 55% +/- 5%	72	68	50

Initial findings from this field demonstration suggest that G36 sequences may not be well-suited for facilities with tight humidity control requirements. Unlike typical commercial spaces where thermal demand varies with occupancy and weather, cleanrooms often experience constant loads, limiting the flexibility of control strategies. However, the demonstration revealed that implementing G36

sequences often requires first identifying and resolving major issues in the existing building systems, followed by reassessing G36's suitability. For example, a psychrometric analysis for the demonstration building indicated that raising the dewpoint setpoint could yield energy savings under certain outdoor conditions—specifically when the outdoor dewpoint is below the AHU's setpoint (e.g., 50°F).

However, applying this strategy in practice may present challenges not captured in idealized models, such as sensor drift, aging controls, and imperfect actuators. These real-world limitations can compromise setpoint stability and overall Energy Savings from Plant Optimization. Ultimately, G36 should only be pursued in sensitive applications after verifying that the system is reliable and capable of supporting its advanced control logic. The project team also faced a G36 deployment challenge in the Site 2 building. On several occasions, the boilers would not meet the hot water setpoint written by the G36 T&R controls, which Site 2's facility management team believes was due to issues with the boilers' burner controller. Site 2 facility management would perform a manual reset of the burner controller to correct the issue, but it reappeared a few more times at seemingly random intervals, increasing uncertainty for M&V calculations.

Energy and Cost Savings Analysis

The research team used IPMVP Option B (Retrofit Isolation with All Parameter Measurement) and IPMVP Option C (Whole facility) to quantify energy savings for Site 1 and Site 2 respectively. Differences in energy were wholly attributable to the retrofit.

The team determined two sets of energy usage results, as described below.

1. **Measured energy usage difference:** In this approach the team compared the raw measured energy consumption data for baseline and G36. Due to the use of rapid M&V, the research team believes that the two data sets are comparable since outside air temperature and building operation variations are small between days. However, the team performed further analysis using TOWT models to account for the (small) differences in weather conditions encountered on the days when one or the other control strategy was operating.

2. **Normalized energy usage estimation:** In this approach, the team applied typical weather data to the models described in the approach above over a year to determine energy use and savings during a typical year.

   The weather and building operation conditions are expected to be similar between the two strategies, especially due to the use of rapid M&V. However, the team looked at weather normalization for typical weather data over a year for a more comprehensive comparison, and to allow for normalization to a typical meteorological year.

Weather Conditions

Figure 8 and Figure 9 below show the outside air temperature distribution for baseline and G36, and for typical weather data from TMY3 dataset. Overall, the M&V period covers most of the typical outside air temperatures, with similar density of hours in each temperature range. The monthly variation of outside air temperatures during the M&V period behaves as expected based on the TMY3 data, where the months of August and September represent the warmest weather as expected in Berkeley, California.

TMY3 data also has cooler conditions that neither baseline nor intervention cover, with temperatures below 5°C (approximately 40°F) not represented in the M&V period. The team believes that the M&V period fell on a slightly warmer winter than the TMY3 data, which averages data from 1976 to 2005.

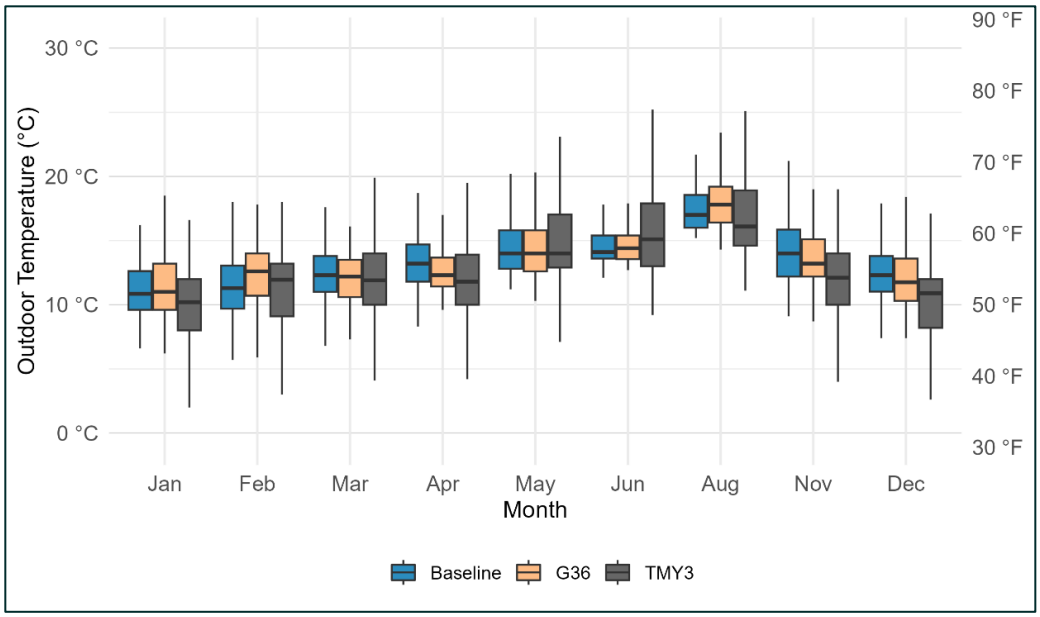

Figure 8: Distribution of outside air temperature by month for measured baseline, measured G36, and TMY3 data.

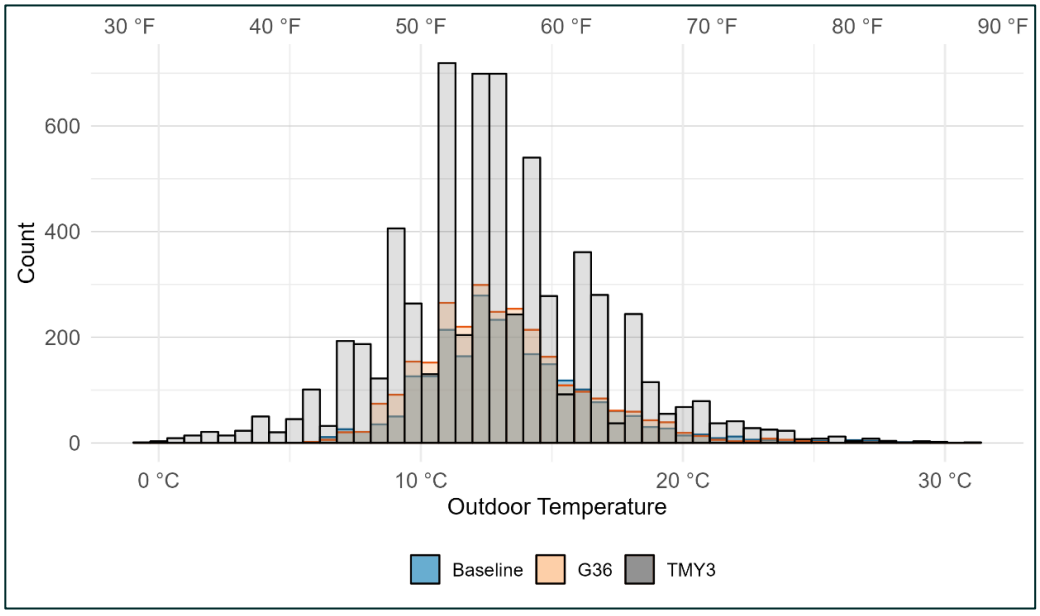

Figure 9: Outside air temperature distribution histogram for measured baseline, measured G36, and TMY3 data.

Energy Consumption Analysis – Site 1 Chilled Water Plant

The research team implemented a rapid M&V schedule, which randomly alternated between baseline and G36 strategies; the resulting distribution of these two strategies is nearly equal. Below, Figure 10 shows the number of days each strategy was run for each day of the week, while Figure 11 presents the daily average energy usage with the control strategy (baseline or G36) indicated by color, illustrating how both strategies were applied across various weather conditions and building operational states (e.g., weekdays vs. weekends) throughout the M&V period. This distribution ensured that both baseline and intervention strategies were representative of a broad range of environmental and operational conditions, contributing to a more comprehensive assessment.

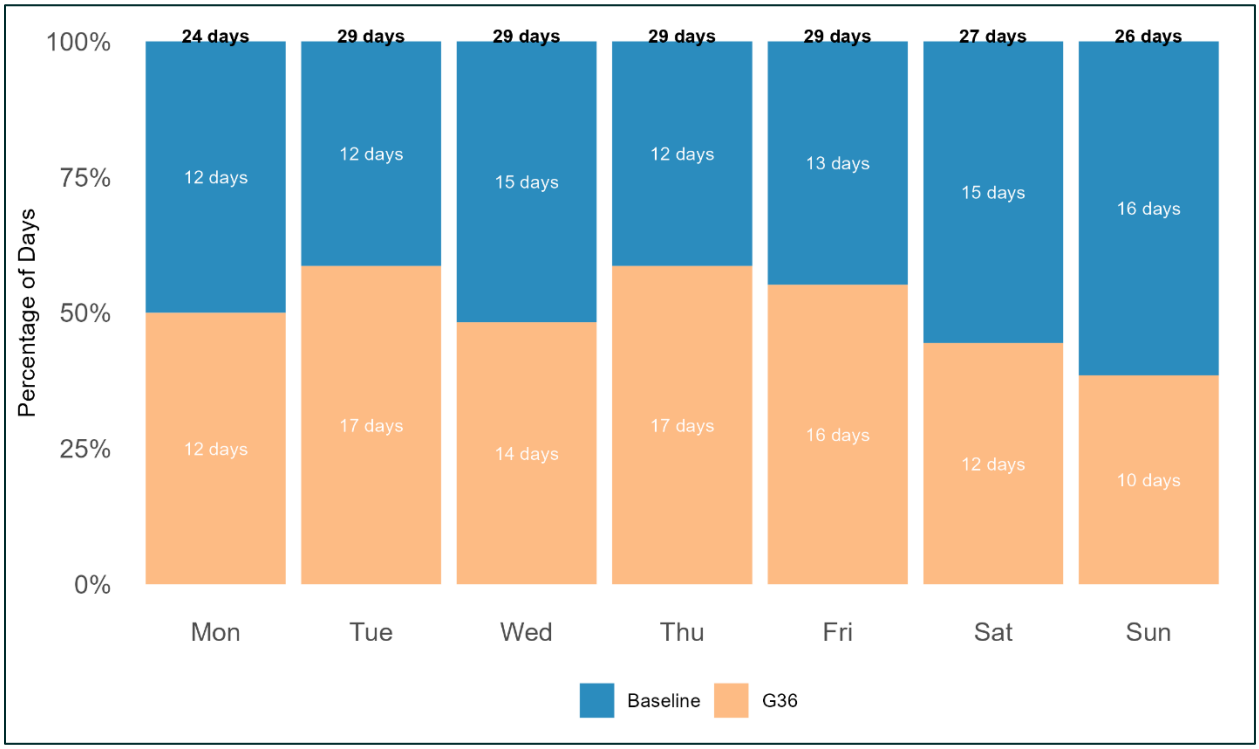

Figure 10: Rapid M&V schedule: Comparison of number of days sampled by different strategy

The baseline condition maintained a fixed supply water temperature of 43°F, whereas the G36 strategy employed a reset logic that modulated supply water temperature between 43°F and 52°F using a trim and respond approach. Table 11 illustrates the distributions and hourly averages for supply chilled water temperature and flow rate under both conditions.

Under the G36 strategy, the supply water temperature consistently remained higher than in the baseline condition. This increase in temperature corresponds to reduced electrical energy use by the chiller. Conversely, the chilled water flow rate was higher in G36, indicating a slight increase in chilled water pump energy use. As shown in Figure 11, flow rate trends moved inversely to the temperature profile to cater to a similar level of cooling demand within the building.

Despite the slightly higher pump energy use under G36, the overall electricity consumption was lower. This outcome reflects the fact that the increase in pump energy was marginal compared to the substantial energy savings achieved through reduced chiller operation.

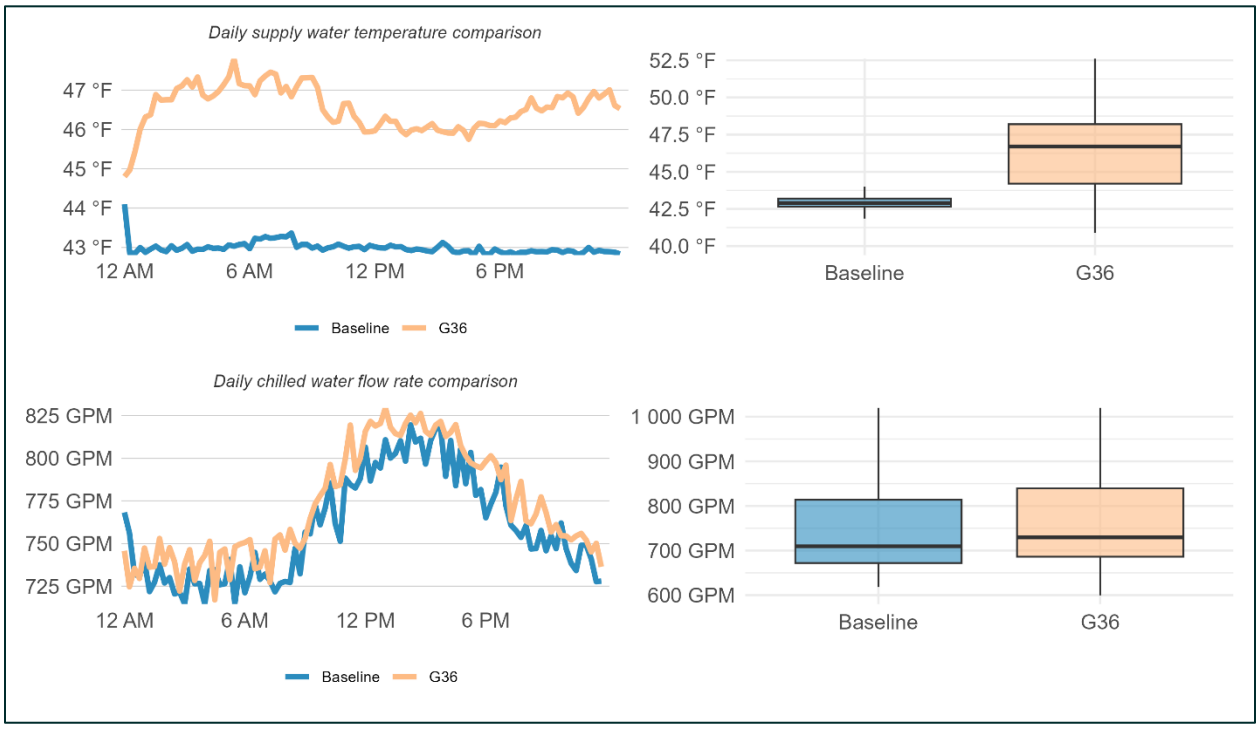

Figure 11: Distribution and hourly average profiles of chilled water supply temperature and chilled water flow rate for baseline and G36 for the whole monitoring period.

DAILY AVERAGE ENERGY USE

Figure 12 presents the daily average energy use, with baseline and G36 strategies represented in blue and orange, respectively. The figure also illustrates the alternating pattern of the two strategies implemented during the rapid M&V schedule, confirming a well-distributed deployment across the evaluation period.

Total electrical energy accounts for the combined energy consumption of the chiller, pumps and cooling tower. Several days were excluded from the analysis due to data quality issues or operational disruptions in the plant, which are shown as gaps in the figure.

The team observed that energy use during June through August period was higher than the remainder of the year. Upon further investigation, the team noticed changes to the dew point measurement, setpoint, and AHU supply air temperature setpoint; we did not investigate the exact reason for this change and decided not to use this data for the M&V analysis. The measured data shown in this section does not include June through August period. Additionally, when predicting energy using the TOWT model, the team did not predict energy use for this period since the plant operation is fundamentally different.

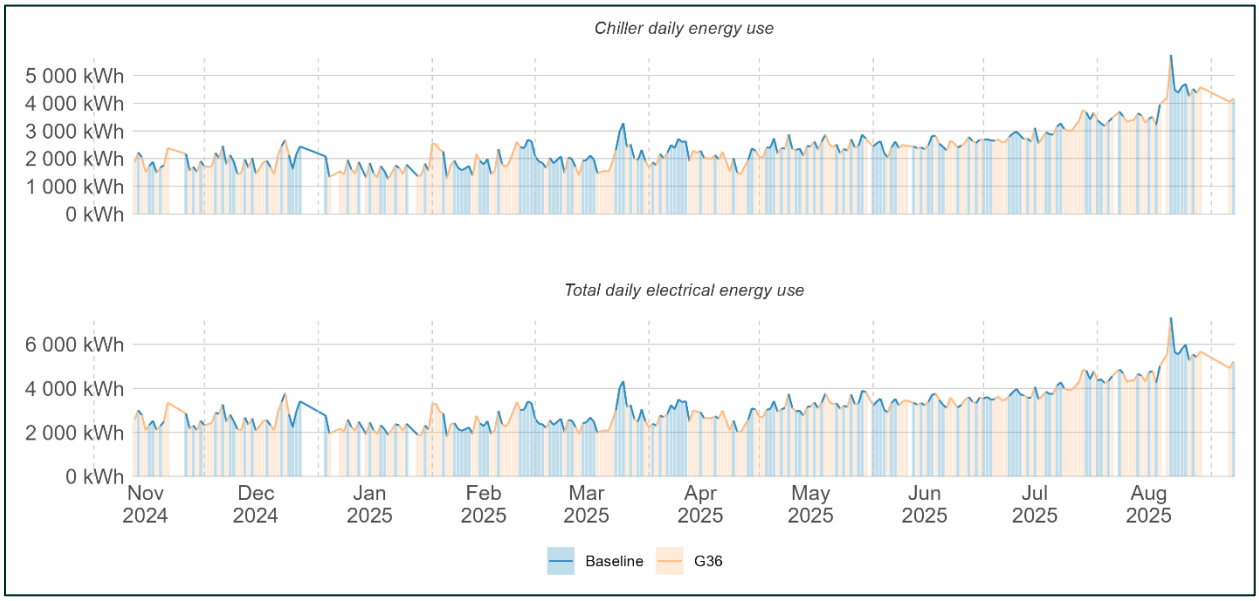

Figure 12: Daily chiller and total electrical energy use with the rapid M&V approach.

Figure 13 below shows density distributions of 15-minute electric power use, separated by month for baseline and G36. While the available data includes limited coverage of the summer months, the research team anticipates increased cooling energy use during that period due to higher ambient temperatures and corresponding building cooling loads.

Among the winter months, February stands out, with notably higher cooling energy use under the G36 strategy compared to January and March. This suggests that even within the winter season, specific operational or weather-related factors may drive elevated demand for chilled water.

Within each month, the distribution and the average line (red) indicate the hourly average energy consumption within a day. This follows the expected pattern of higher cooling energy use during late morning to afternoon when the outside air temperature is at its highest.

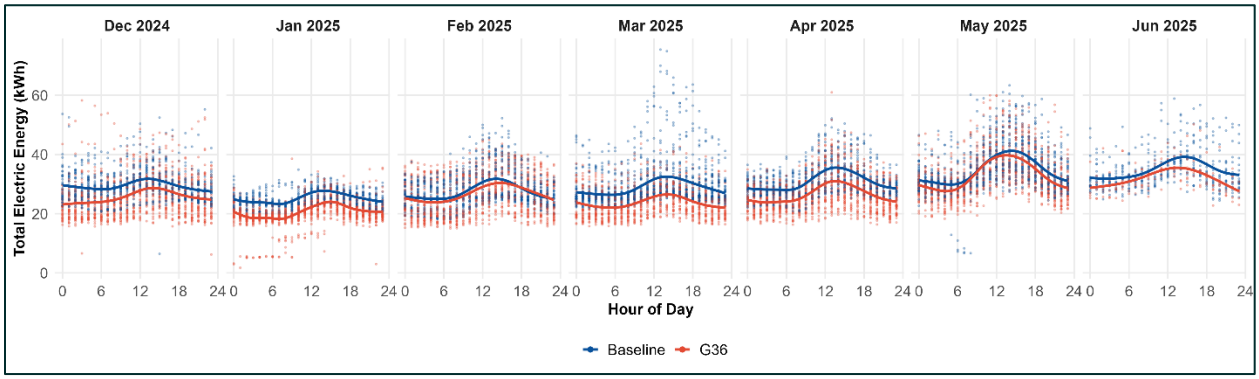

Figure 13: Measured 15-minute electrical energy use comparison throughout the day split monthly between baseline and G36.

Figure 14 below illustrates the hourly total electrical energy use for both the baseline and G36 strategies. Across all hours of the day, G36 consistently demonstrates lower energy consumption compared to the baseline. For both strategies, energy use follows a typical daily pattern, rising from morning to mid-afternoon as outdoor air temperatures increase and cooling demand within the building intensifies. This trend aligns with expected daily load profiles and shows the effectiveness of G36 in reducing energy use throughout the day.

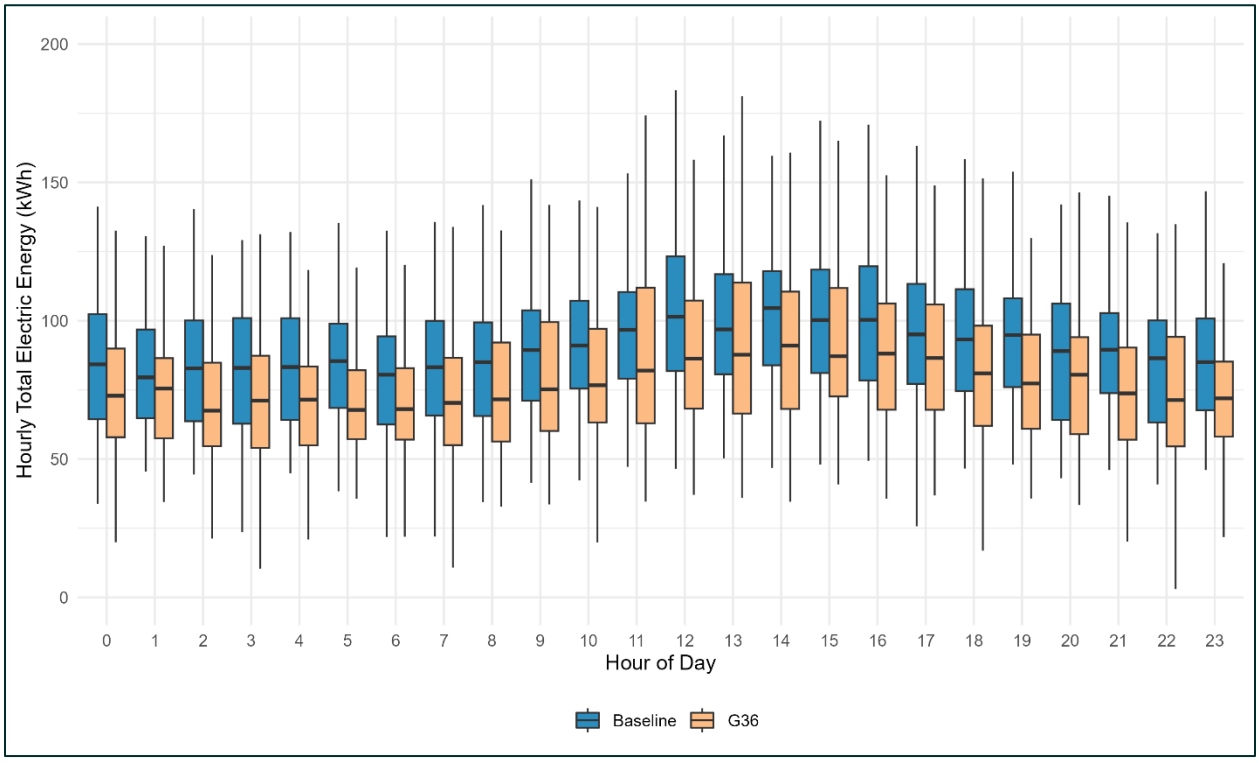

Figure 14: Total electrical energy use for each hour of the day for both baseline and G36.

Figure 15 and Figure 16 below show the distribution of daily electrical energy use and chiller energy use for baseline and G36 measurements. The analysis includes a p-value that represents the probability of the null hypothesis being true. In this context, the null hypothesis states that the mean daily energy usage from the G36 measurement set is greater than or equal to that of the baseline measurement set.

The results demonstrate that G36 reduces total daily electrical energy use by an average of 332 kWh, representing an 11.6 percent reduction compared to baseline. Most of this saving, approximately 330 kWh, is attributable to reduced chiller energy consumption. The associated p-value is well below 0.0001, and this low p-value indicates this null hypothesis to be statistically improbable, leading to the conclusion that energy usage in G36 is less than baseline.

Two main factors contribute to the reduced chiller energy use under G36. First, the use of higher supply water temperatures in G36 reduced thermal energy load by minimizing pipe heat losses. Second, chillers operated with slightly higher efficiency at elevated supply water temperatures. Additionally, aligning implementations of both chilled water and hot water plants improved the efficiency of both systems together that is represented in these savings.

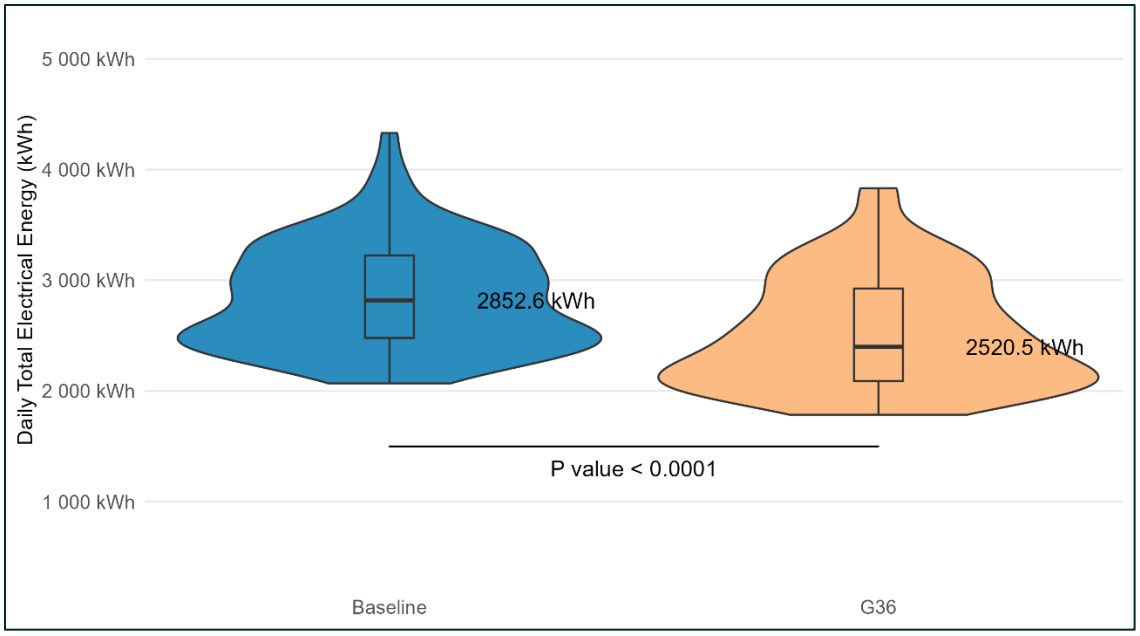

Figure 15: Distribution of total electrical energy use between baseline and G36.

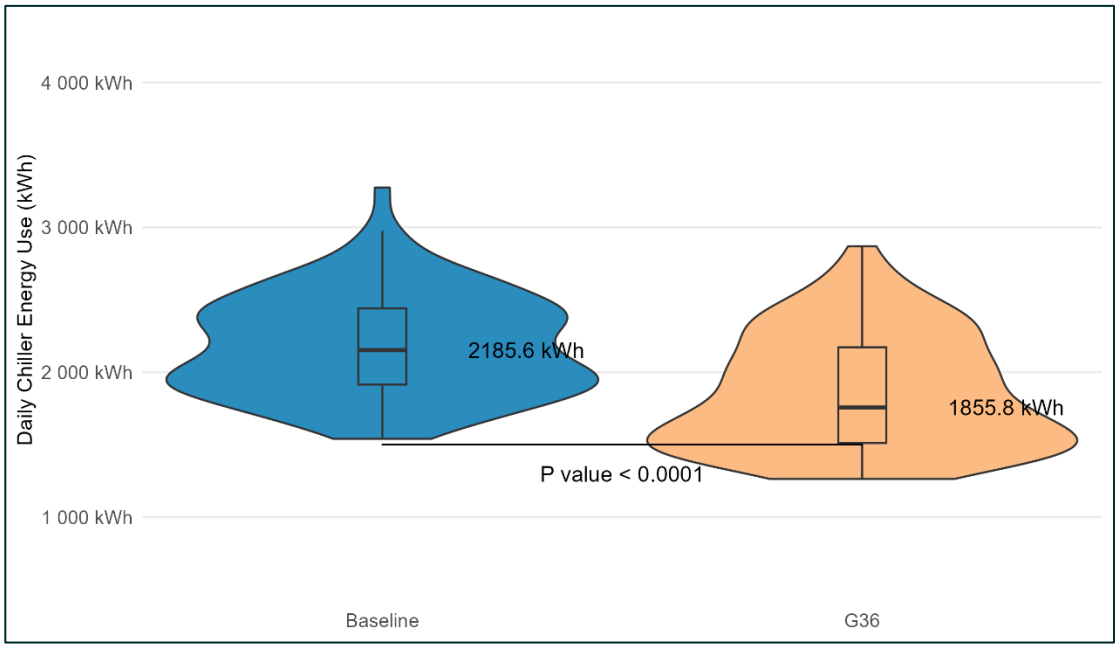

Figure 16: Distribution of chiller electrical energy use between baseline and G36.

Figure 17 below illustrates the daily average energy use by the chilled water and condenser water pumps under both the baseline and G36 strategies. The pump energy use remained consistent between the two strategies, with only minor variation in magnitude. When compared to the substantial chiller energy savings observed under G36, the differences in pump energy use were minimal and did not significantly impact the overall energy performance.

The p-value associated with this comparison was relatively large, indicating weak statistical evidence to support the null hypothesis that G36 uses less pump energy than baseline. As a result, it was not possible to conclude with confidence that either baseline or G36 consistently resulted in lower pump energy use.

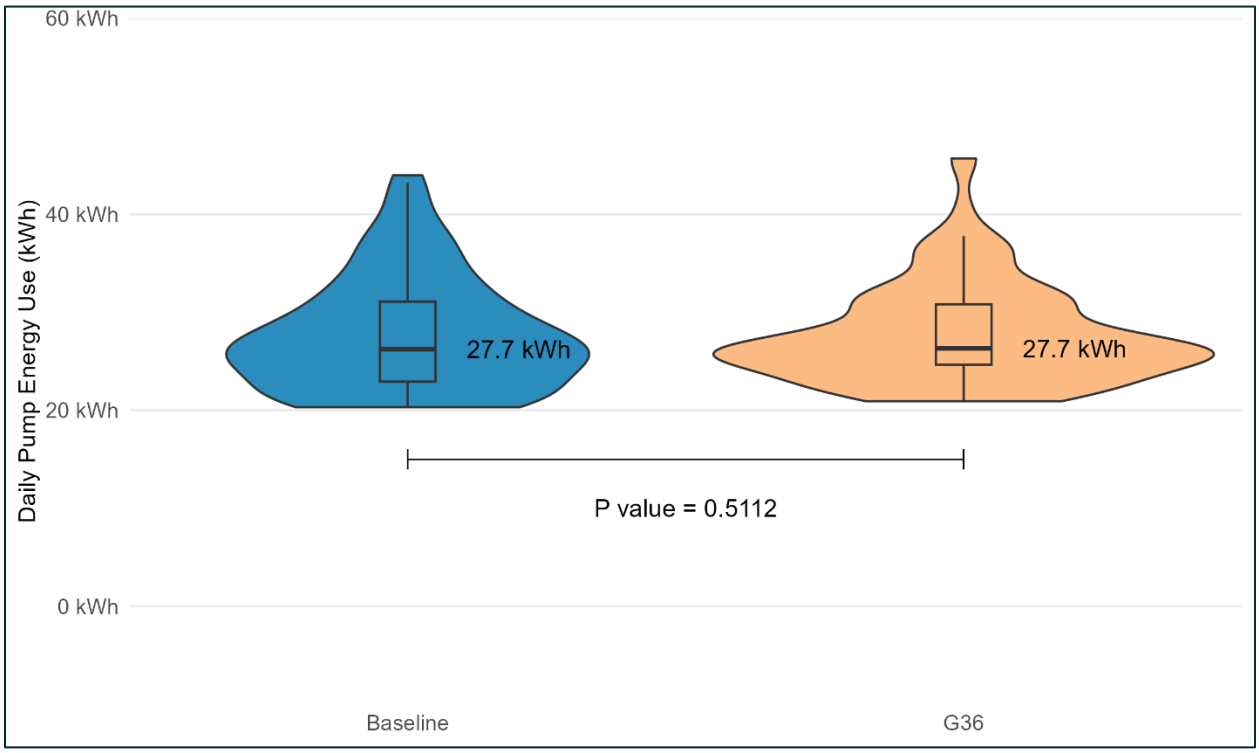

Figure 17: Distribution of chilled and condenser water pump energy use between baseline and G36 intervention.

In addition to electrical energy, the research team also evaluated thermal energy use to support and validate the findings related to chiller and total electrical energy savings above. Thermal energy was calculated using chilled water supply and return temperatures, along with the corresponding flow rates.

Figure 18 below presents the daily thermal energy consumption derived from this data.

Results indicate that G36 achieved an average daily thermal energy savings of 4,480 kBtu, representing a 9.8 percent reduction compared to baseline. While this reduction was notable, it was smaller than the observed electrical energy savings, as part of the latter is attributed to improved chiller efficiency rather than a direct reduction in thermal load.

The thermal energy savings were primarily the result of reduced pipe heat losses, made possible using higher chilled water temperatures, and improved chiller efficiency when operating at higher chilled water temperatures. For the development of the TOWT model and the analysis of normalized energy consumption, the research team used electrical energy as the basis for evaluation, given its direct correlation to operational cost and chilled water plant performance.

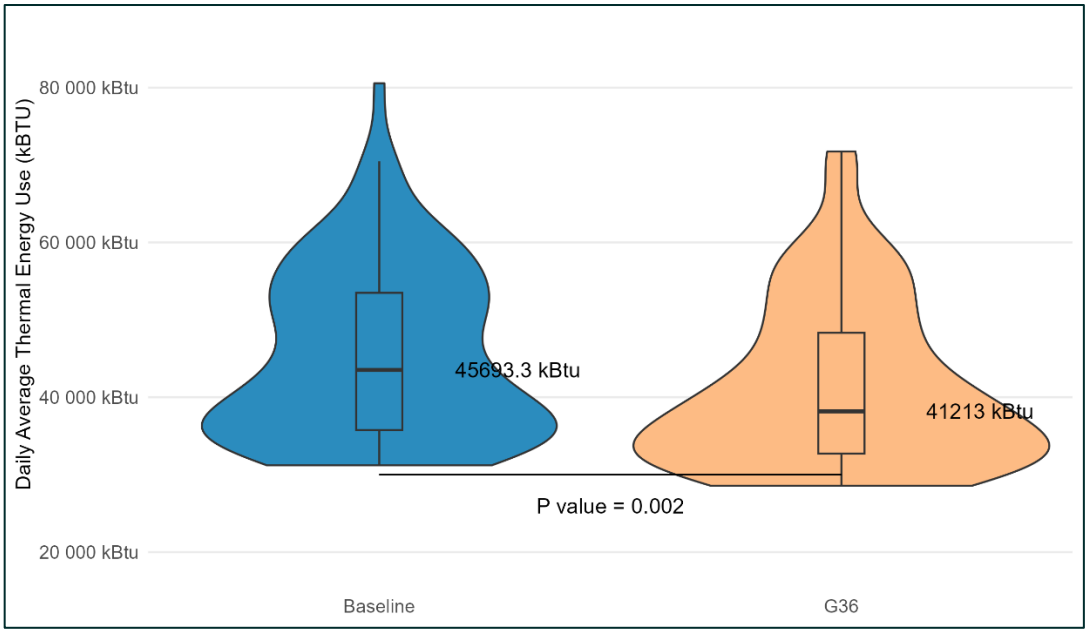

Figure 18: Distribution of chiller thermal energy use between baseline and G36 intervention.

Figure 19 below displays the peak electrical power usage for both the baseline and G36 strategies. Analysis of the data showed that the average daily peak power remained approximately the same for both cases. The corresponding p-value offered no strong statistical evidence to suggest that peak power demand under G36 was significantly higher or lower than that of baseline.

Peak chiller power typically occurred during periods of highest cooling demand, often in the early afternoon when outside air temperatures reached their daily maximum. The similarity in peak power across both strategies indicates that each could meet these peak cooling demands with comparable power input. Consequently, the energy savings observed with G36 were primarily realized during partial load conditions, when cooling demand was lower, and the system operated more efficiently through temperature reset and demand-based control. The high p-value also indicated that there was no strong evidence to suggest G36 has lower peak power use compared to baseline or vice versa.

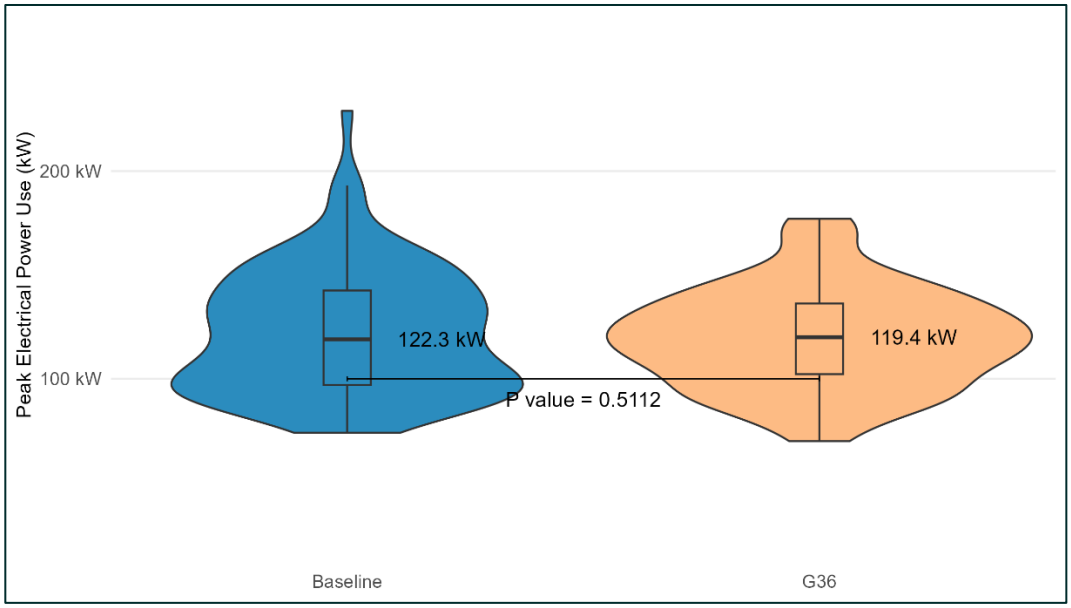

Figure 19: Distribution of daily chiller peak electrical power use between baseline and G36 intervention.

ENERGY SAVINGS FROM PLANT OPTIMIZATION

The G36 Sequences Implementation and Plant Optimization section outlines the adjustments the research team made to temperature and dew point setpoints specifically for the nanofabrication lab. These changes were aimed at reducing the cooling energy load by enabling the cooling coils to operate under partial load conditions rather than running continuously at full capacity.

Figure 20 below compares daily average thermal power across three conditions: the original baseline from a 2023 study in the same building, the updated baseline following setpoint adjustments, and the G36 strategy after implementation. Results indicate a 16.4 percent reduction in energy use from 2,429 kBtu per hour to 1,904 kBtu per hour by following the setpoint optimization alone, amounting to a savings of 525 kBtu per hour on average, or 3.7 Btu per hour per square foot. In total, with the G36 implementation, the savings increased to 29 percent.

This comparison highlights the significant energy-saving potential of targeted retrofits and operational optimizations when combined. Even in the absence of advanced control strategies like G36, optimizing key setpoints can lead to substantial reductions in energy consumption. Implementation and commissioning of advanced control sequences require examination of the existing HVAC system, including controls, sensors, and setpoints; it is also important to ensure retro-commissioning the system will maximize energy saving potential when combined with the advanced control sequences.

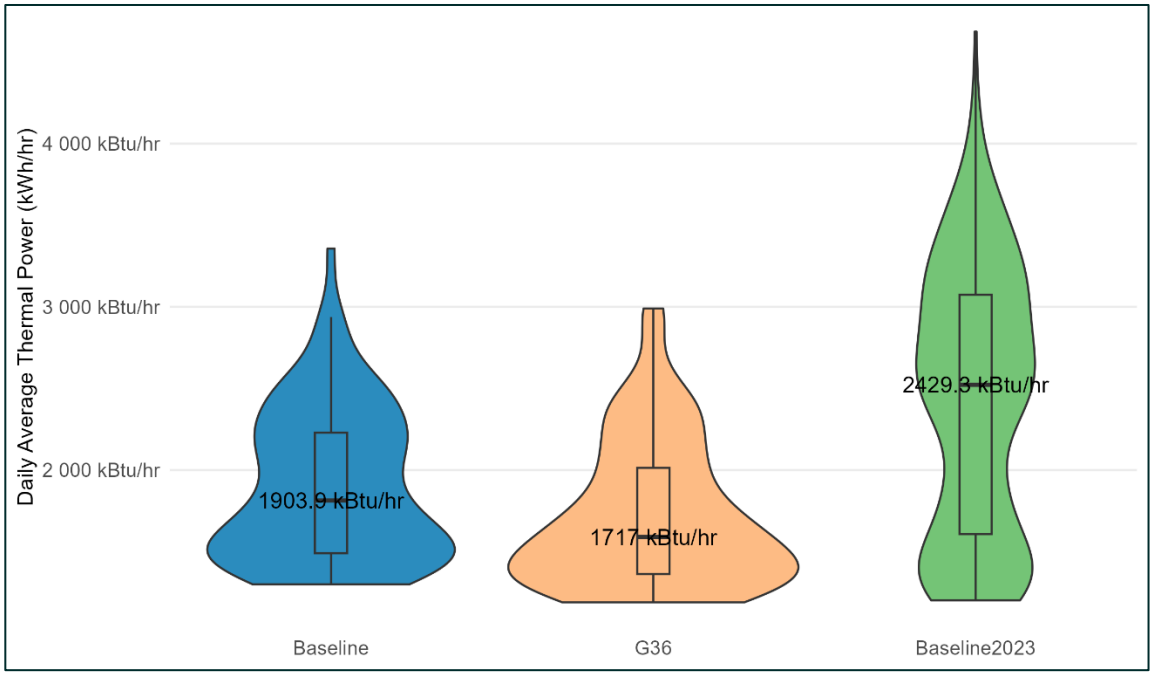

Figure 20: Daily average thermal power distribution for baseline and G36 compared with baseline from 2023 before plant optimization.

TOWT MODEL

The research team developed TOWT models to represent energy consumption patterns for both the baseline and G36 strategies. Using 15-minute interval energy consumption data, we employed the nmecr package developed by kW Engineering within the R programming environment to construct and evaluate these models.

Table 10 below summarizes the regression model statistics for each strategy and each type of energy analyzed. Model performance was assessed against benchmark criteria, and all models met or exceeded the benchmark thresholds, indicating an acceptable fit and validating the suitability of the models for normalized energy comparison and further analysis.

Table 10: Model fit parameters for TOWT model for baseline and G36 for total electrical energy and chiller energy.

	Baseline				G36			
Energy type	**No. of days**	**R2**	**CVRMSE%**	**NDBE%**	**No. of days**	**R2**	**CVRMSE%**	**NDBE%**
CHW plant elec energy	95	0.62	14.56	3.9E-12	98	0.457	21.32	-1.2E-11
Chiller elec energy	95	0.0.663	13.23	5.3E-12	98	0.444	23.23	9.3E-12

Figure 21 and Figure 22 below display the relationship between chiller electrical energy consumption and outside air temperature, comparing measured data with model predictions for baseline and G36. Red dots represent the measured 15-minute chiller electricity use, while blue dots show the corresponding TOWT model predictions based on the recorded outside air temperatures.

A visual inspection of the plots indicated a relatively better model fit at lower outside air temperatures, which likely corresponded to partial load conditions typically observed during nighttime and early morning hours. This alignment suggested that the TOWT model captures energy behavior more accurately under reduced cooling demand, which was consistent with how the system operated during off-peak periods.

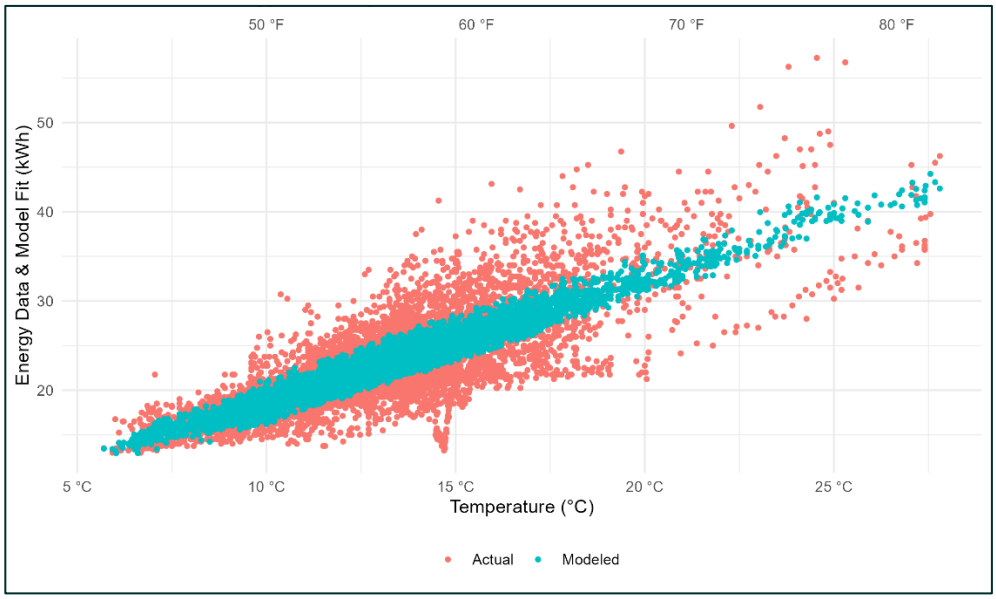

Figure 21: Measured and model predicted chiller electrical energy use in 15 minutes against outside air temperature for baseline strategy.

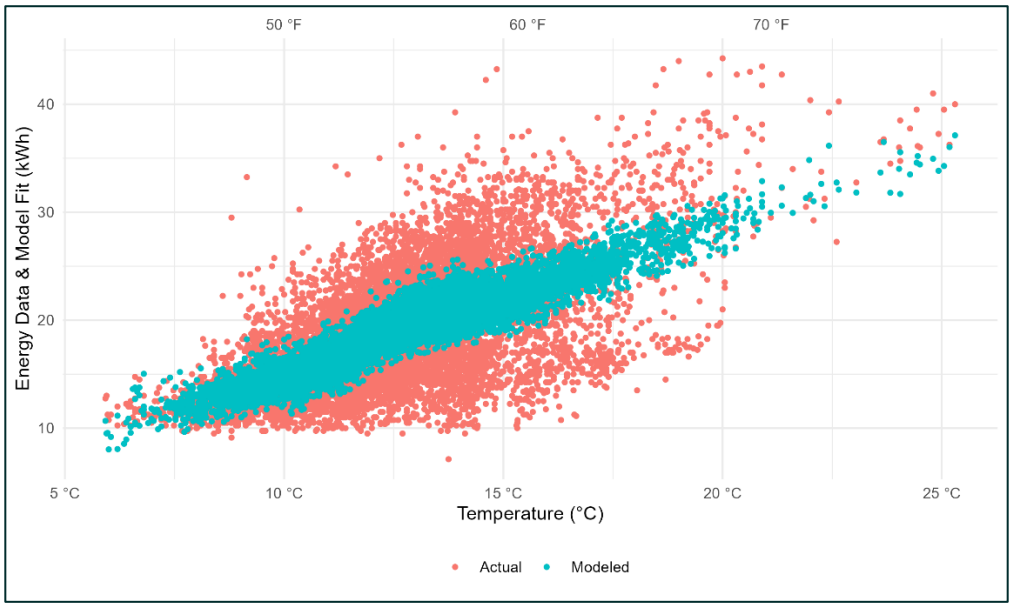

Figure 22: Measured and model predicted chiller electrical energy use in 15 minutes against outside air temperature for G36 strategy.

To evaluate normalized energy savings, the research team used the TOWT models to predict daily energy consumption for both the baseline and G36 strategies under standardized weather conditions. Weather data from a typical meteorological year sourced from the TMY3 database (NREL, 2020) served as the input for this analysis to ensure consistency and comparability across scenarios.

Figure 23 below presents a comparison of the predicted daily chiller plant energy consumption for both strategies throughout a typical year except for June through August period. The team decided not to use the TOWT model to predict energy use during these months since the plant operation was fundamentally different, as explained above. Figure 24 shows the monthly chiller plant energy use comparison between the two strategies.

Based on the model outputs, the predicted cooling related electrical energy savings for G36 in the demonstration site is 86,672 kWh, equivalent to 0.61 kWh per square foot per year, a 14.6 percent reduction compared to baseline. These findings highlight the long-term energy saving potential of implementing the G36 control sequences.

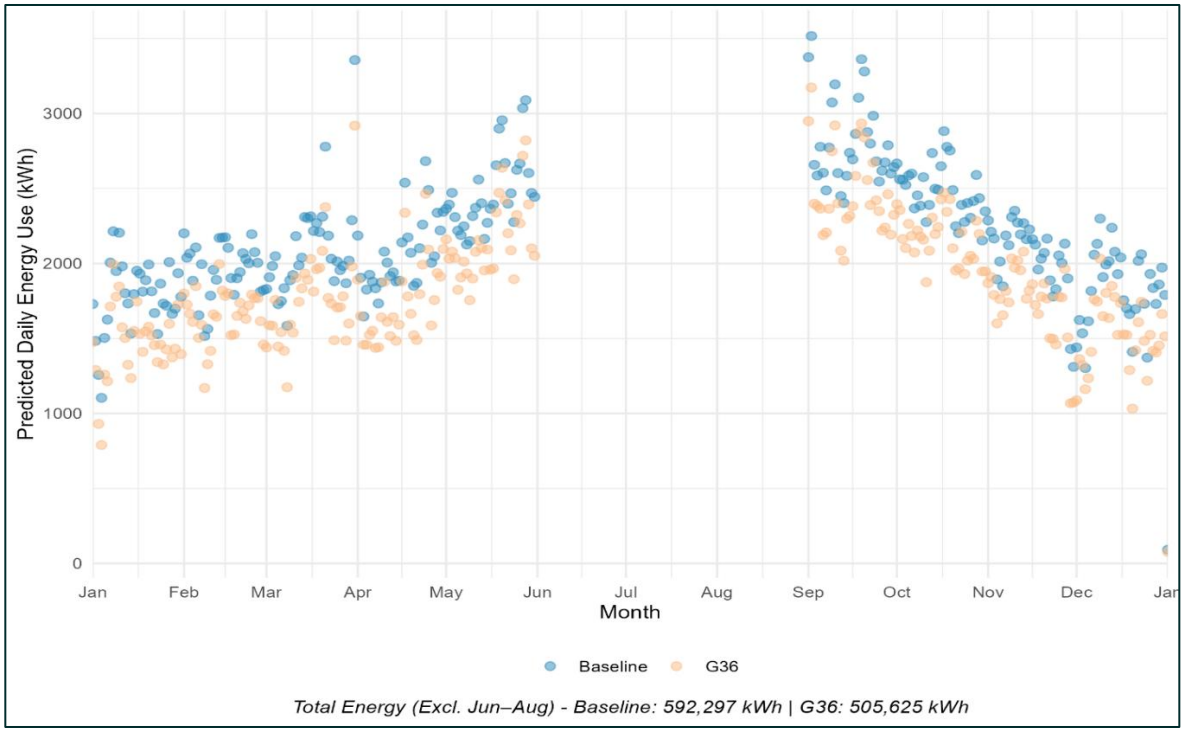

Figure 23: TOWT model predicted normalized daily chiller plant energy consumption for baseline and G36.

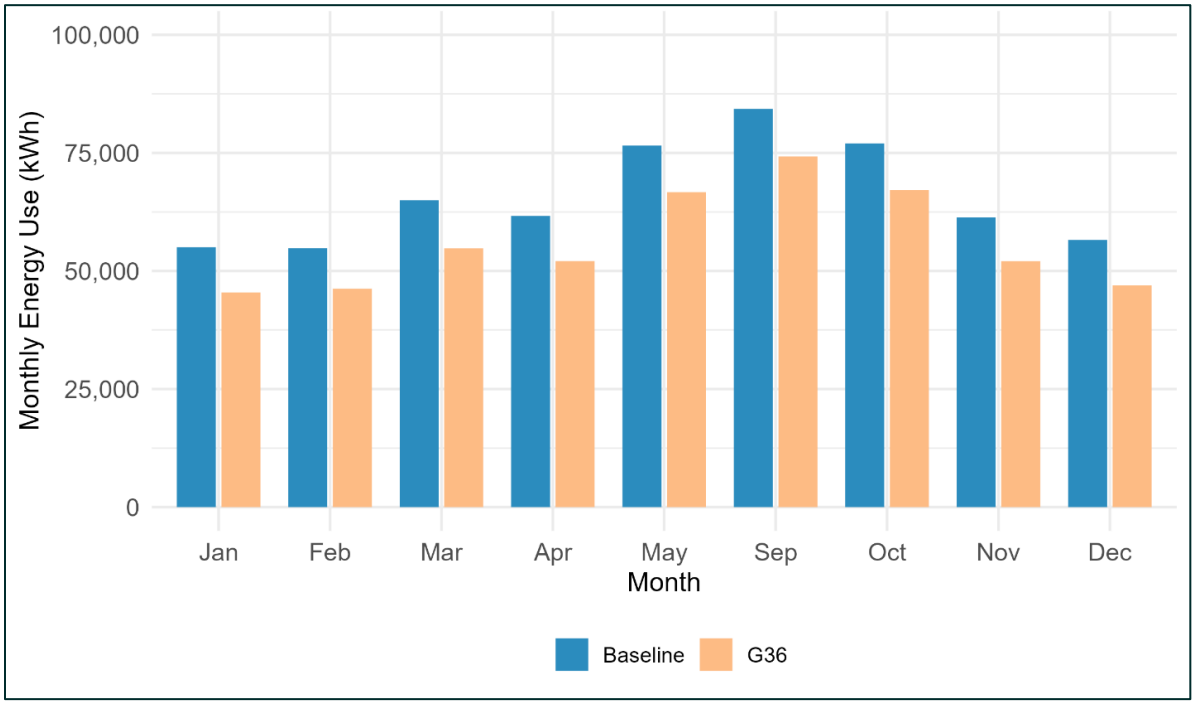

Figure 24: TOWT predicted chiller plant energy use comparison between baseline and G36.

Based on the model-predicted energy savings of 86,672 kWh at the demonstration site, and using an estimated average commercial electricity rate of $0.20 per kWh in California, the annual cost savings would be approximately $17,334.

Energy Consumption Analysis – Site 1 Hot Water Plant

The rapid M&V schedule implemented for the hot water plant—as shown in Figure 25—mirrored the schedule used for the chilled water plant, with the key difference being an earlier start date for the hot water system. This adjustment provided additional data at the beginning of the evaluation period.

By aligning the rapid M&V schedules for both the chilled and hot water plants, the research team was able to assess the combined impact of the G36 control strategy across both systems. This alignment was particularly important for capturing interactive effects, such as increased heating demand that may result from overcooling zones due to inefficiencies in the cooling system. Evaluating both systems together enabled an overall understanding of the energy performance of the full G36 sequence when implemented.

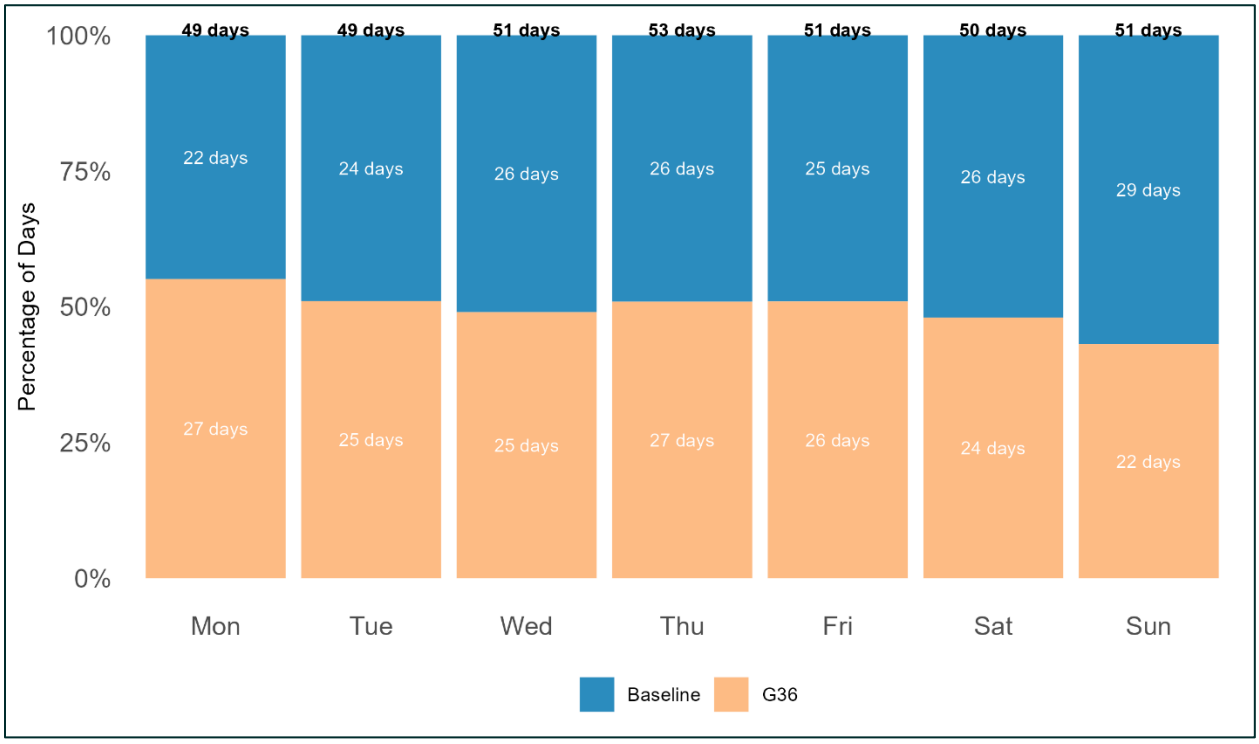

Figure 25: Rapid M&V schedule: Comparison of number of days sampled by different strategies.

In the baseline condition, the hot water plant operated with a fixed supply water temperature of 190°F. Under the G36 control strategy, the supply temperature was reset dynamically between 190°F and 120°F using a T&R logic to better match heating demand.

Figure 26 below illustrates the typical operation of G36 throughout the day. During morning hours, particularly after night setbacks when the building begins to reheat, G36 maintained the supply temperature near the upper end of the reset range to meet the increased heating demand. As the

day progressed and the building became thermally stabilized, the control logic reduced the hot water temperature, especially during the afternoon and nighttime periods.

This reduction in temperature resulted in a corresponding increase in hot water flow rate, following a similar pattern to that observed in the chilled water plant. The elevated flow rate helped maintain the necessary thermal output despite lower water temperatures, ensuring comfort while enabling energy-efficient operation.

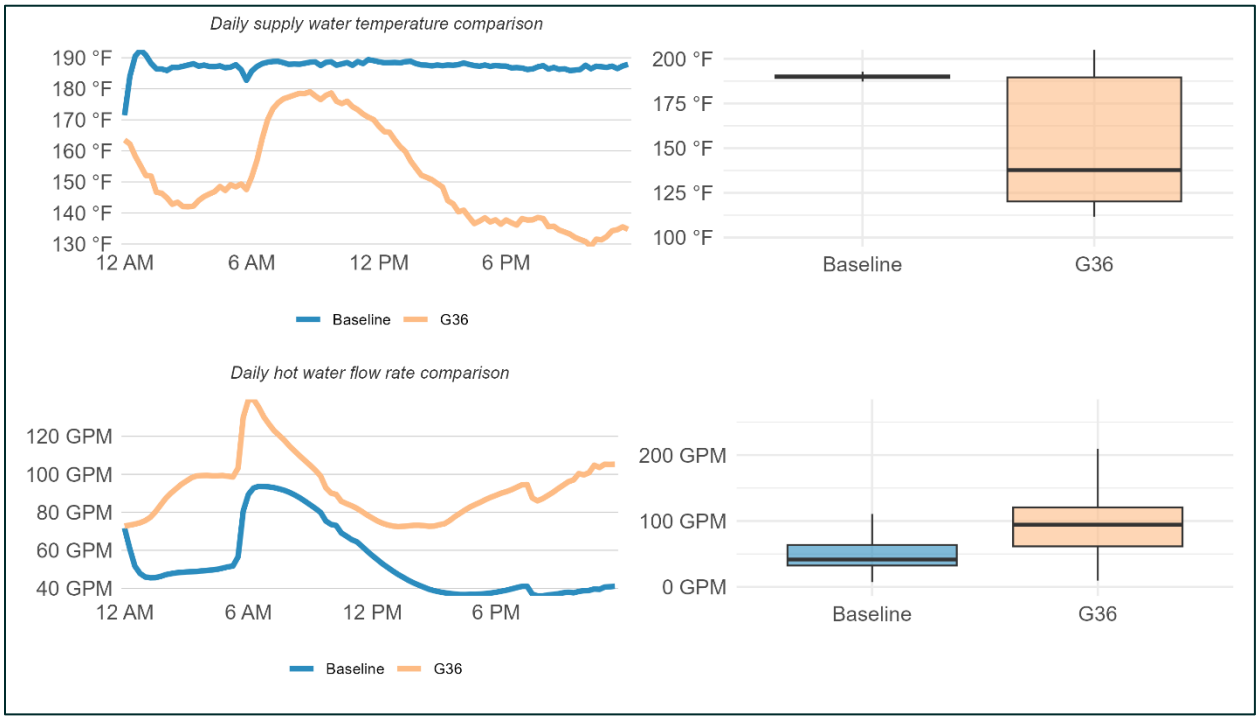

Figure 26: Hot water supply temperature and hot water flow rate comparison between sampled intervention days and baseline days.

DAILY AVERAGE ENERGY USE

Figure 27 below presents the daily average thermal energy use for the hot water plant, with baseline operation shown in blue and G36 operation in orange. The rapid M&V framework alternated between the two strategies throughout the M&V period, enabling a direct comparison of their performance under varying conditions.

The team calculated thermal power for the hot water plant using the measured supply and return water temperatures, along with the water flow rate. This approach provided an accurate representation of the thermal energy delivered to the building under each control strategy.

Several data gaps are present in the figure, primarily due to hot water flow meter communication issues during August and September, as well as sMAP data communication disruptions in the later months. These affected periods were excluded from the analysis to maintain data quality and reliability.

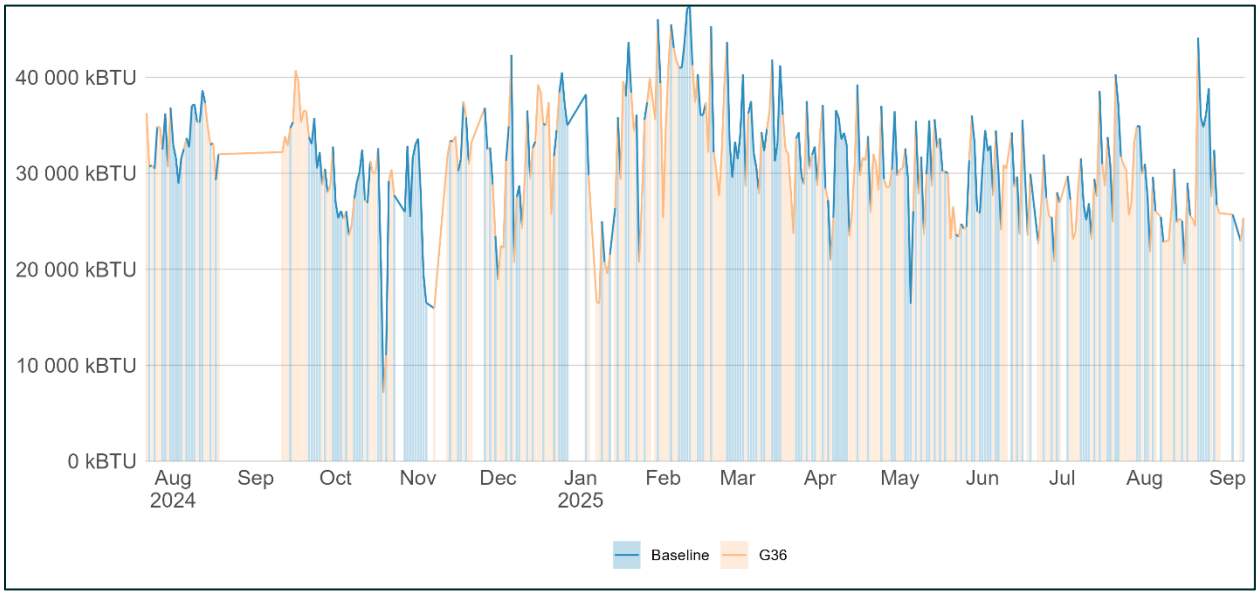

Figure 27: Daily hot water plant thermal energy use with the rapid M&V approach.

Figure 28 below displays the distribution of 15-minute thermal energy use for the hot water plant, separated by month. These plots provide insight into the variability and intensity of heating demand across different times of the year.

Measured data for the summer months was limited due to the M&V period. However, based on typical building operation and seasonal trends, the research team expected significantly lower heating energy use during the summer. This is consistent with reduced heating demand when outdoor temperatures are higher.

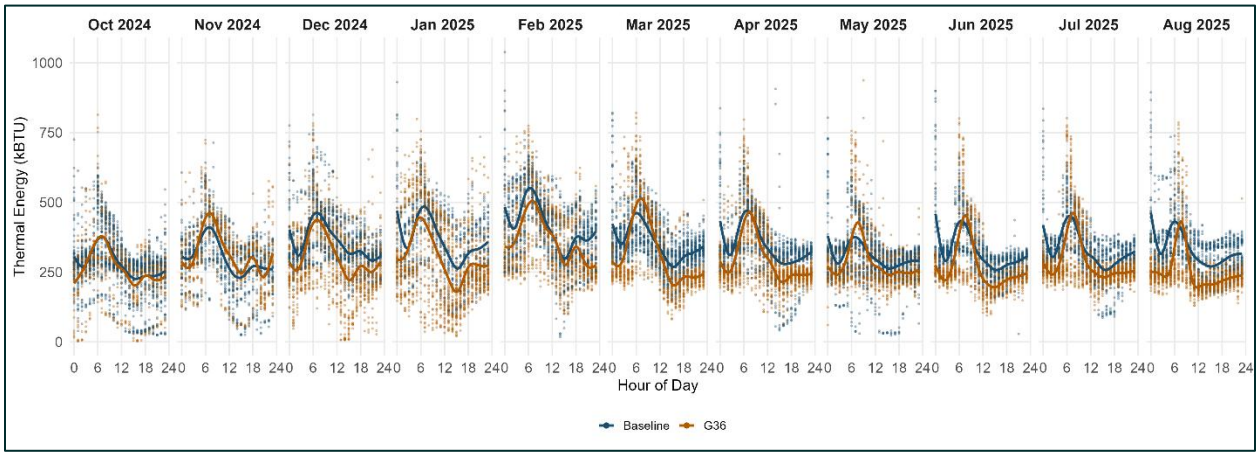

Figure 28: Measured 15-minute thermal energy use throughout the day split monthly between baseline and G36.

Figure 29 below illustrates the hourly thermal energy use for both the baseline and G36 strategies. As expected, thermal energy use peaked in the morning hours due to the building's transition from night setback to occupied conditions, which required a surge in heating to meet comfort setpoints.

During these morning hours, G36 used more thermal energy than baseline. This was likely due to the higher reset temperatures used by G36 at startup to quickly respond to heating demand. However, for the remainder of the day—including afternoon and evening hours—G36 consistently used significantly less thermal energy compared to baseline. These sustained reductions more than offset the higher morning usage, resulting in the overall energy savings shown in Figure 30.

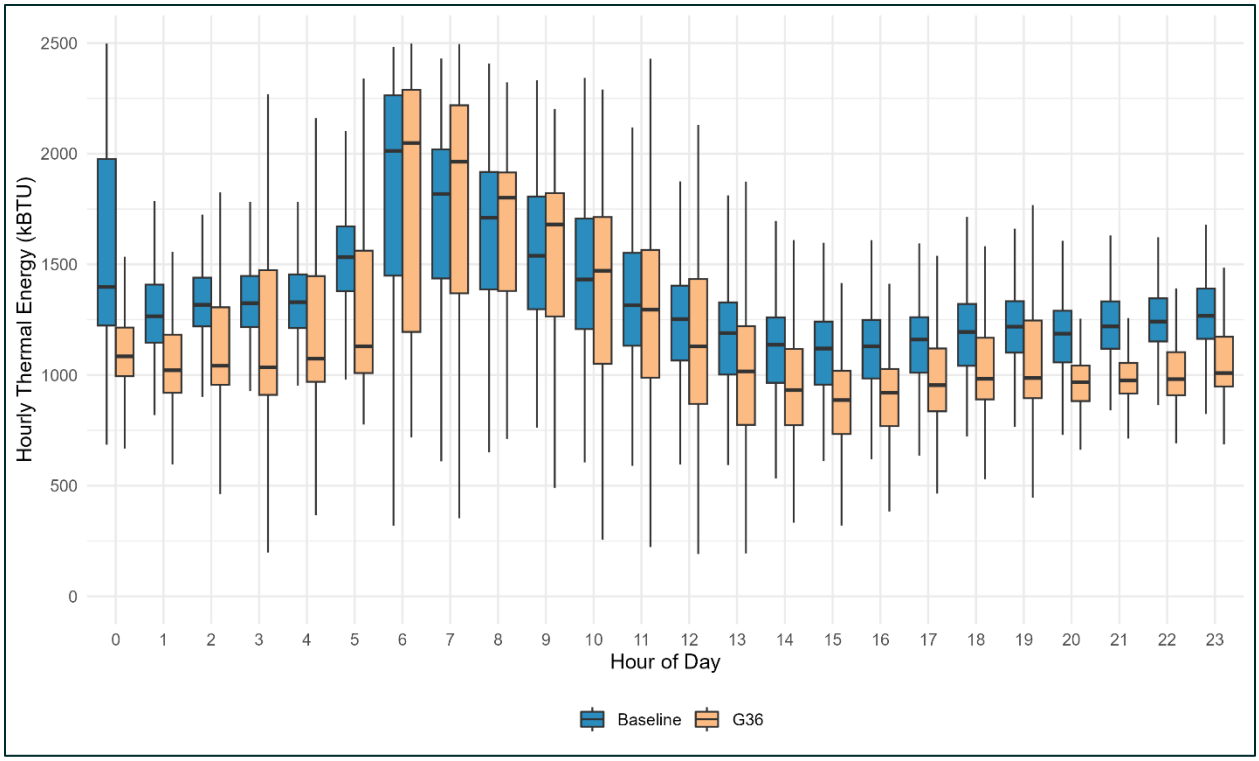

Figure 29: Hourly thermal energy calculated by hour of day in baseline and G36.

The team conducted a one-tailed hypothesis test to evaluate the null hypothesis: that mean daily thermal power usage under the G36 strategy would be greater than or equal to that of baseline. The results indicate that G36 reduced daily average thermal energy consumption from 32,344 kBtu to 29,038 kBtu, representing a 10.2 percent reduction, or approximately 23 Btu per square foot per day.

Notably, this comparison does not account for potential variations in heat exchanger efficiency or upstream steam energy consumption, as those data were not available to the research team. Despite this limitation, the observed savings can be primarily attributed to reduced pipe losses resulting from operating the hot water system at lower supply temperatures under the G36 control strategy. This outcome aligns with the goals of G36 to deliver energy savings through smarter temperature reset logic.

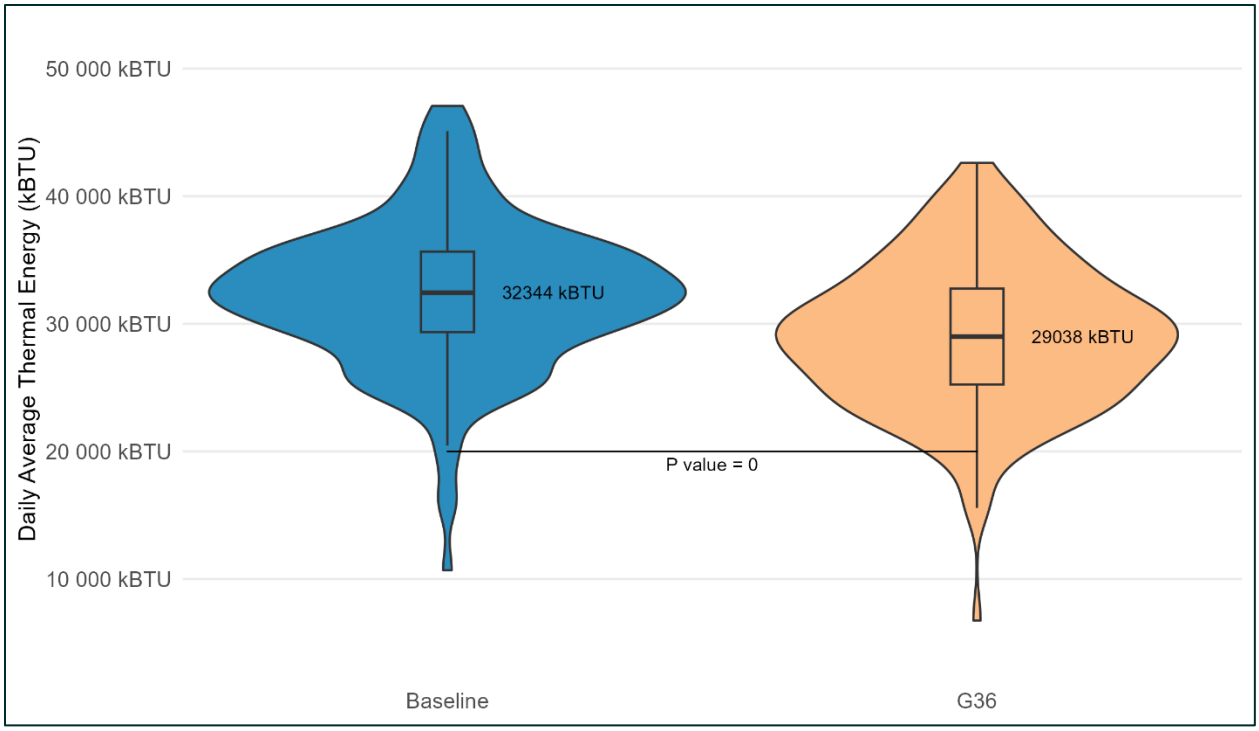

Figure 30: Distribution of thermal energy use between baseline and G36 intervention.

As shown in Figure 31 below, hot water pump power usage was slightly higher (approximately 8 percent) under the G36 strategy compared to baseline. This increase aligns with the higher flow rates observed in G36 operation, as shown in Figure 30 above.

However, the magnitude of pump energy use remained minimal relative to the thermal energy delivered. While daily thermal energy consumption was around 30,000 kBtu per day, the corresponding hot water pump energy use was only about 400 kBtu per day, with an average increase of about 30 kBtu per day. Due to its relatively small contribution, pump energy was not included in the energy savings analysis.

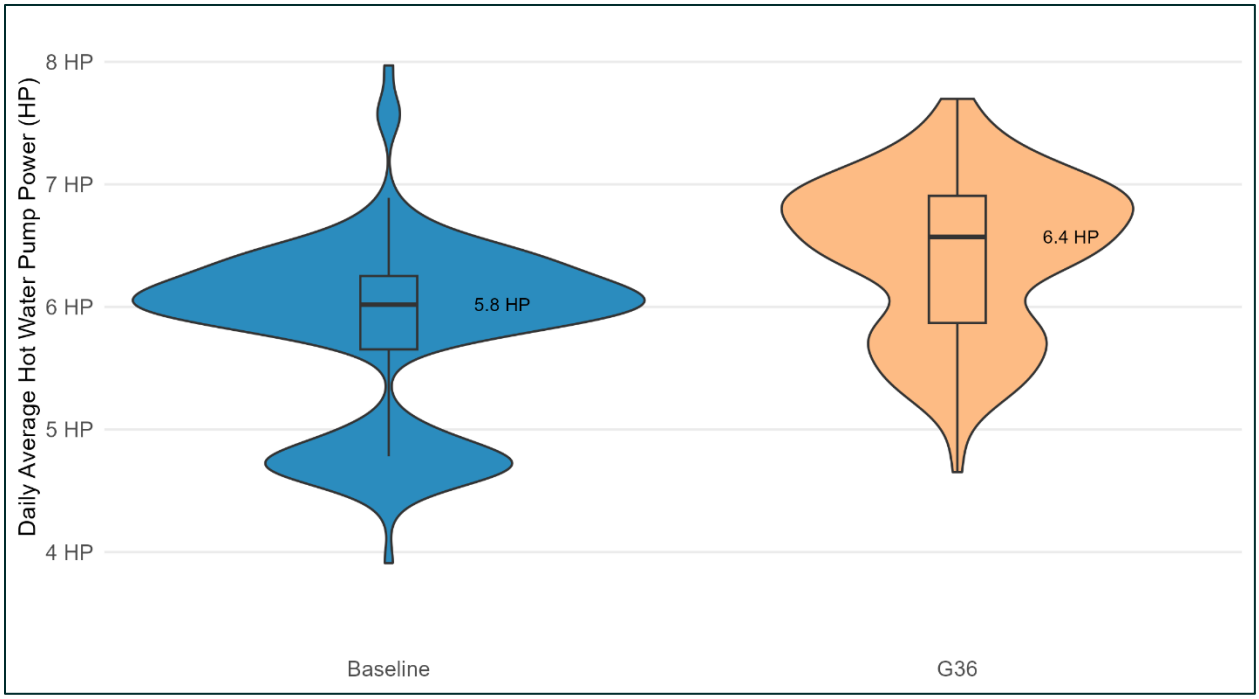

Figure 31: Distribution of hot water pump power between baseline and G36 intervention.

TOWT MODEL

The research team developed TOWT regression models to characterize energy consumption patterns for both the baseline and G36 strategies. These models were constructed using 15-minute interval energy consumption data and the nmecr package.

The table below presents the regression model statistics for each strategy. The team evaluated the goodness-of-fit metrics against benchmark criteria established, and all models met the standard thresholds, indicating that the fits were acceptable

Table 11: TOWT model fit statistics for baseline and G36: Site 1 HW plant.

	Baseline				G36			
Energy type	**No. of days**	**R2**	**CVRMSE%**	**NDBE%**	**No. of days**	**R2**	**CVRMSE%**	**NDBE%**
HW plant thermal energy	178	0.543	21.18	-1.33E-11	176	0.51	29.06	3.6E-11

Figure 32 compares measured thermal energy use with the model-predicted values for both the baseline and G36 strategies. Red dots represent the measured 15-minute thermal energy consumption, while blue dots indicate the TOWT model's predicted energy use for the corresponding conditions.

The general trend aligned with expected behavior: As outside air temperature increases, the building's heating energy use decreases.

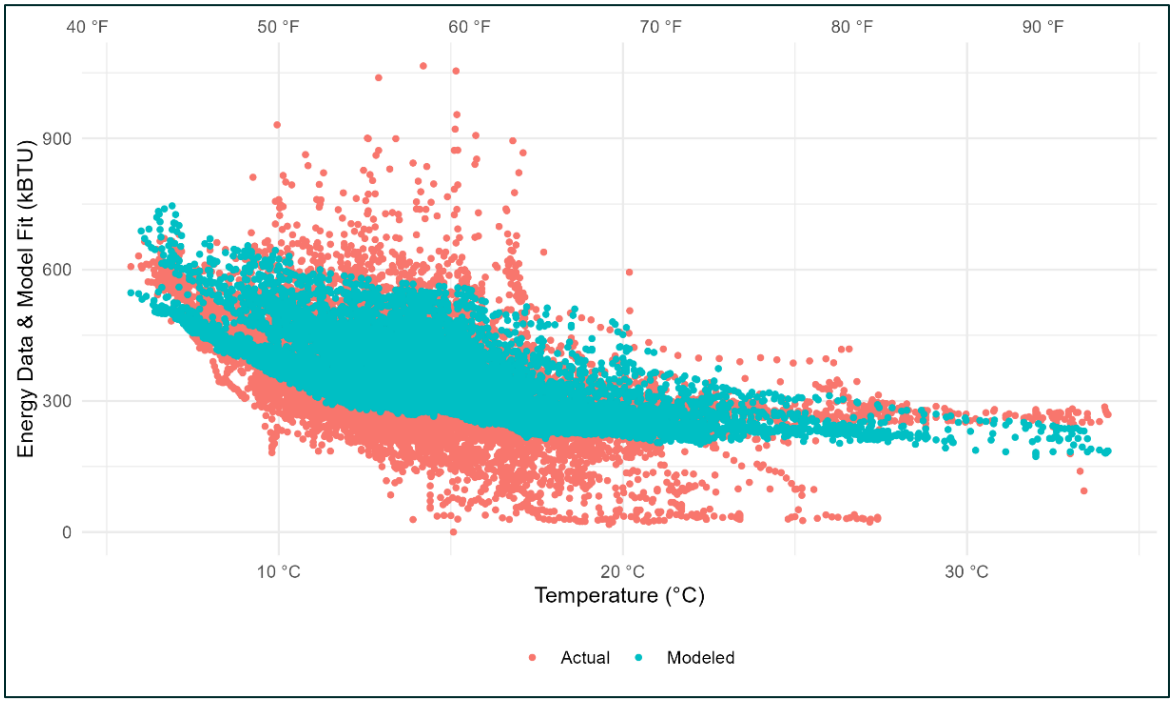

Figure 32: Measured and model predicted thermal energy use in 15 minutes against outside air temperature for baseline strategy.

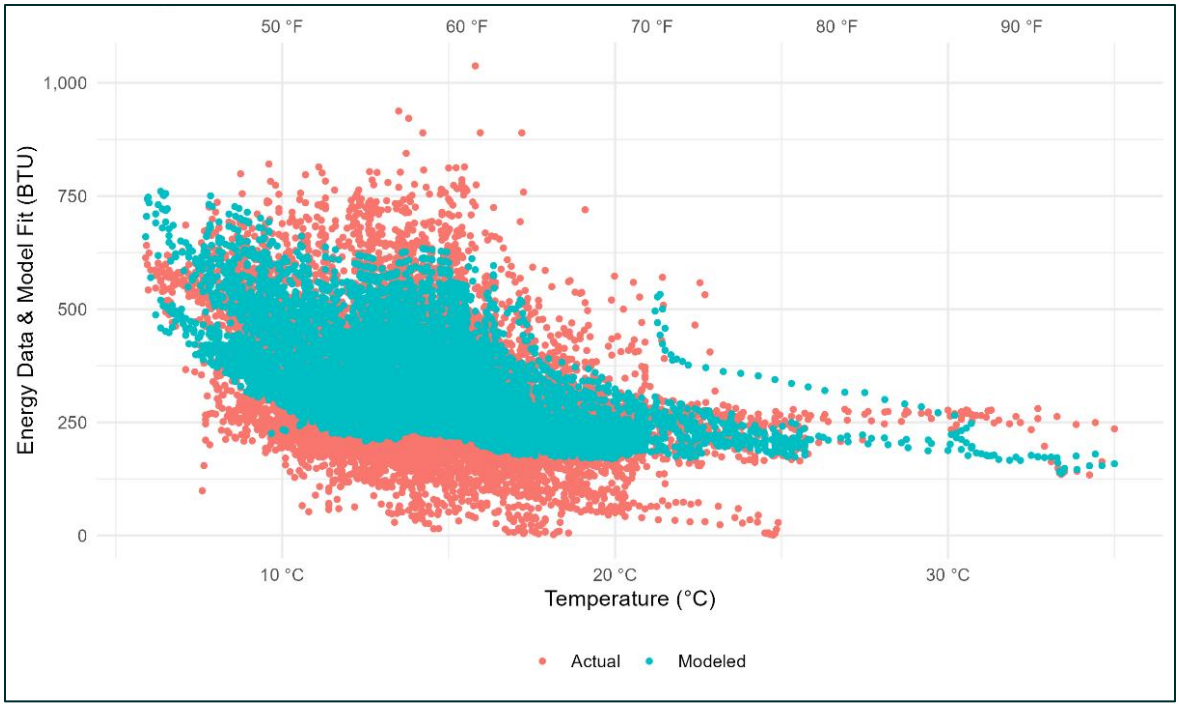

Figure 33: Measured and model predicted thermal energy use in 15 minutes against outside air temperature. for G36 strategy.

The research team utilized the TOWT regression models to predict normalized daily energy consumption under typical weather conditions, employing data from the TMY3 database for this analysis. This approach allowed for evaluation of each strategy's performance across a representative meteorological year.

Figure 34: TOWT below illustrates the daily predicted energy consumption for both the baseline and G36 strategies over the course of one year, based on TMY3 weather data. Figure 35 compares the predicted monthly energy consumption between the two strategies. The comparison highlights the impact of the G36 control logic on reducing heating energy use under typical climate conditions.

Model predictions indicate an annual average energy savings of 1,431,580 kBtu per year, equivalent to 10.15 kBtu per square foot per year. This represents a 11.5 percent reduction in heating energy consumption at the demonstration site, indicating the effectiveness of the G36 strategy for long-term energy savings.

Assuming a central plant boiler efficiency of 90 percent, and a natural gas utility rate of $15 per million Btu, the predictions above correspond to $23,860 per year in cost savings ($0.17 per square foot per year).

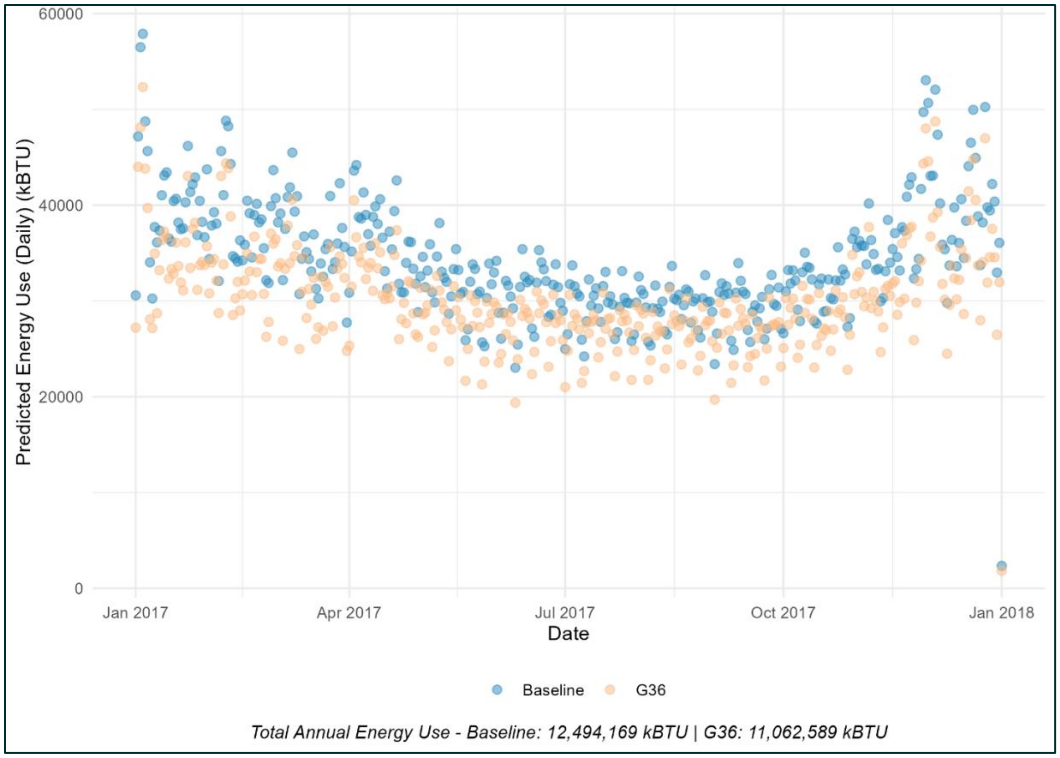

Figure 34: TOWT model predicted normalized daily energy consumption for baseline and G36.

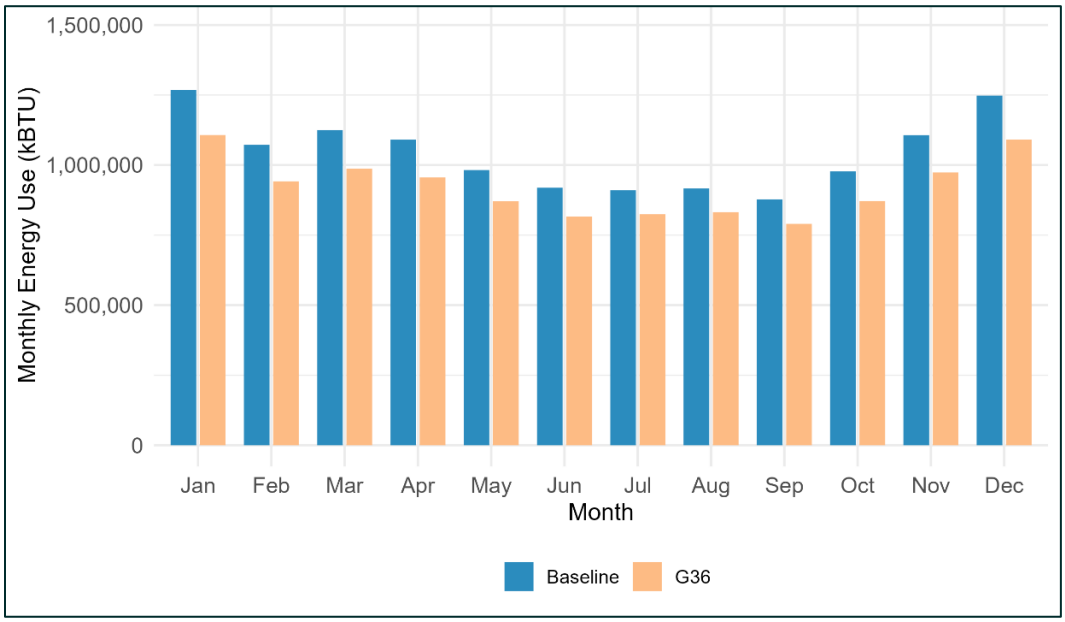

Figure 35: TOWT model predicted monthly energy use comparison between baseline and G36: Site 1 HW plant.

Energy Consumption Analysis – Site 2 Hot Water Plant

The research team implemented a rapid M&V schedule that randomly alternated between the baseline and G36 control strategies. This approach ensured a nearly equal number of operating days for each strategy, allowing for a balanced comparison, as shown in Figure 36 below. To account for the thermal inertia of the building's radiant system, the team adopted a three-day alternating schedule.

Several data points were removed from the analysis due to boiler shutdowns caused by plant-related issues. In order to minimize bias introduced by residual thermal effects, the first day following each strategy change was excluded from the M&V analysis. This ensured that energy use comparisons reflected steady-state conditions under each control strategy.

In addition, the research team excluded the first two days following each data gap, based on the assumption that building-wide warm-up after periods of inactivity would result in abnormally high heating energy use.

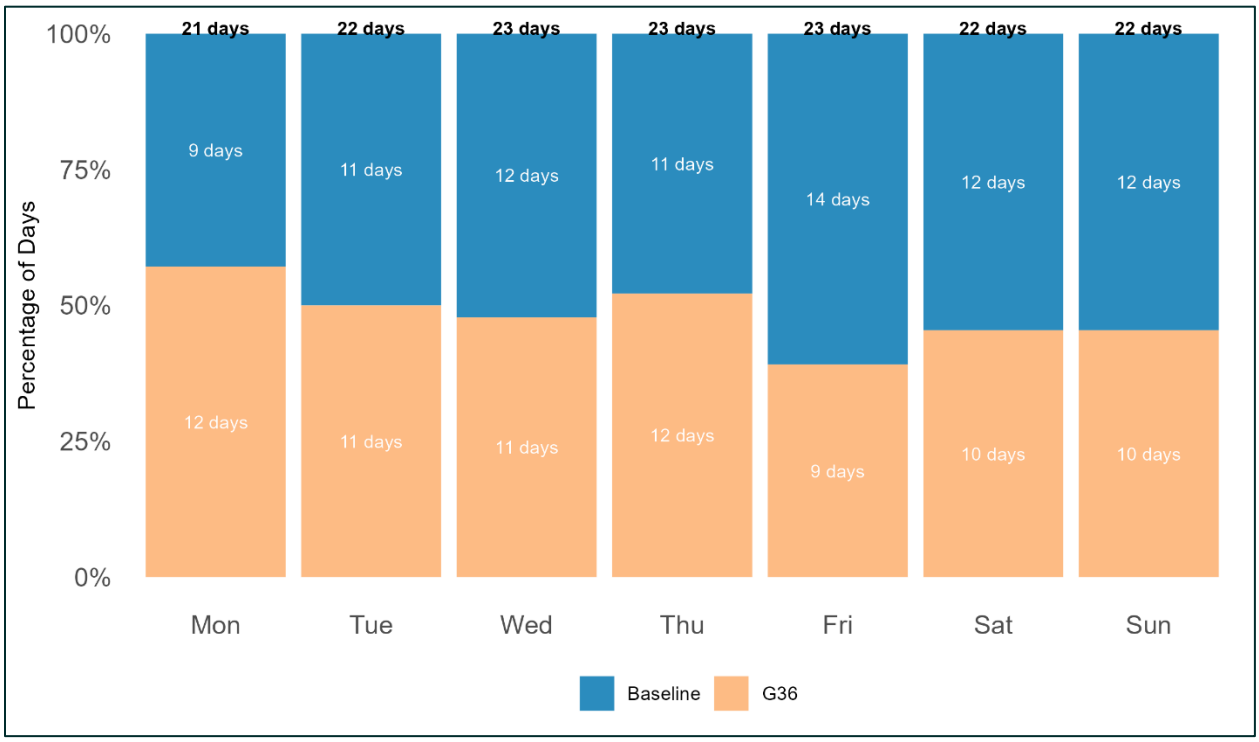

Figure 36: Rapid M&V schedule strategy distribution across days of the week.

The baseline operating condition used a fixed-supply hot water temperature of 130°F, whereas the G36 strategy implemented a dynamic temperature reset between 130°F and 90°F using a T&R logic. Figure 37 below presents the hourly average supply water temperature and flow rate, along with a box plot illustrating the distribution of values throughout the day. Under G36, the supply water temperature is consistently reset to lower levels during afternoon and nighttime hours. To meet the building's heating demand under these reduced temperatures, the system compensates with increased hot water flow rates. Despite this rise in flow, the corresponding increase in pump power is minimal. Overall, the reduced supply temperature leads to a net decrease in thermal energy use, as

demonstrated in Figure 37. This highlights the effectiveness of G36 in achieving energy savings without compromising thermal performance.

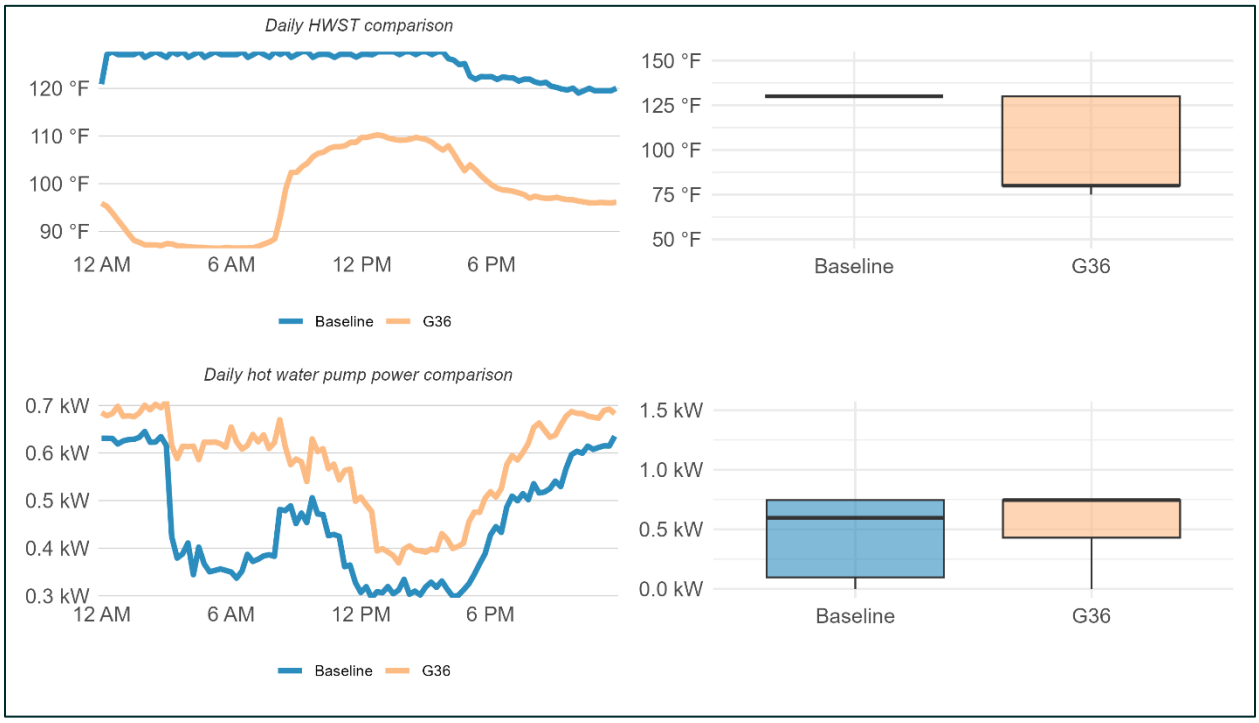

Figure 37: Hot water supply temperature and hot water pump power comparison between G36 days and baseline days.

Figure 38 shows hot water supply and return temperature distributions for the baseline and G36 days. The T&R reset under the G36 approach reduced the mean supply water temperature to 102.6°F compared to 120.2°F in the baseline, as well as reduced the mean return water temperature to 88.2°F compared to 97.2°F in the baseline. For condensing boilers, efficiency is primarily driven by return (or entering) water temperatures, where condensing begins at temperatures of about 130°F but efficiency continues to improve at lower temperatures. Importantly, the boiler plant was already operating efficiently in the baseline condition with return water temperatures mostly within the condensing region. The even lower return water temperatures with the G36 approach, an average reduction of about 9°F, provided incremental improvements in boiler efficiency in this case but larger savings would have been possible if the boilers were not already operating so efficiently in the baseline operation.

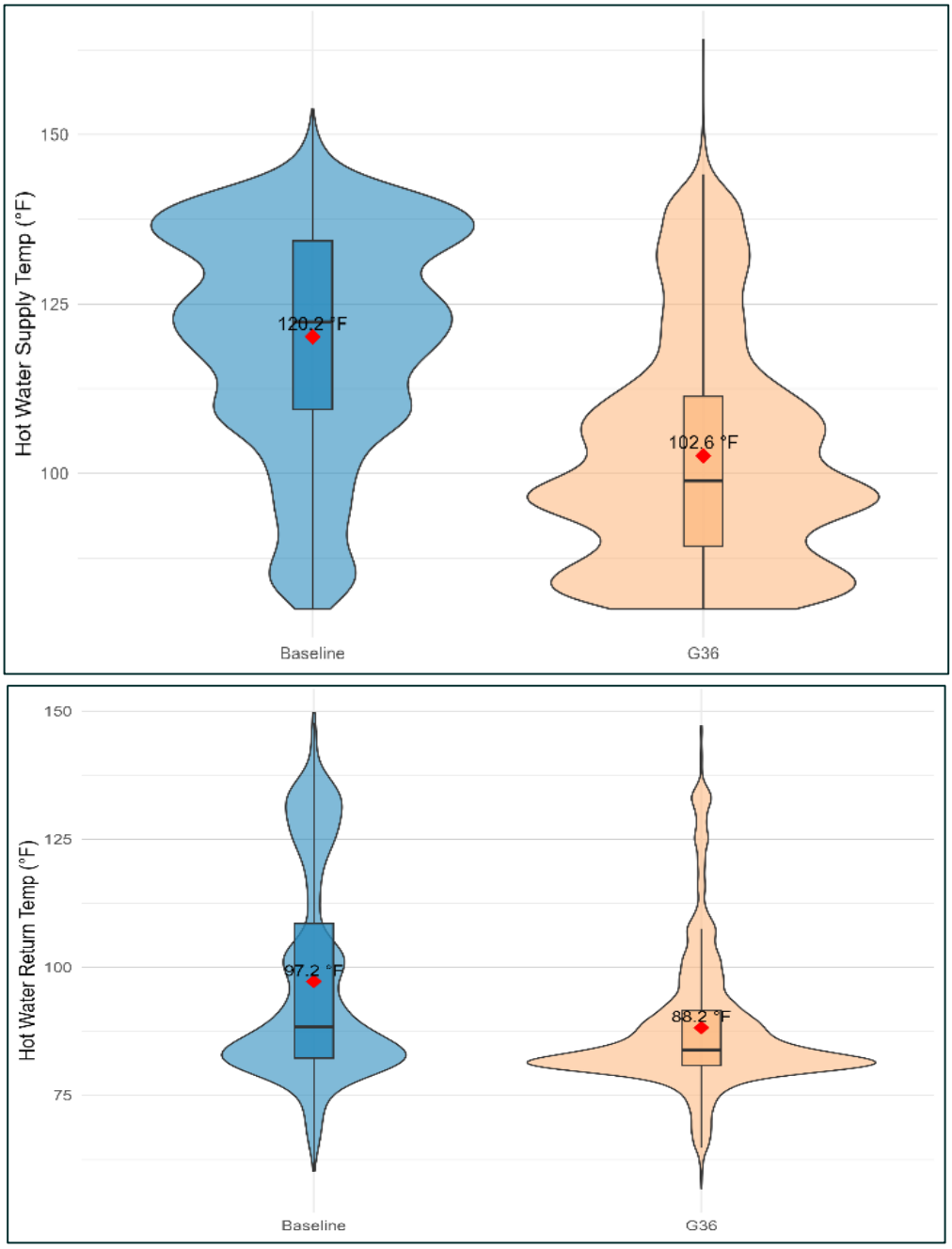

Figure 38: Hot water supply and return temperature distribution for baseline and G36 days.

Figure 39 below illustrates the daily natural gas energy use, with baseline data shown in blue and G36 data in orange. The rapid M&V schedule alternated between the two control strategies throughout the entire measurement period. Daily energy use was derived from utility meter data, expressed in kBtu per day.

Notably, several peak energy use days correspond to the first day after a period of boiler shut off, which the research team believes is due to building warmup. As stated above, the team removed these data points from the analysis.

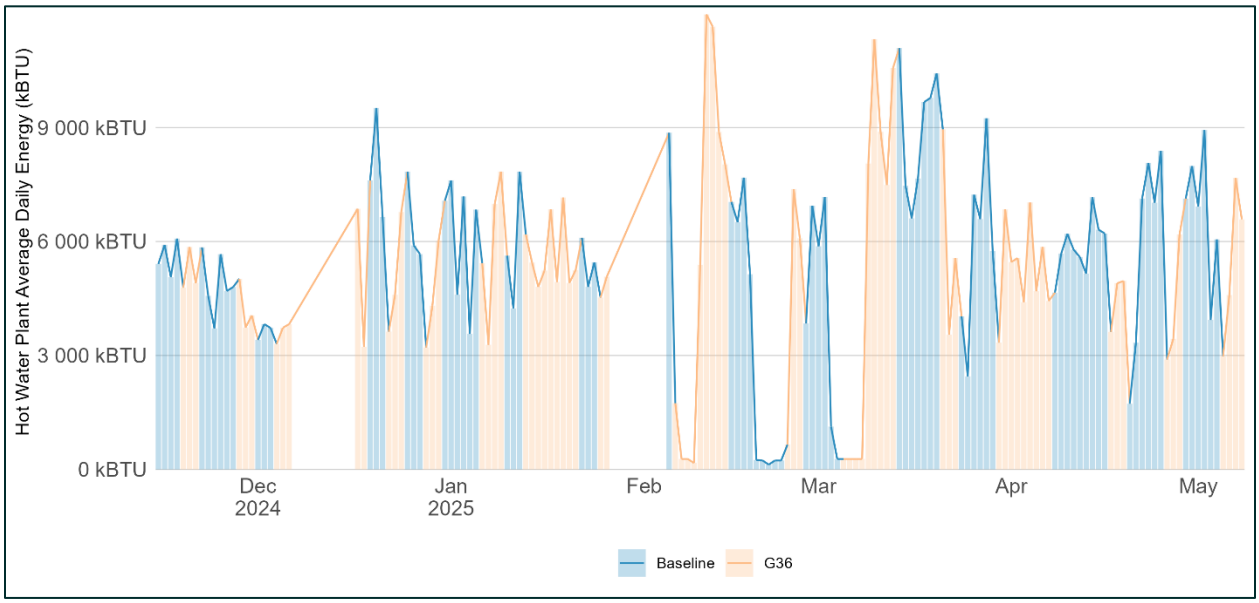

Figure 39: Daily hot water plant natural gas energy use with the rapid M&V approach (utility data).

Figure 40 presents the daily natural gas energy use, which the team measured using an external pulse-counting meter installed at the building's natural gas meter. A period of missing data from January through the end of April was identified and attributed to a drained battery in the VataVerks pulse-counting device, which led to inconsistent and unreliable readings.

For the M&V analysis, the research team opted to separately analyze the daily data available from the utility meter and the sub-hourly data aggregated to 15-minute intervals from the external meter, ensuring that both data sources were utilized to the extent possible while maintaining data integrity.

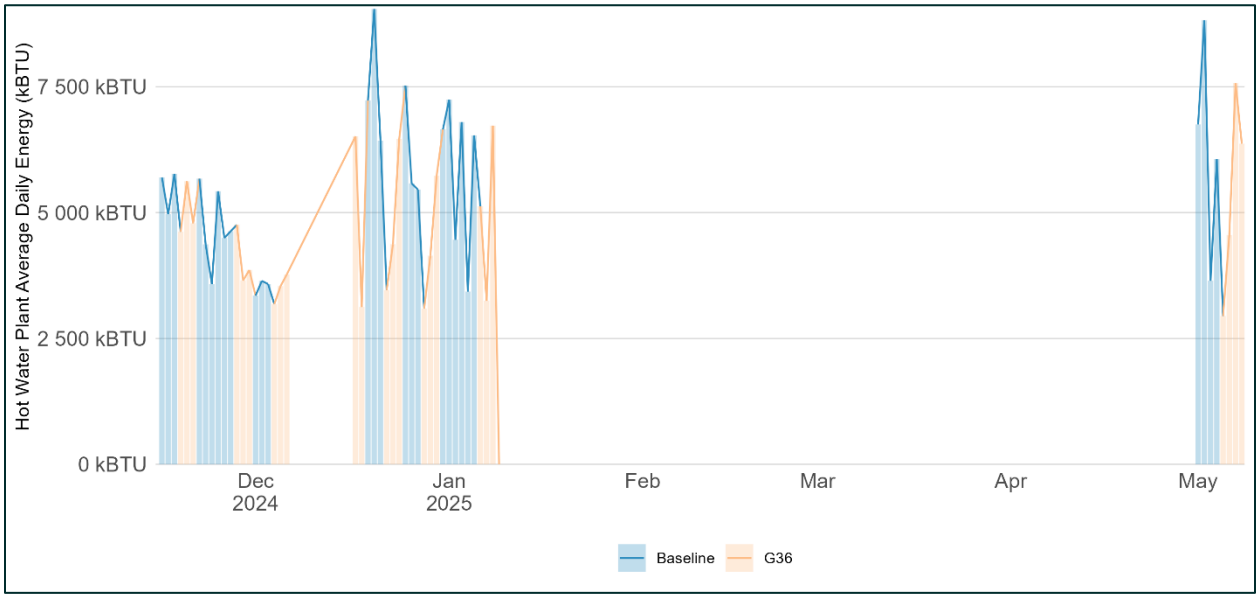

Figure 40: Daily hot water plant natural gas energy use with the rapid M&V approach (measured data).

DAILY AVERAGE ENERGY USE

The team conducted a one-tailed hypothesis test to evaluate the null hypothesis: that the mean daily thermal energy use under G36 is greater than or equal to that under the baseline. Figure 41 below shows daily average energy consumption derived from utility meter data.

Results indicate that daily average energy consumption decreased by 585 kBtu per day (equivalent to 15.1 Btu per square foot per day), representing a 9.4 percent reduction under G36. The observed low p-value provides strong statistical evidence to reject the null hypothesis, confirming that G36 used significantly less energy compared to the baseline.

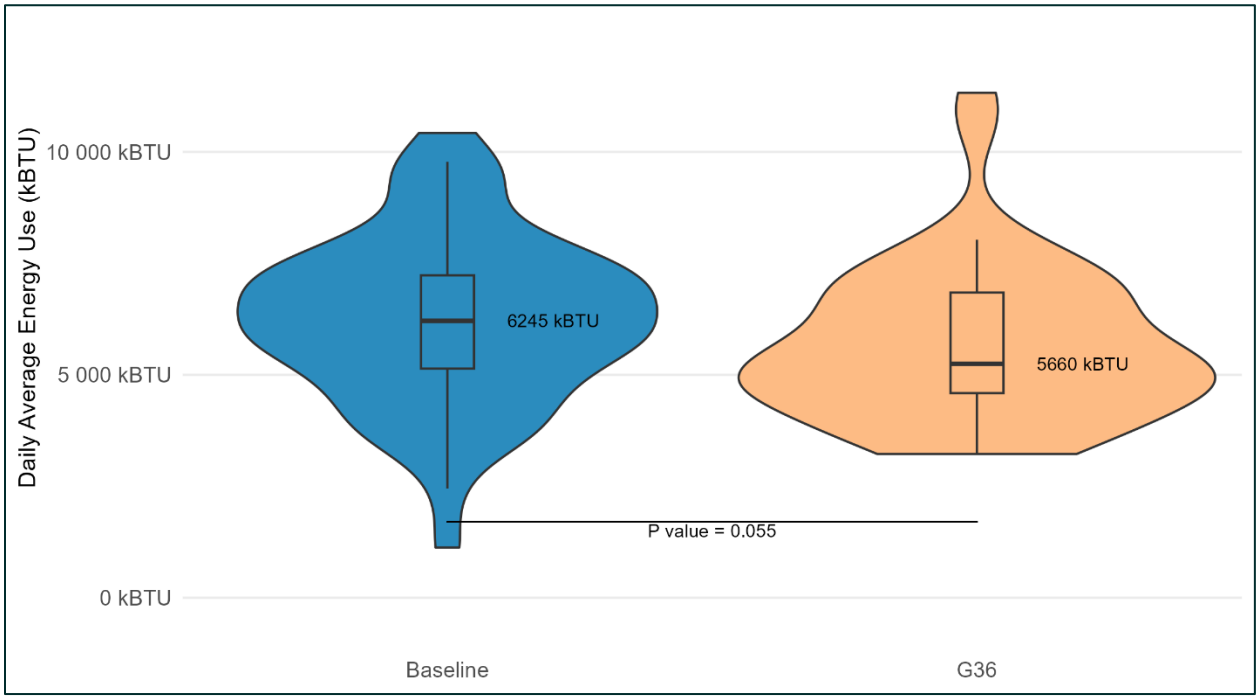

Figure 41: Distribution of natural gas energy use between baseline and G36 intervention (utility data).

The 15-minute natural gas energy use distribution, shown in Figure 42 below, is based on metered data collected by the research team. As previously noted, there are gaps in this dataset due to issues with the pulse meter.

Despite these data limitations, the conclusion remains consistent with the daily utility meter analysis: G36 used less energy compared to the baseline. The analysis indicates that G36 achieved an average daily savings of 816 kBtu (equivalent to 21.1 Btu per square foot per day), representing a 15 percent reduction in energy use.

This result differs somewhat from the daily utility meter-based savings (10.4 percent), which might be caused by missing data from January and February periods that include colder weather. Since G36 was expected to deliver greater savings during shoulder seasons, the reduced presence of cold-weather data in the 15-minute dataset shown in Figure 42 aligns with the observed higher percentage savings.

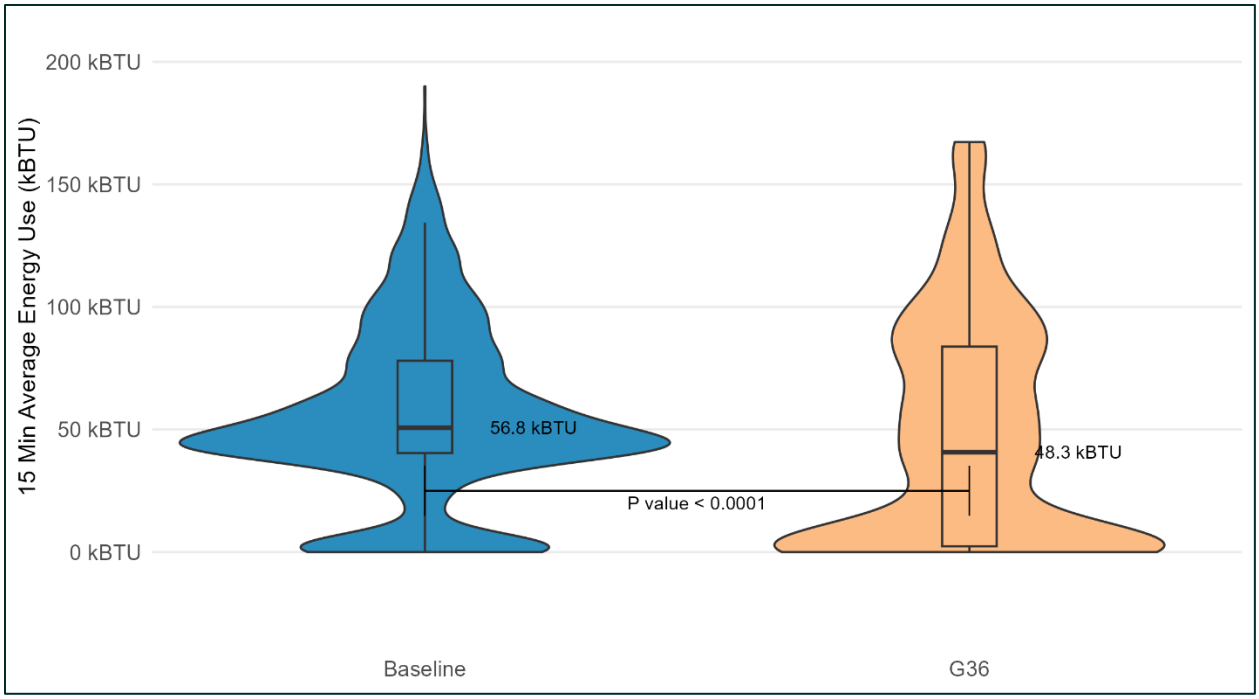

Figure 42: Distribution of 15-min natural gas energy use between baseline and G36 intervention (measured data).

TOWT MODEL

The research team collected five-minute natural gas usage data using an external pulse logger, which was then aggregated to 15-minute intervals for use in TOWT regression models. These models were created using the NMEC R (nmecr) package developed by kW Engineering in the R programming environment.

Model performance statistics for both the baseline and G36 strategies are summarized in Table 12 below. Compared to the benchmark thresholds established, the model statistics are close but do not meet the thresholds. This is due to the limited data when using both daily and 15-minute data sets, and the team expects model fits will be better if additional data is used. The team also believes that the conclusions of this section will not change with additional data that would improve model fit.

During model development, a 20 percent threshold was applied to filter the dataset for metered energy data. This filtering process excluded periods where natural gas was used exclusively for domestic hot water, as well as data points considered outliers due to boiler operation issues. This approach ensured that the models accurately represent energy usage patterns associated with space heating under both baseline and G36 control strategies.

Table 12: TOWT model fit statistics for baseline and G36: Site 2 HW plant.

	Baseline				G36			
Energy type	**No. of days**	**R2**	**CVRMSE%**	**NDBE%**	**No. of days**	**R2**	**CVRMSE%**	**NDBE%**
Natural gas energy – utility	57	0.310	27.01	-6.3E-14	46	0.142	33.41	-2.7E-14
Natural gas energy – measured	29	0.638	34.48	4.6E+01	24	0.591	46.16	7.1E-13

Figure 43 and Figure 44 below use daily utility-provided data to compare the measured thermal energy use to the TOWT model predictions for both the baseline and G36 strategies. In these plots, red dots represent the measured daily energy consumption, while blue dots indicate the energy consumption predicted by the TOWT regression model for the corresponding outside air temperature conditions.

The research team expected a trend of lower natural gas energy use with increasing outside air temperature, which is weakly reflected in this trend.

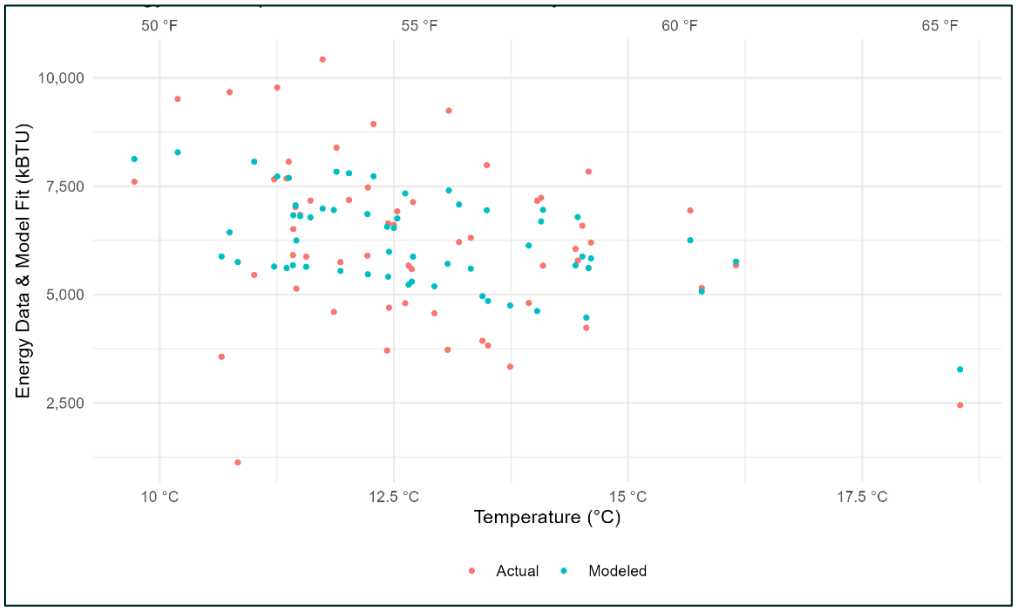

Figure 43: Measured and model predicted daily natural gas energy use against outside air temperature for

baseline strategy (utility data).

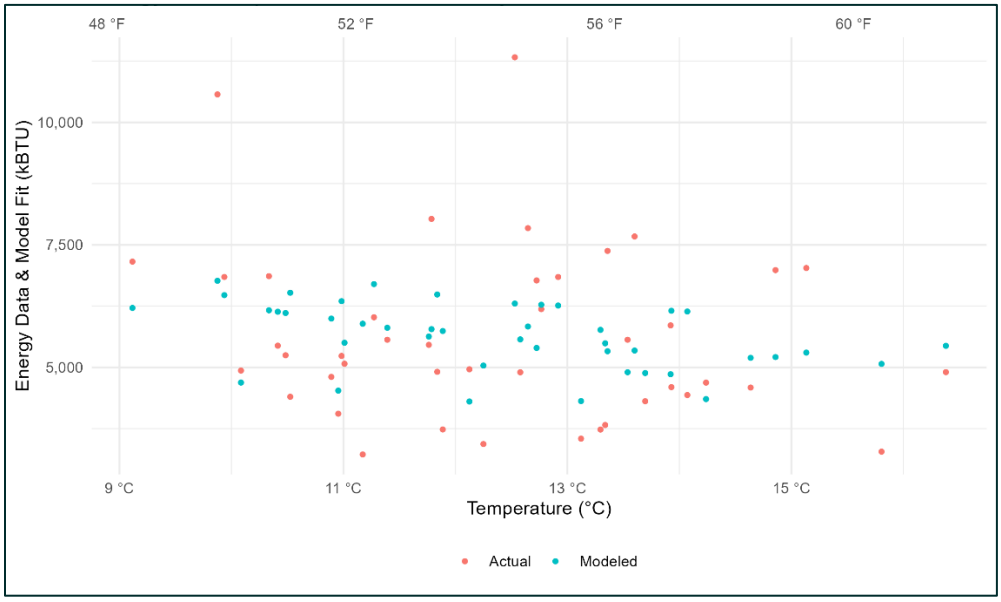

Figure 44: Measured and model predicted daily natural gas energy use against outside air temperature for G36 (utility data).

Figure 45 and Figure 46 below present a comparison between measured thermal energy use and model predicted data for both the baseline and G36 strategies, using 15-minute natural gas usage data collected by the research team. Unlike the trend observed in the daily utility data, where higher outside air temperatures corresponded with lower energy use, the 15-minute data did not clearly show this expected inverse relationship.

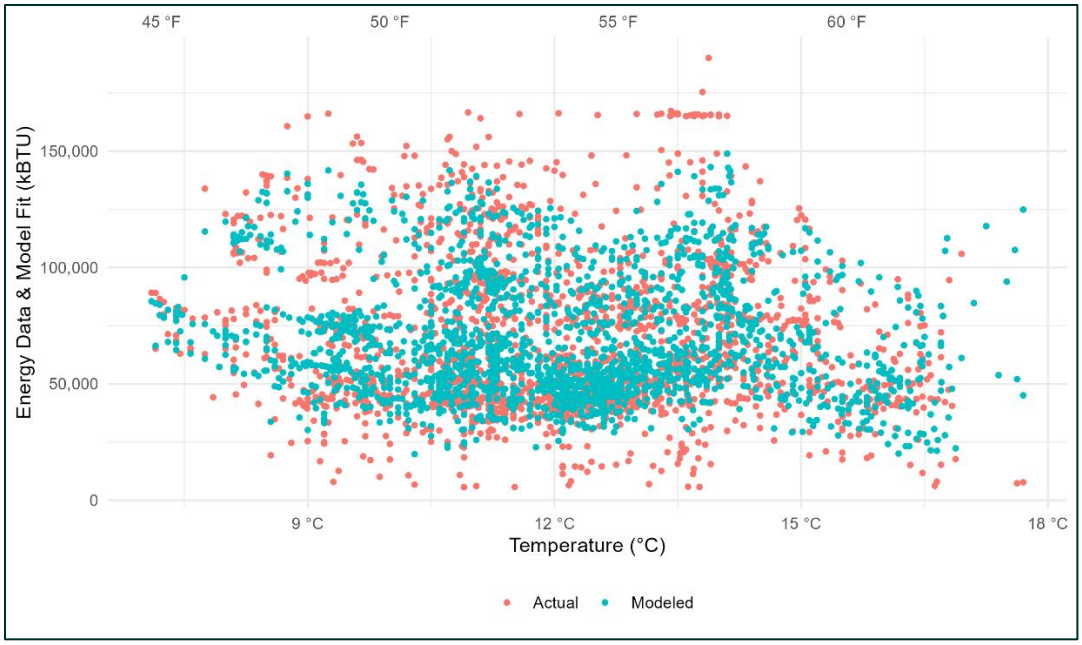

Figure 45: Measured and model predicted natural gas energy use in 15 minutes against outside air temperature (measured data).

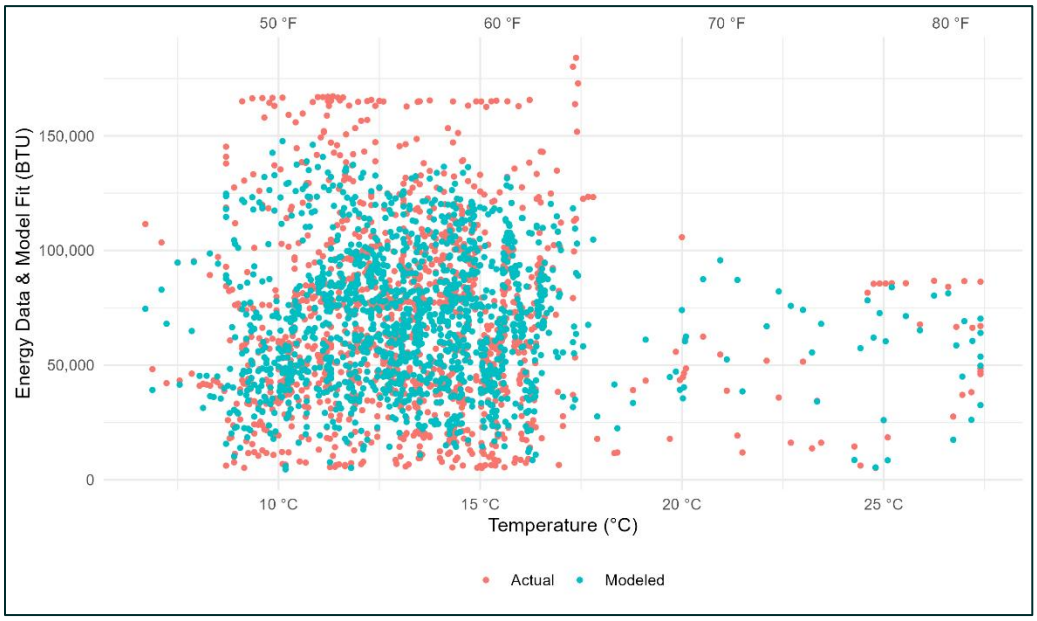

Figure 46: Measured and model predicted natural gas energy use in 15 minutes against outside air temperature (measured data).

To evaluate the long-term performance of the G36 strategy under typical weather conditions, the research team utilized TOWT regression models to predict normalized daily energy consumption. This analysis was conducted using weather data from the TMY3 database, which represents average climate conditions for the project's geographic location. Below, Figure 47 compares the predicted daily energy consumption for both the baseline and G36 strategies, while Figure 48 compares the

predicted monthly energy consumption between the two strategies. Summer months between June and August were ignored for this analysis, since the boiler is typically turned off during this period. The comparison highlights the impact of the G36 control logic on reducing heating energy use under typical climate conditions. Results from the model estimate an annual energy savings of 126,953 kBtu, equivalent to 3.28 kBtu per square foot per year, or approximately 7.5 percent energy reduction for the demonstration site.

Based on an average natural gas utility rate of $2.885 per therm, this leads to a normalized annual cost savings of $3,662 per year, or $0.095 per square foot per year.

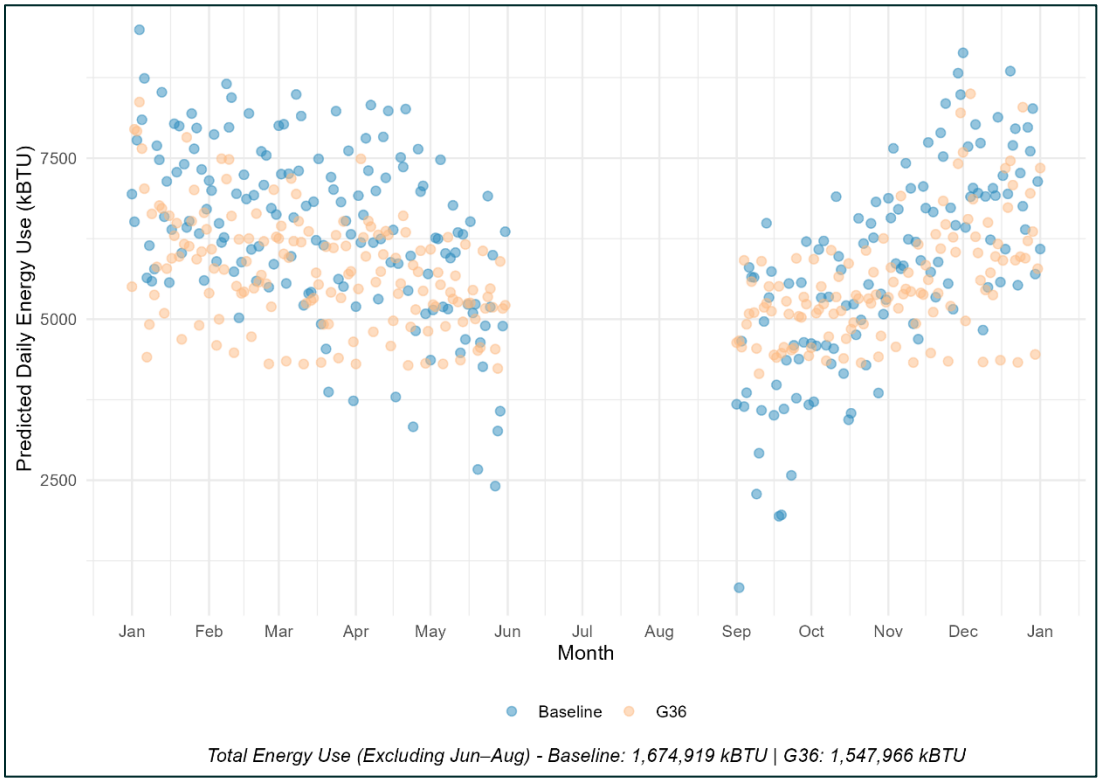

Figure 47: TOWT model predicted normalized daily utility energy consumption for baseline and G36.

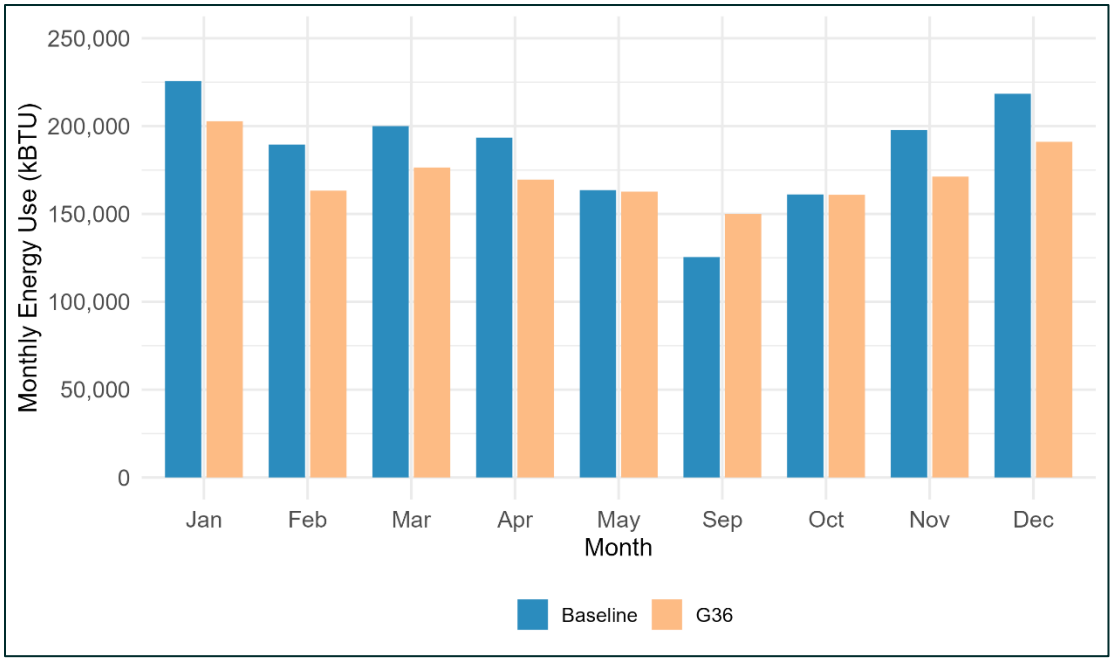

Figure 48: TOWT model predicted monthly energy use comparison between baseline and G36: Site 2 HW plant.

Energy and Cost Savings Summary

Table 13 below summarizes the avoided and annual normalized energy and cost savings for implementing G36 for each plant in the two buildings.

Table 13: Summary of energy and cost savings.

Site	Energy Type	Annual Normalized Energy Saving*			Annual Cost Saving*	
Site 1	CHW plant electricity*	86,672 kWh*	0.61 kWh/ft2*	14.6%*	$17,334/yr *	$0.12 /ft2-yr*
Site 1	HW plant	1,431,580 kBtu/yr	10.15 kBtu/ft2-yr	11.5%	$23,860/yr	$0.17/ft2-yr
Site 2	HW plant natural gas	126,953 kBtu/yr	3.28 kBtu/ft2-yr	7.5%	$3,662/yr	$0.095 /ft2-yr

*Note: Site 1 CHW plant energy electricity predicted energy use calculation does not include Jun-Aug energy use

Market Scalability

This project presents a promising solution for the scalable deployment of advanced, high-performing control sequences in existing buildings with BAS. By decoupling the controls delivery workflow, the approach enables different stakeholders to focus on specialized tasks, improving efficiency and consistency. Control and programming experts can concentrate on developing foundational, vendor-agnostic control blocks based on G36 SOOs that are transparent and verifiable. Ontology experts contribute by creating standardized, machine-readable frameworks (e.g., Brick) for organizing and tagging metadata across building systems. Software developers then integrate the preprogrammed control blocks into complete control applications that query the Brick data model, interact with the building's BAS to retrieve and transmit data, and execute both primary and supporting control logic.

Meanwhile, building, HVAC, and data modeling professionals work with facility-specific information to translate unstructured metadata into a structured Brick model. The resulting control application can run on a BACnet-compatible edge device capable of uploading the building Brick data model and interfacing with a wide range of BAS platforms, as illustrated in Figure 49. In this setup, the Brick model is essential for enabling the application to automatically discover building systems and self-configure, eliminating the need to reprogram G36 SOOs for each control vendor's platform.

Additionally, deploying the application via a BACnet edge device—a device analogous to our small fan-less PC that connects to the building's BACnet network and provides local control and data processing—offers a practical alternative when the existing BAS cannot handle the programming complexity of G36 SOOs or would suffer from performance limitations or high integration costs. This modular, standards-based approach not only has the potential to accelerate control deployment and reduce engineering burden, but also lays the groundwork for a replicable, cost-effective pathway to modernize control systems across the broader existing building stock.

While the proposed supervisory-level implementation offers a flexible and scalable pathway for modernizing existing BAS, several inherent limitations must be acknowledged to ensure reliable and robust operation. Supervisory controllers generally operate at slower update rates of one-to-five-minute intervals, making them unsuitable for fast-acting feedback loops. The performance of supervisory control depends heavily on the quality of the underlying field devices and control loops.

Poorly tuned PIDs, drifted sensors, or unverified actuators can undermine higher-level optimization. Furthermore, supervisory systems have limited access to real-time safety functions and cannot enforce mechanical interlocks, which must remain at the equipment level. Communication and IT-related constraints present additional challenges, as network congestion, bandwidth limitations, and security policies can restrict data exchange or delay control actions. Cyber-resilience concerns also arise when edge devices need to connect to external cloud services. Finally, legacy BAS often provides sparse or inconsistent point data, while operator overrides and limited staff training can introduce conflicts between local and supervisory control layers.

The team encountered some of these limitations in our study, such as poorly tuned PIDs, drifted sensors, cybersecurity concerns of an additional BACnet device, and a lack of knowledge of the supervisory layer. However, we worked with management to resolve these issues by retro-commissioning, limiting access to the fan-less PC, and communicating the expected behavior of the supervisory control on their BAS.

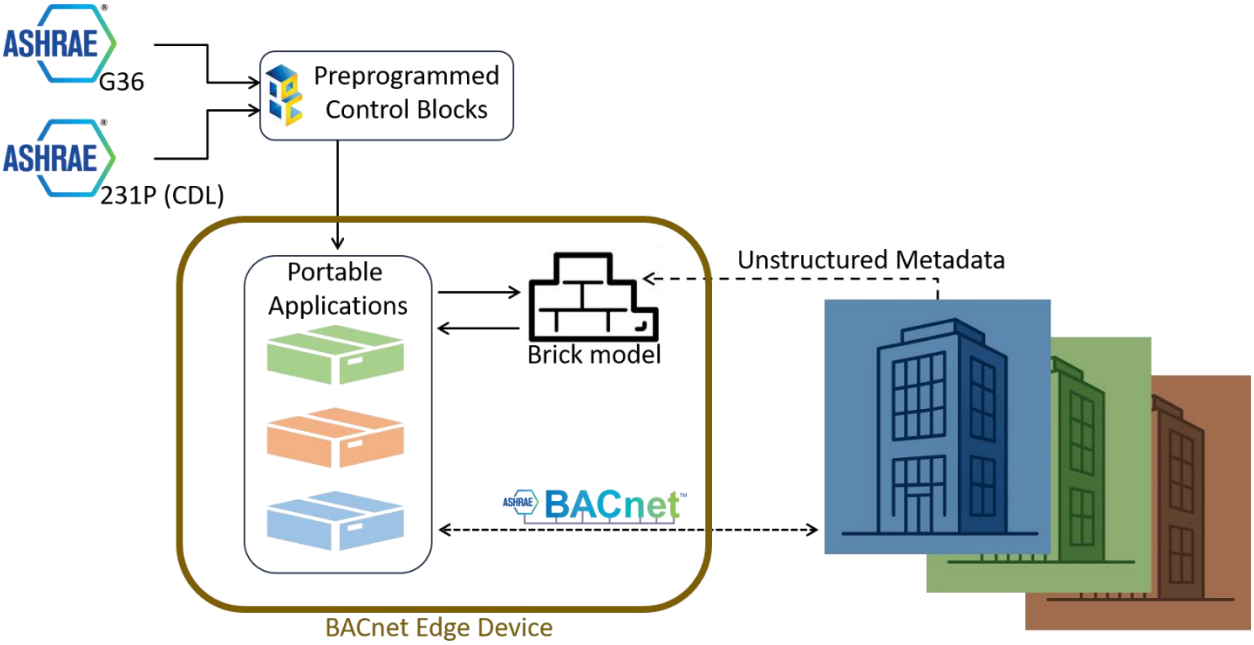

Figure 49: Schematic of how the standardization methods used in these field demonstrations can serve as building blocks to create high-performing, portable, scalable control applications.

Market scalability of G36 adoption is supported by multiple pathways that lower implementation barriers and promote broader adoption. One key strategy involves pre-programming G36 sequences in control systems at the manufacturer level. This approach reduces the need for on-site customization and accelerates project timelines by simplifying design and commissioning tasks. Pre-programmed controls ensure consistency in implementation and improve reliability across different projects and building types. These embedded sequences can be particularly beneficial for smaller design firms or contractors who may lack the in-depth expertise to fully customize advanced control strategies.

This can be further enhanced by standardizing designs around G36 with an accessible and easy-to-use tool. A LBNL-developed website, *ctrl-flow,*[1] provides users with a G36 sequence based on high-level project information, such as climate zone and system type. The solution demonstrated in this project can get wide adoption in the design and specifying phase, which leads to more consistent and implementable design requirements for G36. The *ctrl-flow* output can also be tailored to provide outputs that help with adoption of ASHRAE 231P and 232P efforts in conjunction with G36.

G36 is also well-positioned to be included as a utility program measure, either as a deemed or custom offering. Its demonstrated energy savings make it a compelling candidate for demand-side management portfolios. Utility programs can play a key role in market transformation by providing financial incentives, offering technical assistance for integration into building automation systems, and supporting training efforts. Additionally, the use of rapid M&V methods can help quantify savings

[1] https://ctrl-flow.lbl.gov/

in a timely and cost-effective manner, encouraging broader implementation by streamlining the performance verification process.

Further, the savings measured by implementing HW supply temperature and CHW supply temperature resets are larger than those typically estimated for these energy conservation measures. However, the models used to generate those estimates do not accurately capture all aspects of real system performance. For example, they omit losses from the heat transfer from and to distribution piping, which is likely part of the reason why they underestimate savings. These results indicate the savings in practice are larger than estimated. Though clearly further investigation in a larger sample of buildings is needed to more accurately quantify the benefit in a typical building, these are very low-cost measures that are broadly applicable to the building stock, and as such, should be further incentivized or required in current codes to improve adoption.

Finally, the integration of G36 into codes and standards will be instrumental in accelerating adoption. The 2025 California Title 24 update already includes elements of G36, laying the groundwork for more comprehensive inclusion in future code cycles. Expanding hydronic sequences from G36 into either prescriptive or performance-based compliance pathways would increase market penetration while raising the baseline of system performance. As codes evolve to include more of these sequences, adoption will shift from being an innovative option to a standard expectation, further reinforcing G36's role in high-performance HVAC design.

Conclusions and Recommendations

This implementation of selected ASHRAE G36 hydronics sequences of operation leveraged an advanced control framework that included a supervisory control layer, CDL programming, and Brick schema-based ontology. This approach enabled structured, scalable deployment of the G36 sequences across multiple air handling units and plant systems. The supervisory control layer provided centralized coordination of zone-level and plant-level sequences, while CDL ensured readable, transparent, and modular control logic that can be scaled easily. Brick ontology allowed standardized equipment and point tagging across buildings, facilitating faster configuration, improved fault diagnostics, and integration with data processing workflows. This procedure streamlined G36 adoption in this demonstration and presented the proof of concept for a replicable path for broader market deployment in new and retrofit applications.

In terms of energy performance, ASHRAE G36 showed consistent and significant energy savings across the three hydronics plants in Site 1 and Site 2 compared to the existing control systems in these plants. Based on TOWT annual normalized savings, the selected G36 measures saved 14.6 percent (86,672 kWh, 0.61 kWh per square foot) and 11.5 percent (1,431,580 kBtu per year, 10.15 kBtu per square foot per year) plant energy, as well as $0.12 per square foot and $0.17 per square foot per year cost in Site 1 chilled water and hot water plants, respectively.

In Site 2, the selected G36 measures saved 7.5 percent (126,953 kBtu per year, 3.28 kBtu per square foot per year) and $0.095 per square foot per year plant energy and cost. These consistent savings across datasets and timeframes highlight the significant energy efficiency potential of G36 sequences when appropriately implemented. The results also highlight a clear opportunity for

broader G36 deployment through manufacturer pre-programming, utility program adoption, further integration into codes and standards, and through tools like *ctrl-flow*.

The research team conducted a thorough review of the existing system prior to implementation of G36 and optimized the controls to address identified issues, saving an estimated 16 percent energy over the baseline during the monitoring period, not normalized to typical weather conditions. These findings indicate that both thoroughly reviewing the existing system operation and correcting any issues save energy, as well as enable G36 deployments to operate more efficiently than they would have over the existing condition. Therefore, a key recommendation is to conduct a thorough review and retro-commissioning of existing systems before implementing advanced sequences like G36. This includes validating sensor calibration, ensuring actuator reliability, and tuning control loops where necessary. For critical or tightly controlled spaces, support systems such as dedicated dehumidification control should be considered as part of the overall strategy.

References

ASHRAE. (2020). *ASHRAE Handbook - HVAC Systems and Equipment.* Retrieved from https://www.ashrae.org/technical-resources/ashrae-handbook

ASHRAE. (2020). *BACnet - A Data Communication Protocol for Building Automation and Control Networks.* Atlanta, GA: ASHRAE Standard 135.

ASHRAE. (2021). *High Performance Sequences of Operation for HVAC Systems.* ASHRAE.

ASHRAE. (2023). *Guideline 14-2023 - Measurement of Energy, Demand and Water Savings.* ASHRAE. Retrieved from https://www.techstreet.com/standards/ashrae-guideline-14-2023-measurement-of-energy-demand-and-water-savings?product_id=2569793

Bender, J. (2018). *BACpypes Documentation.*

Bergmann, H., Mosiman, C., Saha, A., Haile, S., Livingood, W., Bushby, S., . . . Pritoni, M. (2020). Semantic Interoperability to Enable Smart, Grid-Interactive Efficient Buildings. *ACEEE 2020 Summer Study on Energy Efficiency in Buildings.*

Bharathan, B., Bhattacharya, A., Fierro, G., Gao, J., Gluck, J., Hong, D., . . . Whitehouse, K. (2016). Brick: Towards a Unified Metadata Schema For Buildings. *Proceedings of the 3rd ACM International Conference on Systems for Energy-Efficient Built Environments.*

Blochwitz, T., Otter, M., Akesson, J., Arnold, M., Clauss, C., Elmqvist, H., . . . Viel, A. (2012). Functional Mockup Interface 2.0: The Standard for Tool independent Exchange of Simulation Models. *Proceedings of the 9th International Modelica Conference.* Munich, Germany: The Modelica Association.

Brick Consortium. (2015). *What is Brick?* Retrieved from Brick: A Uniform Metadata Schema for Buildings: https://brickschema.org/

Butler, J. F., & Veelenturf, R. (2010). Point Naming Standards. *ASHRAE*, B16-B20.

Delgoshaei, P., Heidarinejad, M., & Austin, M. A. (2022). A Semantic Approach for Building System Operations: Knowledge Representation and Reasoning. *Sustainability*.

Duarte Roa, C., Paul, R., Sun, R., Paul, L., Prakash, A. K., Pritoni, M., . . . Peffer, T. (2022). Towards a Stronger Foundation: Digitizing Commercial Buildings with Brick to Enable Portable Advanced Applications. *2022 Summer Study on Energy Efficiency in Buildings.* Pacific Grove, CA.

Lawrence Berkeley National Laboratory. (2024). *Performance Evaluation, Specification, Deployment and Verification of Building Control Sequences*. Retrieved from OpenBuildingControl: https://obc.lbl.gov/

Lin, G., Pritoni, M., Chen, Y., Vitti, R., Weyandt, C., & Granderson, J. (2023). Implementation and test of an automated control hunting fault correction algorithm in a fault detection and diagnostics too. *Energy and Buildings*.

Nmap. (2022). Nmap: The Network Mapper - Free Security Scanner.

NREL. (2020). *TMY3 Weatehr*. Retrieved from https://doe2.com/Download/Weather/TMY3/

Raftery, P., Cheng, H., & Wendler, P. (2024). Are we prioritizing the right thing? Cutting carbon emissions in California's large office buildings before installing a heat pump. *ACEEE Summer Study.* Pacific Grove: CA.

Raftery, P., Zou, A., Parkinson, T., & Hancock, G. (2023). *Reliably Estimating the Impact of a New Control Strategy in a Building.* Retrieved from SSRN: https://papers.ssrn.com/sol3/papers.cfm?abstract_id=4531516

Singla, R., Paliaga, G., Koli, S., Chu, Y., Chappell, C., Cheng, H., & Eubanks, B. (2022). *Nonresidential HVAC Controls Final CASE Report.* California Statewide Utility Codes

and Standards Team.
Taylor Engineering, TRC, Integral Group. (2022). *Best-in-class Optimized Solutions.* California Energy Commission.
Wetter, M., Ehrlich, P., Gautier, A., Grahovac, M., Haves, P., Hu, J., . . . Zhang, K. (2022). OpenBuildingControl: Digitizing the control delivery from building energy modeling to specification, implementation and formal verification. *Energy*.
Wetter, M., Grahovac, M., & Hu, J. (2019). Control Description Language. *American Modelica Conference*, (pp. 17-26). Cambridge, MA.
Wetter, M., Zuo, W., Nouidiu, T. S., & Pang, X. (2014). Modelica Buildings Library. *Journal of Building Performance Simulation*, 253-270.